Iowa Research Online
The University of Iowa's Institutional Repository

University of Iowa
Iowa Research Online

Theses and Dissertations

Spring 2010

Enzymatic regulation of phosphatidylcholine synthesis via protein ubiquitination

Phillip Louis Butler
University of Iowa

Copyright 2010 Phillip Louis Butler

This dissertation is available at Iowa Research Online: http://ir.uiowa.edu/etd/473

Recommended Citation
Butler, Phillip Louis. "Enzymatic regulation of phosphatidylcholine synthesis via protein ubiquitination." PhD (Doctor of Philosophy) thesis, University of Iowa, 2010.
http://ir.uiowa.edu/etd/473.

Follow this and additional works at: http://ir.uiowa.edu/etd


Part of the Biochemistry Commons

ENZYMATIC REGULATION OF PHOSPHATIDYLCHOLINE SYNTHESIS VIA PROTEIN UBIQUITINATION

by

Phillip Louis Butler

An Abstract

Of a thesis submitted in partial fulfillment of the
requirements for the Doctor of Philosophy degree
in Biochemistry in
the Graduate College of
The University of Iowa

May 2010

Thesis Supervisor: Professor Rama K. Mallampalli

ABSTRACT

Pulmonary surfactant is a critical surface-active substance consisting of dipalmitoylphosphatidylcholine (DPPtdCho) and key apoproteins that are produced and secreted into the airspace from alveolar type II epithelial cells. Deficiency of the surfactant leads to severe lung atelectasis, ventilatory impairment, and gas-exchange abnormalities. The generation of DPPtdCho in cells occurs via two integral routes: the *de novo* and remodeling pathways. The interplay between these pathways has not been investigated. Overexpression of the remodeling enzyme, acyl-CoA:lysophosphatidylcholine acyltransferase (LPCAT1), in epithelia decreases *de novo* PtdCho synthesis without significantly altering cellular phospholipid mass; this occurs through increased degradation of cholinephosphotransferase (CPT1), the terminal enzyme of the *de novo* pathway. CPT1 is degraded by multi-ubiquitination and trafficking via the lysosomal pathway. When expressed in lung epithelia, CPT1 mutants harboring arginine substitutions at multiple carboxyl-terminal lysine residues exhibited proteolytic resistance to effects of LPCAT1 overexpression. Cellular expression of these CPT1 mutants also restores *de novo* PtdCho synthesis to levels normally observed in lung epithelia. Further studies demonstrate that the SCF (Skip-Cullen-F-box) ubiquitin E3 ligase component, β-TrCP, was sufficient to degrade CPT1. Similar to CPT1, LPCAT1 levels are also regulated at the level of protein stability. However, LPCAT1 is a poly-ubiquitinated enzyme processed within the proteasome. Similar to CPT1, β-TrCP may be the putative E3 ubiquitin ligase subunit responsible for LPCAT1 ubiquitination. β-TrCP appears to dock and ubiquitinate LPCAT1 within its amino-terminus. Collectively, these observations indicate the presence of cross-talk between the phospholipid remodeling and *de novo* pathways; this involves tight regulation by site-specific ubiquitination of indispensable regulatory enzymes catalyzed by SCF ubiquitin E3 ligase members that

mechanistically provide homeostatic control of cellular phospholipid content.

Abstract Approved: _____
Thesis Supervisor

_____
Title and Department

_____
Date

ENZYMATIC REGULATION OF PHOSPHATIDYLCHOLINE SYNTHESIS VIA PROTEIN UBIQUITINATION

by

Phillip Louis Butler

A thesis submitted in partial fulfillment of the
requirements for the Doctor of Philosophy degree
in Biochemistry in
the Graduate College of
The University of Iowa

May 2010

Thesis Supervisor: Professor Rama K. Mallampalli

Graduate College
The University of Iowa
Iowa City, Iowa

CERTIFICATE OF APPROVAL

_____

PH.D. THESIS

_____

This is to certify that the Ph.D. thesis of

Phillip Louis Butler

has been approved by the Examining Committee
for the thesis requirement for the Doctor of Philosophy
degree in Biochemistry at the May 2010 graduation.

Thesis Committee: _____
Kris DeMali, Thesis Chair

_____
John Donelson

_____
Robert Piper

_____
Peter Rubenstein

_____
Dan Weeks

To my parents

ACKNOWLEDGEMENTS

Work presented in this thesis was made possible through the assistance and encouragement of past and current members of the Mallampalli lab. In particular, I would like to thank my advisor, Rama Mallampalli for allowing me to grow as an independent thinker and scientist; Diann McCoy for her assistance on animal studies and primary cell isolation; Ron Salome for his assistance on LDH assays; and Alan Ryan and Nancy Ray for their support during my stay in the Mallampalli lab. I would also like to thank Dr. Bill Chen for his scientific enthusiasm and guidance. I am grateful to Kris DeMali for her guidance in this project. Funding was provided by a Merit Review Award from the Department of Veteran's Affairs, and NIH R01 Grants HL068135, HL080229, HL081784, HL096376, HL097376, and HL098174 (to RKM).

ABSTRACT

Pulmonary surfactant is a critical surface-active substance consisting of dipalmitoylphosphatidylcholine (DPPtdCho) and key apoproteins that are produced and secreted into the airspace from alveolar type II epithelial cells. Deficiency of the surfactant leads to severe lung atelectasis, ventilatory impairment, and gas-exchange abnormalities. The generation of DPPtdCho in cells occurs via two integral routes: the *de novo* and remodeling pathways. The interplay between these pathways has not been investigated. Overexpression of the remodeling enzyme, acyl-CoA:lysophosphatidylcholine acyltransferase (LPCAT1), in epithelia decreases *de novo* PtdCho synthesis without significantly altering cellular phospholipid mass; this occurs through increased degradation of cholinephosphotransferase (CPT1), the terminal enzyme of the *de novo* pathway. CPT1 is degraded by multi-ubiquitination and trafficking via the lysosomal pathway. When expressed in lung epithelia, CPT1 mutants harboring arginine substitutions at multiple carboxyl-terminal lysine residues exhibited proteolytic resistance to effects of LPCAT1 overexpression. Cellular expression of these CPT1 mutants also restores *de novo* PtdCho synthesis to levels normally observed in lung epithelia. Further studies demonstrate that the SCF (Skip-Cullen-F-box) ubiquitin E3 ligase component, β-TrCP, was sufficient to degrade CPT1. Similar to CPT1, LPCAT1 levels are also regulated at the level of protein stability. However, LPCAT1 is a poly-ubiquitinated enzyme processed within the proteasome. Similar to CPT1, β-TrCP may be the putative E3 ubiquitin ligase subunit responsible for LPCAT1 ubiquitination. β-TrCP appears to dock and ubiquitinate LPCAT1 within its amino-terminus. Collectively, these observations indicate the presence of cross-talk between the phospholipid remodeling and *de novo* pathways; this involves tight regulation by site-specific ubiquitination of indispensable regulatory enzymes catalyzed by SCF ubiquitin E3 ligase members that mechanistically provide homeostatic control of cellular phospholipid content.

TABLE OF CONTENTS

LIST OF FIGURES

LIST OF ABBREVIATIONS

ABC	ATP-binding cassette transporter protein
ABCA	ABC family transporter within the A sub-family protein
ARDS	Acute respiratory distress syndrome
ALI	Acute lung injury
BSA	Bovine serum albumin
β-TrCP	beta-transducin repeat containing protein
CCT	Choline-phosphate cytidylyltransferase A
CEPT1	Choline:ethanolaminephosphotransferase
CFP	Cyan fluorescent protein
CHM	Cycloheximide
CK	Choline kinase
CPT1	Choline phosphortransferase 1
cDNA	Complementary DNA
DMEM	Dulbecco's modified Eagle's medium
DNA	Deoxyribonucleic acid
DPPtdCho	Dipalmitoylphosphatidylcholine
DTT	Dithiothreitol
EDTA	Ethylenediaminetetraacetic acid
FBS	Fetal bovine serum
GGA	Golgi-localized, gamma-ear-containing, Arf-binding
H. *flu*	*Haemophilus influenza* bacteria
HEPES	N-(2-hydroxyethyl) piperazine-N'-(2-ethanesulfonic acid)
HITES	DMEM F12 cell culture medium
kDa	Kilo Dalton
KGF	Keratinocyte growth factor
Lac	Lactacystin
Leu	Leupeptin
LPCAT1	Acyl-CoA:lysophosphatidylcholine acyltransferase
MLE	Murine lung epithelial
mRNA	Messenger RNA
PA103	Pseudomonas aeruginosa strand 103
PAGE	Polyacrylamide gel electrophoresis
PBS	Phosphate buffered saline
PCR	Polymerase chain reaction
PEMT	Phosphatidylethanolamine *N*-methyltransferase-2
PG	Phosphatidylglycerol
PI	Phosphatidylinositol
PMSF	Phenylmethylsulfonyl fluoride
PtdCho	Phosphatidylcholine
SDS	Sodium dodecyl sulfate
SCF	Skp1-Cullin-F-box
siRNA	Short interfering RNA
YFP	Yellow fluorescent protein

CHAPTER I

INTRODUCTION

Pulmonary surfactant is a critical substance containing dipalmitoylphosphatidylcholine (DPPtdCho) and key apoproteins [1] that are produced and secreted into the airspace from alveolar type II epithelial cells [2]. The acute lung injury syndrome (ALI) and chronic disorders such as cystic fibrosis result in functional surfactant deficiencies leading to severe lung collapse, ventilatory difficulties, and gas-exchange abnormalities that can lead to right heart failure. Clinical treatment of these disorders with surfactant replacement therapies is now underway [3, 4]. However, effectiveness of exogenous surfactant treatment in these disorders is limited because of the presence of infection with highly virulent strains of bacteria that greatly suppress surfactant phospholipid biosynthesis and surfactant secretion. Thus, these observations have led to investigations of molecular mechanisms for phospholipid generation (specifically DPPtdCho) that would pave the way for newer strategies directed at optimizing the pool of surfactant in the setting of lung inflammation. These strategies might entail use of small molecular inhibitors (e.g. ubiquitin E3 ligases) or activators (e.g. CPT1) of novel molecular targets that could someday prove beneficial for inflammatory lung disorders.

Eukaryotic PtdCho synthesis

Phosphatidylcholine (PtdCho) accounts for ~60-70% of surfactant phospholipids (Fig. 1) [5]. The major surface-active form of surfactant is DPPtdCho. DPPtdCho biosynthesis in eukaryotic cells mainly utilizes one of two pathways: the *de novo* pathway or the recycling/remodeling pathway (Fig. 2). *De novo* PtdCho synthesis involves three steps as shown in Figure 2A : (i) an ATP-dependent phosphorylation of choline catalyzed by choline kinase (CK) to synthesize cholinephosphate, (ii) a transfer

of cholinephosphate to CTP to form CDP-choline catalyzed by CTP:phosphocholine cytidylyltransferase (CCT), and (iii) a transfer of cholinephosphate from CDP-choline to diacylglycerol to form PtdCho catalyzed by cholinephosphotransferase (CPT1) [6]. In this pathway, kinetic studies show that the formation of CDP-choline from cholinephosphate catalyzed by CCT is rate-limiting and regulatory [7]. CCT alpha is the major isoform in the lung and in surfactant-producing alveolar epithelial cells [8].

The remodeling pathway is important in the lung because, in most mammalian cells, PtdCho has an unsaturated fatty acid linked to the *sn*-2 position of the glycerol backbone (Fig 2B), which is not a substantial component of surfactant. In type II cells of the lung, this unsaturated PtdCho species has to be converted to saturated DPPtdCho (a molecule lacking unsaturated acyl groups), a feature that confers surface-tension lowering activity to surfactant. Thus, the unsaturated moiety from PtdCho is removed first by a calcium-independent phospholipase A_2 (PLA_2), generating the toxic phospholipid termed LysoPtdCho. Although the mechanism by which LysoPtdCho is toxic to cells has not been well studied, evidence suggests that the lipid may be secreted and act as a chemotactic signal mediating attraction of monocytic cells to apoptotic cells [9]. In the second step, LysoPtdCho is re-acylated using palmitate by another enzyme. Until recently, the identity of this enzyme was unknown. The enzyme that catalyzes the acyltransferase reaction has recently been cloned from lung alveolar cells and is termed acyl-CoA:lysophosphatidylcholine acyltransferase (LPCAT1) [10, 11]. The CDP-choline and remodeling pathways are not the only means by which cells can produce PtdCho. In the liver, *de novo* PtdCho synthesis also proceeds via the sequential *N*-methylation of phosphatidylethanolamine (PE) as an auxiliary (PEMT) pathway. However, this pathway is minimally active in the liver and serves primarily in an auxiliary role.

The *de novo* pathway: CDP-choline:1,2-diacylglycerol cholinephosphotransferase (CPT1)

The terminal step in the *de novo* PtdCho synthesis pathway involves a transfer of cholinephosphate from CDP-choline to diacylglycerol to form PtdCho catalyzed by CPT1. Although the enzymatic activity associated with CPT1 was proposed long ago with the initial PtdCho *de novo* pathway postulation by Kennedy, it was later discovered that there were two enzymes that contributed most of the cholinephosphotransferase activity in eukaryotic cells [12-14]. CPT1 and the dually specific choline/ethanolaminephosphotransferase (CEPT1) are both capable of coupling CDP-choline to diacylglycerol, but CPT1 predominates in lung epithelial as CEPT1 expression levels in lung is very low [15, 16]. The cholinephosphotransferases localize to either the endoplasmic reticulum or Golgi apparatus where available diacylglycerol substrate resides. Study of these enzymes has been difficult as they are transmembrane enzymes which lose much, if not all, of their activity in detergent-mild and rich environments often used to isolate and purify membrane-bound enzymes.

The remodeling pathway: Acyl-CoA: Lysophosphatidylcholine acyltransferase (LPCAT1)

LPCAT1 is a 60kDa enzyme that converts 1-acyl-*sn*-glycero-3-phosphocholine (LysoPtdCho) to DPPtdCho by addition of a palmitoyl fatty acyl group to the *sn*-2 position of LysoPtdCho (Fig 2). This enzyme appears to play a key role in a second pathway involving the remodeling of phospholipids. In this pathway, unsaturated PtdCho (nonsurfactant lipids) are converted to saturated phospholipids (i.e. surfactant lipids, DPPtdCho) - a process critical in lung cells. Here, an unsaturated moiety of PtdCho (usually oleic acid) is first cleaved from the glycerol backbone by PLA_2 generating LysoPtdCho, a molecule toxic to cells; LysoPtdCho has to be rapidly eliminated and can be processed to synthesize DPPtdCho by re-acylation with a palmitic fatty acid catalyzed

by LPCAT1 - without the use of the *de novo* pathway. LPCAT1 is abundant in lung alveolar type II cells compared to other tissues [11]. High-level expression of LPCAT1 suggests that it may be critical for maintaining DPPtdCho production in a salvage pathway or to complement *de novo* synthesis of surfactant during inflammatory stress. Previous estimates indicate a significant portion of DPPtdCho in type II cells is from the remodeling pathway using LPCAT1; however, this has not been investigated *in vivo* [17, 18]. LPCAT1 activity increases with lung development and in response to glucocorticoids, an effect that appears to be to due to increased LPCAT1 gene transcription [10]. Unfortunately, because the identity of LPCAT1 has (until recently) been elusive, published biochemical analysis has been limited. Work on the molecular physiology of glycerol lipid acyltransferases indicate that a conserved $H(X)_4D$ motif [19] is necessary for enzymatic activity.

Surfactant secretion by lung epithelia

Pulmonary surfactant is highly relevant to the prevention and treatment of respiratory distress syndrome (RDS) in preterm infants, a condition characterized by reduced surfactant phospholipid synthesis [20]. These investigations in surfactant metabolism in RDS led to the identification of novel enzymes that regulate the synthesis, secretion, function, and catabolism of alveolar surfactant [21, 22]. The surfactant proteins (SP-A, SP-B, SP-C, and SP-D), PtdCho biosynthetic enzymes, remodeling enzymes, and the surfactant lipid associated transporters (e.g. ABCA3), play critical roles in surfactant homeostasis [23, 24]. SP-A and SP-D are hydrophilic glycoproteins that promote lung immunity and host defense [25] , whereas SP-B and SP-C are hydrophobic proteins that confer the surface tension lowering ability of surfactant [26]. Surfactant is synthesized in alveolar type II cells that contain relatively high levels of the enzymes listed above. Type II cells must produce surfactant phospholipid, package the lipid in organelle

compartments called lamellar bodies, and those organelles must fuse with the apical membrane of the cell during the process of surfactant secretion.

Lamellar bodies are organelles that range in size from 0.1-2.4μm in diameter that consist of roughly 80-85% DPPtdCho, 5-10% neutral lipid, and 10% surfactant proteins [27]. Type II cells normally contain ~100 lamellar bodies; however, they account for less than 5% of all alveolar cells. It is believed that after infancy, PtdCho and DPPtdCho are synthesized in the ER and Golgi, and are trafficked in both Golgi-dependent and independent pathways. Evidence supporting a Golgi-independent pathway involve experiments using brefeldin A, a disruptor of Golgi integrity, that inhibits surfactant protein secretion [28]. Additional experiments using ^{3}[H] choline pulse chase and electron microscopy suggest that trafficking of PtdCho to lamellar bodies to the Golgi may not be direct, however [29]. The identification of PtdCho transport proteins has also been a recent area of investigation for mechanisms of phospholipid sorting to lamellar bodies. Although a highly specific PtdCho carrier protein was previously identified, it appears that either redundancy exists for PtdCho delivery to lamellar bodies or non-specific carriers may be sufficient for delivery [30, 31].

Surfactant phospholipid must also be secreted from lamellar bodies through the apical surface. Secretion to the air lung interface is believed to be a calcium-dependent process, facilitated by ATP-binding cassette dependent (ABC) family lipid transporters within the A sub-family (ABCA). It appears that ATP-binding cassette transporter A1 (ABCA1) is a basal and not apical lipid transporter [32-34]. Another ABCA transporter, ATP-binding cassette transporter A3 (ABCA3), is now believed to be a transporter of lipid within lamellar bodies [35]. It is highly expressed in type II lung epithelia. Additionally, deletion or mutation studies involving the transporter results in abnormal lamellar organelle morphology, immaturity of organelles, reduced PtdCho content of surfactant, and increased surface tension of surfactant [23, 24, 35, 36].

Cellular balancing between surfactant (DPPtdCho) and nonsurfactant (PtdCho) phospholipid generation

Lung epithelia must tightly balance levels of surfactant (DPPtdCho) lipid secreted into airways versus nonsurfactant PtdCho destined for cell membranes. While the *de novo* pathway generates both nonsurfactant PtdCho and DPPtdCho, the remodeling pathway would be predicted to synthesize primarily surfactant. It has been estimated that perhaps ~55-75% of surfactant DPPtdCho is synthesized by the remodeling pathway with the remainder generated by *de novo* synthesis[37, 38]. These results suggest that when LPCAT1 levels are increased, as occurs during alveolar stress when demands for surfactant (DPPtdCho) are high, lung epithelia might coordinately reduce *de novo* synthesis of PtdCho. This cellular mechanism may be favorable to shift the balance toward DPPtdCho enrichment for surfactant secretion into the airways. Conversely, when cells adopt a proliferative state and do not require the type II cell surfactant lipophenotype, the *de novo* pathway appears to be indispensable to enhance new cell membrane formation [39]. However, without coordinate balancing of activities of *de novo* synthesis versus remodeling of membrane and surfactant phospholipids under these scenarios, respectively, the risk for cellular lipotoxicity is high [40].

The interdependency of two pathways in lipid metabolism has been described by Cui and colleagues [41]. In their study, the activity of the PEMT pathway is linked to the CDP-choline pathway in hepatic tissues [41]. Furthermore, overexpression of the enzyme phosphatidylethanolamine *N*-methyltransferase-2 (PEMT2) in hepatoma cells inhibits the CDP-choline pathway at the level of CCT [41]. By analogy, it is possible that LPCAT1 in the remodeling pathway regulates the *de novo* pathway to maintain surfactant lipid homeostasis.

Modification of enzymes by ubiquitin

Protein ubiquitination has emerged as an important post-translational modification responsible for altering protein stability and localization. This reversible modification can also regulate diverse processes such as gene transcription, endocytic vesicle trafficking, histone modification, and DNA repair [42, 43]. Conjugation of one (mono-ubiquitination) or multiple (multi-ubiquitination) ubiquitin peptides to lysine residues within target proteins serves as an important endocytic signal for internalization and targeting of various ion channels, membrane cargo receptors, and junction proteins to the endocytic pathway [44, 45]. Interestingly, although lysine is the most common amino acid modified by ubiquitin conjugation formed by using an isopeptide bond, ubiquitin has less frequently been identified conjugating to serine and threonine residues via ester bond formation [46]. Poly-ubiquitination is a process by which a chain of at least four ubiquitin molecules are linked to a lysine on a substrate protein, most commonly resulting in degradation of the substrate protein via the 26S proteasome. Multi-ubiquitination and poly-ubiquitination differ in that multi-ubiquitination is conjugation of many lysine residues with single ubiquitin peptides (multiple mono-ubiquitination) while poly-ubiquitination is often the conjugation of more than four ubiquitin peptides through ubiquitin-ubiquitin conjugations to a single residue. Orientation of ubiquitin-ubiquitin conjugation within ubiquitin chains can drastically alter trafficking of cargo; conjugated ubiquitin Lys-63 (K63) chains often target proteins to the endosome/lysosome while Lys-48 (K48) chains often target cargo to the proteasome for proteolytic cleavage [45]. There are, however, several other obscure ubiquitin-ubiquitin linkages that are in the process of being fully described , such as K6, K11, K27, K29, and K33 poly-ubiquitin chains [47].

The modification of enzymes by ubiquitin conjugation involves several steps: (i) ubiquitin is activated in a two-step reaction by an E1 ubiquitin-activating enzyme, (ii), ubiquitin is transferred from the E1-activating enzyme to an E2-ubiquitin conjugating enzyme, and (iii), an E3-ubiquitin ligase transfers ubiquitin from the E2-ubiquitin

conjugating enzyme to a lysine residue on a substrate enzyme via an isopeptide bond between the ε-amino lysine of the enzyme and the carboxyl-terminus of ubiquitin [48]. E3 ligases are several-fold more abundant than E1 or E2 ligases, which is likely a result of the necessity for specificity of the E3 ligase that directly binds to substrates before their ubiquitination [49]. There are four major classes of E3 ubiquitin ligases: HECT-type, PHD-type, RING-type, and U-box containing [49]. There are also three major families of E1-E2-E3 ubiquitin ligase complexes: the SCF (Skp1-Cullin-F-box) family, the APC (Anaphase-Promoting Complex) family, and the VCB (VHL-Elongin C/Elongin B) family [50]. Importantly, the SCF complex family has been shown to mediate targeting of transmembrane proteins for degradation [48].

The SCF complex includes Skp1, Cullin1, Ubc (E2 ubiquitin-conjugating enzyme) and an E3 ubiquitin ligase (F-box protein) that serves as an adaptor subunit. E3 ligases target many substrates through specific domain interactions. F-box proteins have two domains: an amino-terminal F-box motif and a carboxyl-terminal leucine-rich repeat motif or WD repeat motif. The SCF complex uses the leucine-rich/WD repeat motif for substrate recognition while the F-box motif is used to bind Skp1. F-box proteins have diverse roles regulating protein stability that can regulate the cell cycle and the circadian clock[51, 52]. Thus far, the SCF family of ubiquitin ligases has attracted significant attention and may be relevant to the processing of surfactant lipogenic enzymes as suggested by preliminary data within this thesis.

Ubiquitination of membrane proteins and receptors:
sorting and degradation signals

Plasma membrane proteins and receptors are key regulators of signaling, important to intercellular communication and as a mechanism to regulate cells interaction and responses to their local environment. The inflammatory cytokine response is important to acute lung injury [53-55]. Tumor necrosis factor (TNF) plays a critical role

in inflammation and is involved in the immune response. Although ubiquitination of tumor necrosis factor receptor 1 (TNF-R1) has yet to be described, the receptor complex does recruit ubiquitination machinery that eventually lead to ubiquitination of the tumor necrosis factor receptor-associated factor (TRAF) adaptor molecules and subsequent activation of NF-kappaB [56, 57].

Epidermal growth factor receptor (EGFR), unlike TNF-R1 is directly ubiquitinated. Unlike many transmembrane proteins, this receptor binds a ligand and then enters the multi vesicular bodies (MVB) in an ubiquitin independent manner. Upon entering the MVB, EGFR it is ubiquitinated and targeted for lysosomal degradation by the modification of one of its cytosolic domains [58]. Ubiquitination, however, is often a initiator and mediator of localization and trafficking. Recently, the glycine transporter GLYT1b has been described to be ubiquitinated at a specific lysine residue leading to its internalization [59]. Indeed, ubiquitination alone is often not sufficient for a proteins trafficking to the lysosome as de-ubiquitinating enzymes (DUBs) constantly cleave ubiquitin modifications allowing many receptors and membrane proteins passage back to their original membranes [60].

The platelet-derived growth factor (PDGF) is a classic example of ligand induced ubiquitination [61]. In response to ligand binding, PDGF is poly-ubiquitinated and processed through the proteasome [62, 63]. A recent study, refutes claims made in the 1990s, regarding PDGF poly-ubiquitination and have implicated the role of mono-ubiquitination in the internalization and trafficking of PDGF and other tyrosine kinase receptors [64]. Evidence also supports the role of different ubiquitin modifications regulating a single receptor, such as the epithelial sodium channel (ENaC) [65].

Murine lung cell line

A major limitation of surfactant phospholipid research is the inability to easily isolate rodent type II cells in sufficient numbers for investigation; furthermore, primary type II

cell isolates lose their lipid phenotype (i.e. ability to secrete surfactant lipids) within hours to days. Until the last decade, the lack of an ideal *in vitro* cell model that recapitulates the lipid phenotype remained an important obstacle to studies of surfactant biology. This hurdle has been overcome, in part, by the use of a murine lung epithelial (MLE) cell line used in this thesis. This line has been successfully used in research of pulmonary surfactant production and regulation, lung development and tumorigenesis studies [8, 38, 66-68]. This line was first established in 1992 by Kathryn A. Wikenheiser from pulmonary tumors in a mouse transgenic for the SV40 large T antigen under the control of the human surfactant protein C gene promoter [37]. Specifically, lung tumors were collected from female transgenic mice within 4-5 months of age. The excised tumors and adjacent tissue were minced and washed with medium. Pooled washes and remaining tumor were cultured separately in HITES medium. Colony selection was used as a method of isolation [38]. MLE cell lines exhibit rapid growth, lack of contact inhibition, and epithelial cell morphology for 30-40 passages in culture. Microvilli, cytoplasmic multivesicular bodies, and multilamellar inclusion bodies (morphologic characteristics of alveolar type II cells) have been detected by electron microscopic analysis [37]. This cell line also maintains functional characteristics of distal respiratory type II epithelial cells, including the expression of surfactant proteins B, C, and D and mRNAs. Importantly, these cells exhibit a critical feature of primary mouse type II epithelia - the ability to secrete surfactant phospholipids in response to agents known to stimulate lipid secretion (e.g. phorbol esters and ATP) which can be initiated by agonists that activate P_2Y_2 or A_{2B} receptors [69, 70]. MLE cells provide an alternative to alveolar type II cells and maintain important characteristics of primary type II cells for our studies including lipid secretion and characteristic protein expression while foregoing the need for continued primary cell isolation.

Inhibitors of protein degradation pathways

A multitude of inhibitors are used in molecular and biochemical analyses of cellular function. My studies utilize inhibitors of two cellular degradation pathways: the proteasome or lysosome. The bulk of proteins in mammalian cells are hydrolyzed in an ATP-dependent process by the proteasome and substrates are ubiquitinated before they are recognized for degradation [71, 72]. The 26S proteasome consists of a central 20S complex and two 19S complexes which provide substrate specificity and recognition of ubiquitinated substrates [73]. Aldehyde peptide inhibitors of the proteasome are substrate analogues, which act as transition-state inhibitors of the chymotrypsin-like active site of the proteasome, and are therefore reversible inhibitors [74]. MG-132 is one such inhibitor I have used in my studies. Another inhibitor, lactacystin, acts as a pseudosubstrate. Upon association with the proteasome active site, it becomes covalently linked to the hydroxyl groups of the threonine residues of the 20S complex, which results in inhibition of activity [75]. Unlike MG-132, lactacystin is thought to be a less reversible inhibitor, as hydrolysis from the active site occurs slowly [76].

My studies also used inhibitors of the lysosomal pathway. The lysosome is mainly involved with the degradation of membrane-associated proteins and receptors [77]. Inhibitors of lysosomal acidification (e.g. NH_4Cl), or inhibition of lysosomal proteases (e.g. leupeptin), are used in the study of proteins degraded though the lysosomal pathway [78]. Of these two mechanisms of lysosome inhibition, protease inhibitors are more specific, since the many proteases within the endosome/lysosome are active at a broad pH range [79].

The focus of this thesis

The goal of this research is to determine the molecular and biochemical basis of regulatory factors for the PtdCho remodeling and *de novo* pathways. Chapter II of this thesis addresses how the remodeling pathway acyltransferase enzyme, LPCAT1, reduces

de novo phospholipid synthesis to maintain lipid homeostasis. For this purpose, a novel acyltransferase, LPCAT1, was cloned and expressed, and was determined to be abundantly expressed and highly active in type II lung epithelia, the cells responsible for lung surfactant production. Upon cellular expression of LPCAT1, I demonstrated that total *de novo* synthesis of PtdCho was reduced while leaving total cellular lipid composition unchanged. These results suggest feedback inhibition within the *de novo* synthesis pathway to maintain total cellular lipid balance. Further studies reveal that lipid balance was maintained in response to LPCAT1 overexpression by reduction in *de novo* PtdCho production via reducing immunoreactive levels of the terminal enzyme, CPT1. Using immunofluorescence, I determined that the reduction in CPT1 activity was secondary to CPT1 degradation through processing within the endosome/lysosome pathway. From chapter III experiments, I discovered LPCAT1 overexpression lead to site-specific CPT1 ubiquitination, CPT1 trafficking to the endocytic pathway, and eventual degradation and loss of cellular CPT1 activity.

Enzymes processed through the endocytic pathway are often ubiquitinated. The focus of Chapter III is to examine how LPCAT1 up-regulation in cells leads to CPT1 degradation. I first determined if CPT1 was a substrate for ubiquitination. Co-expression of CPT1 with ubiquitin leads to decreased CPT1 levels suggesting CPT1 may be ubiquitinated. By performing co-immunoprecipitation experiments for CPT1, I was able to detect multiple higher migrating bands indicative of multiple CPT1-ubiquitin conjugates. To identify ubiquitin acceptor sites within CPT1, several candidate lysine residues were mutated to arginine based on proposed models of CPT1 topologic orientation [80]. $CPT1_{K4R}$ and $CPT1_{K6R}$ mutants, containing four and six mutated lysine residues, respectively, were overexpressed and determined to produce a different ubiquitination profile with fewer higher molecular weight signals indicative of loss of ubiquitination on the mutated residues compared to wild-type CPT1. To assess protein stability of the CPT1 and $CPT1_{K6R}$ mutants with or without LPCAT1 co-expression,

cellular protein synthesis was inhibited by cycloheximide treatment and cells were harvested at various time points. Following collection of cells, immunoblot analyses and densitometry was performed. The data, overall, suggest while LPCAT1 significantly decreases CPT1 stability, LPCAT1 did not significantly reduce $CPT1_{K6R}$ stability. To determine if $CPT1_{K6R}$, like CPT1, was properly localized and trafficked through the endosome/lysosome pathway for its degradation, I performed immunofluorescence co-localization studies. These studies suggest no difference in CPT1 and $CPT1_{K6R}$ localization to the Golgi apparatus; $CPT1_{K6R}$ did not display significant localization within the endocytic compartments after LPCAT1 co-expression, suggesting that $CPT1_{K6R}$ is not, or is less efficiently, targeted to the lysosome for degradation. Further support for the ability of ubiquitin to act as a CPT1 degradation signal was explored by performing immunofluorescence on cells overexpressing a CPT1-ubiquitin fusion protein. I determined that the addition of the ubiquitin fusion peptide significantly increased endocytic compartment localization. Last, I observed that $CPT1_{K4R}$ and $CPT1_{K6R}$ mutants are enzymatically active, and overexpression was sufficient to restore *de novo* synthesis in response to LPCAT1 overexpression.

Our studies of CPT1 processing by acyltransferase-induced ubiquitination led us to determine the molecular control of LPCAT1. To date, no studies have investigated how this enzyme is regulated pre-or-post-translationally in cells, as it was only recently characterized. Much like CPT1, LPCAT1 is a membrane-bound enzyme and both are terminal enzymes in the biosynthesis of DPPtdCho. While preliminary studies suggest a role for phosphorylation in LPCAT1 modification, ubiquitination appears to serve as a central method of cellular regulation of lipogenic enzymes CCT and CPT1[81, 82]. Phosphorylation, however, can act as a marker for docking of SCF E3 ubiquitin ligases[83-86]. Therefore, the identification of a LPCAT1 putative E3 ubiquitin ligase and consensus of phosphorylation modification sites are the focus of Chapter IV. To determine if LPCAT1 was ubiquitinated, I first co-expressed LPCAT1 with HA-tagged

ubiquitin in MLE cells and determined that ubiquitin is bound to LPCAT1 by co-immunoprecipitation studies. Because LPCAT1 appears to be phosphorylated (an important recognition signal for some SCF member E3 ubiquitin ligases), I overexpressed several candidate plasmids encoding SCF member E3 ubiquitin ligases and observed that the SCF member, β-TrCP, downregulates endogenous LPCAT1 protein levels. Furthermore, cells containing overexpressed β-TrCP and LPCAT1 protein suggest that the E3 ubiquitin ligase was also able to promote the degradation of recombinant LPCAT1. Co-expression of these plasmids significantly reduced LPCAT1 activity in cells, suggesting, as expected, that the loss of LPCAT1 protein regulates enzymatic behavior. Next, cells were treated with proteasomal and endosomal inhibitors, and cell lysates were analyzed using SDS-PAGE and immunoblot analysis. Lysates from cells overexpressing β-TrCP and treated with proteasome or lysosome inhibitors appear to contain several, higher molecular weight conjugates. Cell lysates were also immunoprecipitated with LPCAT1 antibody. Immunoblots of these immunoprecipitation experiments suggest that only cells treated with MG-132, a proteasomal inhibitor, accumulate detectable higher molecular weight species indicative of LPCAT1 poly-ubiquitination (K48 chain linkages), although these results do not exclude lysosomal degradation of the enzyme. I also determined that LPCAT1 and β-TrCP may be binding partners through immunoblot analysis of immunoprecipitation experiments using LPCAT1-V5 and β-TrCP co-expression. Lastly, preliminary mapping studies using LPCAT1 truncation mutants suggest that the deletion of the carboxyl-terminus of LPCAT1 is not sufficient to completely inhibit LPCAT1/ β-TrCP binding. Although further study is needed to identify the sites within LPCAT1 which are targets for ubiquitin modification, and a site or sites responsible for β-TrCP docking, the current studies will fill a void in the field of phospholipid biochemistry as they relate to the molecular regulation of the newly discovered acyltransferase, LPCAT1, the major enzyme involved in surfactant phospholipid remodeling.

Figure 1. Surfactant composition

A diagram depicting the three major components of lung surfactant in a pie graph: phospholipid, protein (surfactant proteins A-D (SP-A-D)), and neutral lipid. Dipalmitoylphosphatidylcholine (DPPtdCho) is the major phospholipid component of surfactant responsible for the important surface-tension lowering abilities of lung surfactant: its basic structure is pictured. Surfactant proteins A-D either assist in surface-tension lowering (SP-B, SP-C) or are involved in innate immunity (SP-A, SP-D).

Surfactant Composition

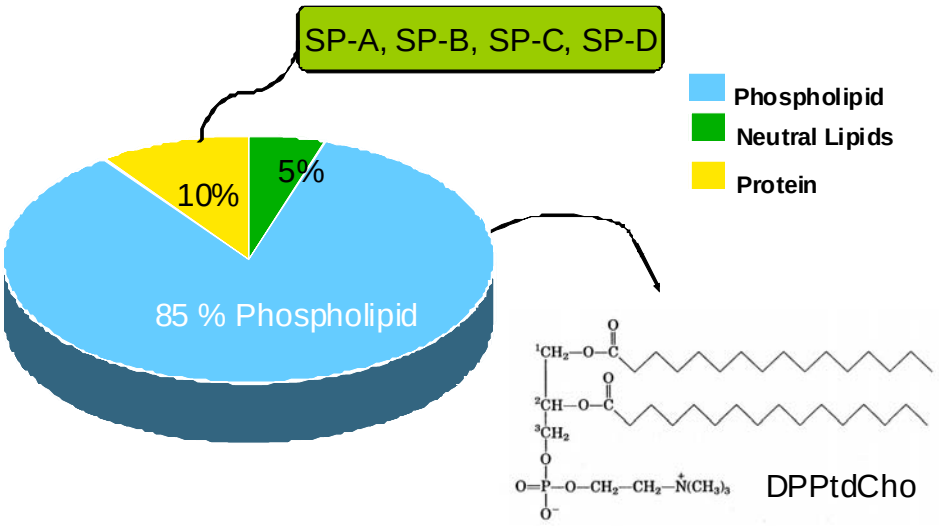

Figure 2. Two main pathways for lung PtdCho synthesis

A diagram of *de novo* PtdCho synthesis. (A) *de novo* PtdCho and (B) remodeling enzyme substrates and products. Both pathways have the potential to produce DPPtdCho. (A) *de novo* PtdCho synthesis involves three major enzymes: (i) choline kinase (CK), (ii) CTP:phosphocholine cytidylyltransferase (CCT), and (iii) cholinephosphotransferase (CPT1). (B) The remodeling pathway involves the re-acylation of a PtdCho degradation product (LysoPtdCho) by acyl-CoA:lysophosphatidylcholine acyltransferase (LPCAT1) for the synthesis of DPPtdCho.

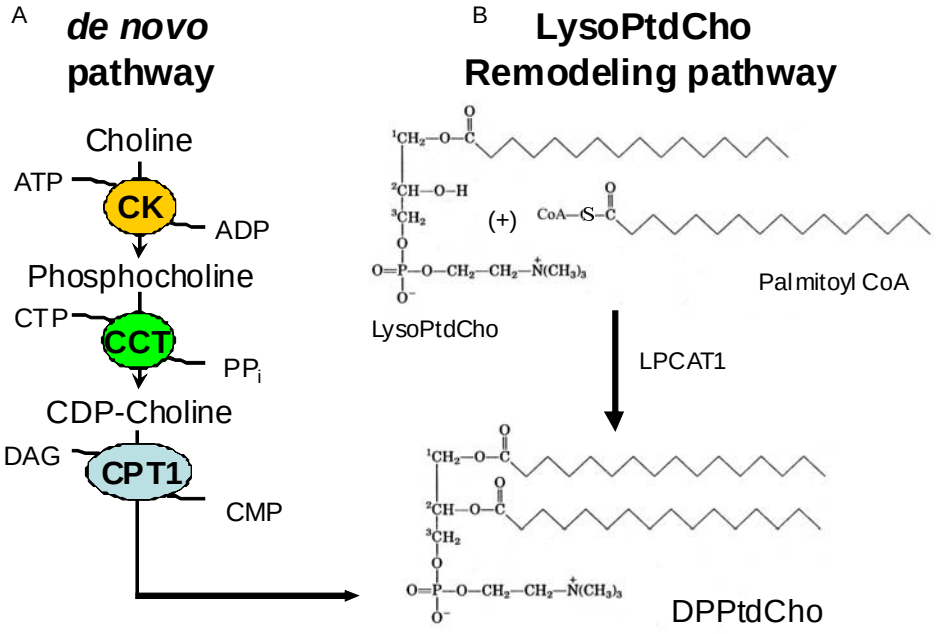
A
de novo pathway
Choline
ATP
CK
ADP
Phosphocholine
CTP
CCT
PPi
CDP-Choline
DAG
CPT1
CMP
B
LysoPtdCho Remodeling pathway
(+)
CoA—S—C
Palmitoyl CoA
LysoPtdCho
LPCAT1
DPPtdCho

CHAPTER II

CROSS-TALK BETWEEN REMODELING AND *DE NOVO* PATHWAYS MAINTAINS PHOSPHOLIPID BALANCE

Abstract

Phosphatidylcholine (PtdCho), the major phospholipid of mammalian membranes, is generated by both remodeling and *de novo* synthesis. Overexpression of the remodeling enzyme, acyl-CoA:lysophosphatidylcholine acyltransferase (LPCAT1) in epithelia decreased *de novo* PtdCho synthesis without significantly altering cellular PtdCho mass. Overexpression of LPCAT1 increased degradation of cholinephosphotransferase (CPT1), a resident Golgi enzyme that catalyzes the terminal step for *de novo* PtdCho synthesis. CPT1 degradation involves trafficking and processing via the lysosomal pathway. Thus, cross-talk between phospholipid remodeling and *de novo* pathways involves possible ubiquitin-lysosomal processing of a key molecular target that mechanistically provides homeostatic control of cellular PtdCho content.

Introduction

Mammalian membranes are enriched with PtdCho, a zwitterionic phospholipid that serves as a major component of various secretory products including bile, high-density lipoproteins, and pulmonary surfactant. With the exception of hepatic tissues where PtdCho synthesis may involve sequential *N*-methylation of phosphatidylethanolamine, PtdCho biosynthesis in mammalian cells occurs primarily via the CDP-choline or the *de novo* pathway. This pathway requires three enzymes: choline kinase (CK) (EC 2.7.1.32) that catalyzes the first committed step, CTP: phosphocholine cytidylyltransferase (CCT) (EC 2.7.7.15), the penultimate enzyme, and cholinephosphotransferase (CPT) (EC 2.7.8.2), which catalyzes the terminal reaction within the CDP-choline pathway generating PtdCho [87]. Of these enzymes, CCT is rate-

limiting and rate-regulatory. CCT is an amphitrophic enzyme, and thus can switch between an inactive soluble or cytoplasmic form to an active, membrane-bound species. There are four isoforms of CCT, and deficiency of a major species, CCTα, is associated with impaired cell growth, apoptosis, and embryonic lethality [87]. CK may also be critical for embryonic development and genomic deletion of the CK gene results in bone deformities and muscular dystrophy[88]. CPT (CPT1) catalyzes the transfer of the phosphocholine moiety from CDP-choline to diacylglycerol (DAG). A second human choline/ethanolaminephosphotransferase (CEPT1) that displays dual specificity using either CDP-choline or CDP-ethanolamine as substrates with significant primary sequence identity to CPT1 may also regulate PtdCho availability [88]. CPT1 exists in the Golgi whereas CEPT1 is detected within the endoplasmic reticulum [88, 89]. The substrate requirements of CPT1 and CEPT1 for DAG would impact the molecular species profile of the newly synthesized PtdCho. Genetic inactivation of CPT genes results in reduced phospholipid synthesis, and its inhibition by isoprenoids and ceramides triggers apoptosis, underscoring CPT as a key regulator of PtdCho synthesis[6-8, 88, 89]. Unlike CCT, there is limited information on the molecular control of CK, CPT1, and CEPT1.

In addition to the CDP-choline pathway, the generation of PtdCho in tissues involves its remodeling. In the lung, this remodeling mechanism constitutes a major route for generation of dipalmitoylphosphatidylcholine (DPPtdCho), the major component of surfactant that lowers alveolar surface-tension [18]. In this pathway, a phospholipase A_2 de-acylates PtdCho at the *sn*-2 position of the glycerol backbone, typically releasing an unsaturated fatty acid. The resultant lysophosphatidylcholine (LysoPtdCho) is then re-acylated with a saturated fatty acid (typically 16:0 or 14:0), generating surfactant DPPtdCho. The de-acylating phospholipase A_2 is a calcium-independent, acid pH optimal lysosomal enzyme [90]. Recently, acyl-CoA:lysophosphatidylcholine acyltransferase (LPCAT1) has been identified as an important enzyme that catalyzes the re-acylation step of the remodeling pathway [10, 11]. A conserved $H(X)_4D$ motif is necessary for

enzymatic activity [19], and LPCAT1 expression increases with lung development and in response to glucocorticoids [10]. LPCAT1 mRNA levels have also been shown to be regulated by keratinocyte growth factor (KGF) in cultured rat type II cells [10]. The biochemical and molecular regulation of LPCAT1 and its role in PtdCho synthesis *in vivo* is largely unknown.

Lung epithelia must tightly balance levels of surfactant (DPPtdCho) lipid secreted into airways versus nonsurfactant PtdCho destined for membranes. While the *de novo* pathway generates both nonsurfactant PtdCho and DPPtdCho, the remodeling pathway would be predicted to synthesize primarily surfactant. Thus, it is possible that cross talk between these pathways exists to modify pulmonary lipid composition depending on cellular needs. In other systems, such interdependency exists between lipogenic pathways. For example, rates of PtdCho synthesis are coupled to its degradation[18, 19, 39]. Overexpression of CCT in COS cells increases PtdCho mass only modestly and yet triggers a 3-fold increase in its degradation rate [91]. This coupling between biosynthetic and degradative pathways indicates close regulation of PtdCho metabolism perhaps as a means to avoid cellular lipotoxicity. Furthermore, overexpression of phosphatidylethanolamine *N*-methyltransferase-2 (PEMT2) in hepatoma cells results in feedback inhibition of CCT by reducing its transcriptional rate without altering PtdCho content [41]. These latter data suggest interdependency between the *N*-methylation and CDP-choline pathways for PtdCho biosynthesis. The relationship between the remodeling and *de novo* pathways for PtdCho synthesis has not been investigated.

Herein, I hypothesized that the remodeling pathway regulates the CDP-choline pathway to maintain PtdCho balance. Overexpression of the remodeling enzyme, LPCAT1, in lung epithelia significantly decreased *de novo* PtdCho synthesis without altering cellular PtdCho levels. LPCAT1 expression increased degradation of the final enzyme within the CDP-choline pathway, CPT1, an enzyme trafficked and processed through the lysosomal for elimination. The data provide new insight into the

interdependency between remodeling and *de novo* pathways to preserve lipid homeostasis.

Results

LPCAT1 is highly expressed in distal lung epithelia

Lung epithelial type II cells synthesize and secrete surfactant comprised of the major surface-active species, DPPtdCho. At least three acyltransferases might participate in remodeling of PtdCho within lung epithelia generating DPPtdCho. These proteins include LPCAT1 and two variants harboring similar catalytic domains, termed LPCAT2 [92] and LPCAT3 [93] (AGPAT7 and LPEAT2); these enzymes exhibit similar substrate requirements with regard to saturated (16:0) fatty acyl-CoA donors, but LPCAT2 and LPCAT3 appear to be less specific with respect to different fatty acyl-CoA groups and lysophospholipids in which they interact [94][92, 95]. To evaluate which species may represent the primary acyltransferase involved in surfactant remodeling, I isolated mouse epithelial type II cells, alveolar macrophages, and lung fibroblasts. *qRT-PCR* shows that LPCAT1 mRNA is highly expressed in surfactant-producing mouse primary type II cells, with markedly reduced expression in macrophages or fibroblasts (Fig. 3A). Lung epithelia also expressed mRNAs encoding LPCAT2 and LPCAT3 albeit at lower levels (Fig 3B,C). Of the three homologues, LPCAT2 expression was highly expressed within macrophages and LPCAT3 was most predominant within fibroblasts (Fig 3B,C) Thus, LPCAT1 appears to be a major regulator of surfactant remodeling, but the data do not exclude redundancy with other related acyltransferases.

Overexpression of LPCAT1 reduces PtdCho de novo synthesis

Because LPCAT1 was highly expressed in surfactant-producing lung cells, this enzyme was cloned and expressed in murine lung epithelia to test its regulatory activity

on PtdCho metabolism. Using Amaxa nucleofection (electroporation), hereon referred to as transfection, I was able to achieve high-level (>90%) transfection efficiency in mammalian epithelia within a strong CMV-driven mammalian expression vector (Adv-CMV-LPCAT1). Following expression of this plasmid, I detected a ~10-fold increase in LPCAT1 mRNA (Fig. 4A), a 28-fold increase in immunoreactive LPCAT1 (Fig. 4B, [inset]), a ~7-fold increase in LPCAT1 activity (Fig. 4B), and a nearly 3-fold increase in [^{3}H]-LysoPtdCho incorporation into DPPtdCho (Fig. 5A). The discrepancy between observed increases in protein and mRNA levels may be due to differences in detection efficiencies of assays employed, altered translational efficiencies of coding mRNAs, or unique post-translational modification rates (e.g. relatively slow turnover rates of immunoreactive LPCAT1 versus turnover of corresponding mRNA) in transfected cells. Differences in LPCAT1 protein levels with respect to observed enzyme activity in transfected cells may be due to limits of substrate availability within the *in vitro* assay, presence of endogenous inhibitors in cells, or presence of a pool of physiologically inactive immunoreactive LPCAT1 in cells. Importantly, despite upregulation of LPCAT1 expression and remodeling activity, total levels of cellular PtdCho and DPPtdCho (Fig. 5B) remained unchanged. This suggests existence of a compensatory feedback mechanism(s) to preserve PtdCho balance. LPCAT1 overexpression also did not alter cellular mass of phosphatidylinositol (PI) or phosphatidylglycerol (PG). Although PtdCho and DPPtdCho remained constant in cellular samples, surfactant secretion increased two-fold in cells overexpressing LPCAT1 (Fig 5C). These data are consistent with the ability of type II epithelia to rapidly mobilize intracellular DPPtdCho for export [96], and suggest a novel mechanism for increased surfactant secretion without alteration of cellular PtdCho mass. Thus, type II cells are readily able to adapt to modest surges in surfactant secretion by multiple homeostatic control mechanisms to maintain steady-state levels of lipid mass.

Next, I tested the hypothesis that LPCAT1 overexpression coordinately down-regulates *de novo* synthesis of PtdCho to maintain steady-state levels of phospholipid mass. This might occur by inhibiting the CDP-choline pathway. LPCAT1 overexpression decreased cellular ^{3}[H]-choline incorporation into PtdCho, a marker of *de novo* synthesis, by nearly 80% versus empty vector transfected cells (Fig. 6A). LPCAT1 overexpression reduced PtdCho synthesis within the CDP-choline pathway in MLE cells by significantly reducing CPT activity without altering activities of either CK or CCT (Fig. 6B-D). These effects were also seen in primary type II cells transduced with lentivirus encoding LPCAT1-V5 (Fig. 7A-B).

I next modulated LPCAT1 expression using non-transfectional approaches to assess physiological relevance. KGF increases type II cell surfactant synthesis by increasing LPCAT1 content [10]. KGF treatment increased LPCAT1 protein levels and cellular LPCAT activity, and also decreased CPT activity in lung epithelia (Fig. 8A-B). In preliminary studies, mechanical ventilation of mice using high tidal volumes also increases immunoreactive LPCAT1 levels concomitant with decreased CPT activity in mouse lung (Fig. 8C). Hyperventilation also increases surfactant production [10, 97, 98]. In the primary type II cell, KGF, and ventilated models, LPCAT1 protein levels increase more modestly: 3.5-fold, 5.7-fold and 4.4-fold, respectively, (and not 28-fold as with MLE cells). This demonstrates that the cross-talk between the remodeling and *de novo* pathways occur at more modest levels of LPCAT1 overexpression consistent with what has been shown for other lipogenic enzymes during development and malignant transformation [99, 100]. Collectively, these observations strongly suggest tight control of PtdCho metabolism in lung epithelia; the data also suggest that remodeling and *de novo* pathways in lung epithelia are physiologically linked and biologically relevant.

LPCAT1 overexpression increases CPT degradation via endosomal/lysosomal processing

To evaluate the mechanism whereby LPCAT1 overexpression reduces CPT activity, I expressed recombinant CPT1 and CEPT1 proteins harboring V5 and/or His tags individually or in combination with LPCAT1 coding plasmid in epithelia. CPT1-V5his and V5-CEPT1 cellular expression resulted in increased CPT activity (Fig. 9A). Co-expression of the CPT1 or CEPT1 recombinant plasmids in cells with LPCAT1 resulted in decreased immunoreactive CPT1 protein levels and no significant difference in immunoreactive CEPT1 levels (Fig 9B,C). LPCAT1 overexpression significantly increased CPT1 and CCT mRNA by qRT-PCR ($p<0.05$ vs. control), but effects on CEPT1 mRNA did not reach significance (Fig. 9D). Although the increase in CPT1 and CCT mRNA levels in LPCAT1 transfected cells was unexpected, it is possible that changes in PtdCho/cholesterol species ratio cause an increase in *de novo* gene transcription mediated by sterol regulatory element binding protein (SREBP) transcription factors [101]. These data suggest that LPCAT1 overexpression selectively enhances CPT1 protein degradation or perhaps regulates translational efficiency of the *de novo* biosynthetic enzymes.

Two major avenues for cellular protein disposal include proteasomal degradation and turnover within the endosomal-lysosomal compartment. To identify a role for these pathways in CPT1 degradation, I impaired acidification of endocytic vesicles with NH_4Cl or inhibited proteasomal degradation with lactacystin after cells were transfected with relevant plasmids. In addition, cells were treated with the protein synthesis inhibitor, cycloheximide (CHM) (18μM medium concentration). Fig. 10A demonstrates that co-transfection of CPT1 with LPCAT1 or inclusion of cycloheximide in the medium reduced immunoreactive levels of CPT1. Compared to cells transfected with CPT1 coding plasmid (control), cells transfected with LPCAT1 coding plasmid alone, or in combination with either CHM or lactacystin resulted in lower levels of CPT1. Unlike

effects observed though the use of lactacystin, inclusion of NH_4Cl in the medium significantly blocked LPCAT1 reduction of CPT1 levels (Fig. 10A), suggesting that LPCAT1 induced degradation of CPT1 may involve CPT1 trafficking through the endosome/lysosome system. Surprisingly, extended lactacystin treatment appears to accelerate degradation of CPT1 when compared to cycloheximide treated controls. This observation may be explained by the ubiquitous nature of the ubiquitin modification of proteins within cells. Thus, it is possible that ubiquitin availability within cells has been globally disrupted, upregulating expression of proteins that normally reduce CPT1 levels; alternatively, it is possible that lactacystin treatment modulates expression of transcriptional elements that normally destabilize CPT1 mRNA synthesis in MLE cells [77]. Finally, plasmid co-transfection or NH_4Cl was not toxic to cells (Fig. 10B).

CPT accumulates within lysosomes

To further assess CPT1 degradation involving lysosomal trafficking, I examined CFP-CPT1 subcellular localization in epithelia. Immunofluorescence studies involving expression of plasmid coding for CFP-CPT1 revealed co-localization of CFP-CPT1 with β-1, 3-galactosyltransferase 2 (αβ-GT antibody), indicative of CPT1 localization within the Golgi apparatus (Fig 11A, upper row). As MLE cells are a transformed cell line, cells contained Golgi as represented by larger inclusions rather than by more classic perinuclear labeling as seen with other mammalian cells. When plasmid coding for CFP-CPT1 was co-transfected with a plasmid encoding a fragment of another Golgi resident enzyme, YFP-UDP-gal: β GlcNAc β 1,4-galactosyltransferase (βGT- YFP), the fusion proteins also co-localized (Fig. 11A, lower row). To complement Golgi localization data, cells were once again transfected with CFP-CPT1 and βGT-YFP coding plasmids. After 18 h cells were treated with 20μM nocodazole (microtubule polymerization inhibitor which disrupts Golgi integrity) (Fig. 12 lower) or DMSO vehicle control (Fig. 12 upper) for 4 h and cells were processed for imaging using confocal microscopy. Left panels

show CFP signals, middle panels represent YFP signals, and right panels represent a merged image of YFP and CFP signals.

I also used Lyso-tracker Red, which fluoresces within the acidic pH compartments to examine CPT1 trafficking within lysosome compartments (Fig. 11B). Unlike data from Fig. 11A where CFP-CPT1 co-localizes with β-GT, CFP-CPT1 under native conditions does not appear to significantly co-localize with Lyso-tracker Red. Co-transfection of CFP-CPT1 with LPCAT1 coding plasmids also results in limited CFP-CPT1 immunofluorescence within cells (Fig. 11B, second row). Importantly, only when NH_4Cl was used to impair late endosome/lysosomal function (with or without LPCAT1 transfection) did I detect increased CFP-CPT1 immunofluorescence that co-localized with Lyso-tracker Red (Fig. 11B, lower rows) and the endosomal marker, Rab5 using similar experimental conditions (Fig. 13). CFP-CPT1 co-localization with Lyso-tracker was apparent by small punctate yellow cytosolic signals (arrows). In some cases the visualized lysosomes appear atypical, suggesting that two hours may be an insufficient recovery time following NH_4Cl treatment to allow endocytic compartment reformation. However, it is possible there is a delicate balance between allowing cells to fully re-establish the endocytic pathway (pH) and being able to capture images in the compromised pathway. Thus, if full lysosomal function is restored images would likely resemble conditions lacking NH_4Cl to begin with (Fig. 11B top rows). Together, these data are consistent with LPCAT1–induced CPT1 sorting through the endosomal/lysosomal pathway for its degradation.

Effects of a catalytically-inactive LPCAT1, LPCAT2 and LPCAT3 on CPT1

To further determine the cause of CPT1 degradation, I overexpressed two catalytically inactive LPCAT1 mutants that contain amino acid substitutions at histadine 135 (asparagine or glutamine) to determine if LPCAT activity is required for degradation.

MLE cells were transfected with an empty plasmid, or co-transfected with CPT1-V5his in combination with LPCAT1, LPCAT1 H135N, or LPCAT1 H135Q coding plasmids. Following transfection, after 18 h, cells were labeled with ^{3}[H] choline for 2 h and harvested. Cell lysates were processed for choline incorporation into PtdCho (phospholipid analysis) (Fig. 14A). Cells were also transfected as above and cell lysates were collected at 18 h and lysates were separated by SDS-PAGE, transferred to nitrocellulose, and V5 and β-actin immunoblot analyses were performed (Fig. 14B). Importantly, unlike LPCAT1, the catalytically inactive LPCAT1 mutants fail to reduce *de novo* PtdCho synthesis or CPT1 protein levels.

As acyltransferase activity appears to be necessary for the ability of LPCAT1 to reduce *de novo* PtdCho synthesis and CPT1 protein levels. I next assessed the ability of the closely related LPCAT2 and LPCAT3 to alter PtdCho synthesis and CPT1 protein levels. First, plasmid coding for LPCAT1-V5his, LPCAT2-V5his and LPCAT3-V5his were constructed. Next, MLE cells were transfected with plasmid(s) coding for empty (E), LPCAT2-V5his (L2), LPCAT3-V5his (L3), CPT1 (C), CPT1+Empty (C+E), CPT1+LPCAT2-V5his (C+L2), or CPT1+LPCAT3-V5his (C+L3). Cell lysates were then harvested, protein separated by SDS-PAGE, transferred to nitrocellulose, and V5 and β-actin immunoblot analyses were performed (Fig. 15A-B upper). Densitometry was performed on CPT1 immunoreactive bands and normalized for β-actin (Fig. 15A-B Lower). Later, LPCAT1-V5his, LPCAT2-V5his and LPCAT3-V5his coding plasmids were expressed in cells and after 18 h cell lysates were separated by SDS-PAGE, transferred to nitrocellulose, and V5 immunoblot analysis was performed (Fig. 15C) or cells labeled for 2 h with ^{3}[H] choline under similar transfection conditions as listed above and cell lysates were used to measure *de novo* synthesis (Fig. 15D). Data suggest that overexpression of LPCAT1 but not LPCAT2 or LPCAT3 reduce *de novo* PtdCho synthesis and CPT1 protein levels. Taken together, it appears that LPCAT1 activity is specific in its ability to reduce *de novo* synthesis by reduction of CPT1 protein levels.

LPCAT1 knockdown regulates de novo PC synthesis

I next wanted to determine the effect of LPCAT1 knockdown on *de novo* PtdCho synthesis. LPCAT1 siRNA was packaged into a viral expression system, hemagglutinizing virus of Japan (HJV). Then, primary rat type II cells were cultured and incubated with empty or LPCAT1 containing virus for 72 h prior to collection. Once the infected cells were harvested, lysates were separated by SDS-PAGE, transferred to nitrocellulose and LPCAT1 and β-actin immunoblot analyses were performed confirming LPCAT1 protein reduction with LPCAT1 siRNA transfection (Fig. 16A [inset]). Following immunoblot analysis, LPCAT (Fig. 16A), CPT (Fig.16B), and CCT (Fig. 16C) activity assays were performed on cell lysates. Interestingly, these data indicate that LPCAT1 inhibition of *de novo* PtdCho synthesis may be more complex and perhaps multidirectional as RNA silencing of LPCAT1 significantly decreased CPT activity. A similar observation was made by Kimbrel and colleagues when studying the effects of overexpression and knockdown of an E3 ubiquitin ligase, β-TrCP, on protein levels of the p300 transcription factor [102].

Discussion

Surfactant PtdCho is relatively unique because it is selectively enriched with 16:0/16:0 molecular species (DPPtdCho) on the phospholipid glycerol backbone. This molecular species specificity is essential to optimize surfactant function and is conferred, in part, by a constitutively active LPCAT1 enzyme within lung epithelia. Indeed, perhaps ~55-75% of surfactant PtdCho is synthesized by the remodeling pathway with the remainder generated by *de novo* synthesis [10, 103, 104]. These results suggest that when LPCAT1 levels are increased, as occurs during alveolar stress when demands for surfactant (DPPtdCho) are high, lung epithelia might coordinately reduce *de novo* synthesis of PtdCho by increasing CPT1 degradation through the lysosomal pathway. This cellular mechanism may be favorable to shift the balance toward DPPtdCho

enrichment for surfactant secretion into the airways via LPCAT1-remodeling given that the CDP-choline pathway is also active in membrane (non-surfactant) phospholipid biosynthesis. Thus, our results unveil a previously unrecognized molecular mechanism for feedback control for PtdCho homeostasis.

Comparative analysis of LPCAT mRNAs revealed differential expression of three related acyl-CoA LysoPtdCho acyltransferases that may exhibit synthetic capacity for DPPtdCho. LPCAT1 was a primary candidate based on prior data showing high-level pulmonary expression and preference for saturated (16:0) fatty acids as a donor and 1-myristoyl or 1-palmitoyl-LPtdCho as an acceptor[15, 16]. LPCAT2 and LPCAT3 (AGPAT7 and LPEAT2) also contain similar conserved motifs including acyltransferase, transmembrane, and EF-hand domains [105]. My observations that LPCAT1 mRNA was highest in type II epithelia versus macrophages or fibroblasts underscore its role as a primary regulator of PtdCho remodeling. Confirmation awaits analysis of individual endogenous LPCAT proteins, although unlike LPCAT1, overexpression of either LPCAT2 or LPCAT3 appear to have no effect on CPT1 protein levels (Fig. 15). There may be redundancy in this system because type II epithelia also express modest levels of LPCAT2/LPCAT3 (Fig. 3); their contribution to surfactant remodeling will require more sophisticated *in vivo* genetic ablation systems.

Multiple mechanisms exist that maintain stable steady-state total cellular PtdCho mass despite its reduced *de novo* synthesis and increased surfactant secretion after LPCAT1 expression (Fig. 5A-C). I observed a robust increase (~3-fold) in remodeling activity by LPCAT1 (Fig. 4B). Although LPCAT1 is involved in surfactant synthesis, the enzyme also exhibits some promiscuity with significant substrate activity for other unsaturated fatty acyl species such as oleoyl (C18:1), linoleoyl (C18:2) and alpha-linolenoyl-CoA (C18:3) that may be destined for incorporation into the cell membrane [16]. This would explain, in part, our observation that total cell PtdCho levels are relatively unchanged after LPCAT1 overexpression. Second, type II cells may exploit

other compensatory mechanisms to maintain constant levels of cellular PtdCho including reduced phospholipid degradation rates or increased PtdCho uptake. Overexpression of some biosynthetic lipogenic enzymes reduces degradation rates [91]. Up to 50-85% of secreted PtdCho can be taken up and re-utilized [88]. As the actual mass of lipid secreted by type II epithelia is only 1-2% of total cellular phospholipid per hour, type II cells have significant reserves of intracellular lipid that can offset abrupt alterations in synthetic or secretory rates [96]. Therefore, even a doubling of surfactant secretion as was observed in Figure 5 may not significantly alter lipid homeostasis in lung epithelia over the time period utilized in my experiments. LPCAT1 inhibition of *de novo* PtdCho synthesis may be multidirectional as RNA silencing of LPCAT1 only slightly, but significantly, decreased CPT activity, suggesting a more complex mode of regulation (Fig. 16). Interestingly, LPCAT1-dependent degradation of CPT1 requires an active LPCAT1 enzyme indicating the possibility of a yet unidentified step associated with CPT1 regulation (Fig. 14). Nonetheless, transfection of LPCAT1 coding plasmid in lung epithelia resulted in its robust expression coupled with increases in DPPtdCho synthesis, yet did not alter total cellular phospholipid mass suggestive of feedback inhibition within the *de novo* pathway.

Genetic inactivation of CPT1 and CEPT1 impairs *de novo* PtdCho synthesis in *S. cerevisiae*, but their biochemical and molecular characterization has been hampered because these mammalian enzymes have not been purified to homogeneity [6]. Thus, I transfected cells with plasmids encoding CPT1-V5his and the expressed CPT1-V5his protein was functional and localized to the Golgi [88]. The Golgi pattern in MLE cells was somewhat atypical but CFP-CPT1 was observed to co-localize with known markers, even in the presence of nocodazole treatment which is known to disrupt Golgi integrity by binding β-tubulin and preventing formation of one of the two disulfide linkages, hence, inhibiting microtubule polymerization [106, 107].

Experimental procedures

Materials

The source of murine lung epithelial (MLE) cells, culture medium, immunoblotting materials and radiochemicals were described previously [8]. Rat primary alveolar type II epithelia were isolated as described [54]. The pAmCyan1-C1 and pZsYellow-C1 vector was purchased from Clontech (Mountain view, CA). Lyso-Tracker Red, mouse monoclonal V5 antibody, the To-Pro-3 nuclear staining kit, the PCRTOPO4.1 cloning kit, pcDNA-DEST40, pcDNA3.1/nV5-DEST, pLenti6/V5-Dest cloning vectors, *E. coli* One Shot competent cells, the pENTR Directional TOPO cloning kits, LR clonase II recombinase, Superscript III RT kit, and the Gateway mammalian expression system were purchased from Invitrogen (Carlsbad, CA). Ni^{2+} resin, HIS-select Nickel Affinity gel, Tri Reagent, human KGF, and β-actin primary mouse monoclonal antibody were obtained from Sigma (St. Louis, MO). LPCAT1 antibody was generated by Covance (Princeton, NJ). Amicon Ultra-4 centrifugal filter devices were from Millipore (Billerica, MA). The QuickChange site-directed mutagenesis kit, XL-gold cells, and pCMV-Tag1 vector were from Stratagene (La Jolla, CA). A ubiquitin plasmid was constructed as described [108]. The gel extraction kit and QIAprep Spin Miniprep kits were from Qiagen (Valencia, CA). NucleoBond Xtra Maxi prep kits were obtained from Macherey-Nagel (Bethlehem, PA). Cycloheximide (CHM) and UbiQapture-Q matrix was from Biomol (Plymouth Meeting, PA). HA-tagged ubiquitin was a gift from Dr. Peter Snyder (U. of Iowa). β-1,3-galactosyltransferase 2 goat polyclonal primary antibody was purchased from Santa Cruz Biotechnology (Santa Cruz, CA). Power CYBR Green PCR master mix was from Applied Biosystems (Carlsbad, California). All restriction enzymes and ligases were purchased from New England Biolabs (Ipswich, MA). The TNT-coupled reticulocyte lysate system and RQ1 DNase kit were purchased from Promega (Madison, WI). All DNA sequencing was performed by the University of Iowa DNA Core Facility. Cloning primers were purchased from IDT (Coralville, IA).

The Zeiss LSM 510 confocal microscope is part of the University of Iowa Central Microscopy Research Facility.

qRT-PCR

RNA was purified from primary murine lung cells [99]. Total cellular RNA was isolated using Tri Reagent and cDNA was obtained by reverse transcription followed by DNase I digestion, amplification, and detection by a Chromo 4 Real-Time PCR detector [100]. Levels of transcripts were measured and normalized relative to GAPDH or 18S mRNA.

Expression plasmids

The coding sequence available for LPCAT1, CPT1 and CEPT1 on the NCBI website (NM_145376, NM_144807, NM_133869), were used to construct primers for cloning of genes from cDNA from mRNA via reverse transcriptase PCR from murine liver and kidney tissues. Amplified fragments were subcloned into PCRTOPO4.1, and sequenced, where it was identical to the deposited NCBI LPCAT1 sequence. The resulting PCRTOPO4.1 vector served as a source for cloning into pacAd5 CMV IRES eGFP pA, (University of Iowa DNA core) using ClaI and BamHI restriction sites. For CPT1 and CEPT1, the Invitrogen® Gateway System was used. Primers constructed containing CACC overhangs upstream of the 5' ATG and antisense sequence with (V5-CEPT1) or without (CPT1-V5his) a stop codon were used for amplification using a blunt-end polymerase and pENTR/D-TOPO per manufacturers' instruction. LR clonase II recombinase was used for cloning of CPT1 and CEPT1 sequences into pcDNA-DEST40 or pcDNA3.1/nV5-DEST gateway vectors, respectively (CPT1-V5his, V5-CEPT1). CFP-CPT1 was generated similar to CFP-CCT [100]. The CPT1 construct $CPT1_{K6R}$ was digested with BgIII and SalI, purified, and ligated into pAmCyan-C1 as described generating CFP-$CPT1_{K6R}$ [108]. Flag-CPT1 was constructed by amplifying CPT1 and

ligation into pCMV-Tag1. A βGT-YFP (carboxyl-terminal YFP tag) plasmid was constructed by amplifying or digesting three separate fragments for ligation. First, a human cDNA was used as a template to amplify the first 249 base pairs of UDP-Gal: βGlcNAc β-1,4-galactosyltransferase gene (B4GALT1) (gene bank number BC045773) with flanking ClaI/EcoRV restriction sites. Fragment two was an EcoRV/EcoRI YFP fragment amplified from pZsYellow-C1. Finally, a pacAd5 CMV IRES eGFP pA vector and the two amplified fragments were digested with appropriate restriction enzymes and gel extracted. The B4GALT1 and YFP fragments were ligated into pacAd5 CMV IRES eGFP pA to generate βGT-YFP.

Cell isolation, culture, and transient transfection

Alveolar macrophages, primary type II cells, and fibroblasts were isolated as previously described [109]. MLE cells were maintained in HITES medium (DMEM F12) with 2% fetal bovine serum at 37^{o}C in 5% CO_2. After reaching 80% confluency, the cells were harvested using 0.25% trypsin and 0.1% EDTA, resuspended in medium, and plated onto appropriate culture dishes containing a 3ul per 1ug DNA ratio of FuGENE6 lipofection reagent to appropriate expression vector. After incubation overnight, the medium was replaced with HITES medium with 2% fetal bovine serum for 8 h before harvesting cells. In some studies, an Amaxa electroporation device with program T-013 and solution L was used for plasmid transfection of cells. Cells were maintained as described above, except, after trypsinization, cells were resuspended in a small volume of solution L per manufacturer's directions. Plasmids were transfected into cells or cells were left untransfected. Medium was aspirated 24 h post-transfection and cells were treated an additional 24 h with 0% FBS DMEM F12 medium supplemented with or without NH_4Cl (25 mM). Cell lysates were harvested by brief sonication in 150 mM NaCl, 50 mM Tris-HCl, 1 mm EDTA (no EDTA if Ni^{2+} purification was performed), 2 mM dithiotreitol, 0.025% sodium azide, and 1 mM phenylmethylsulfonyl fluoride (pH

7.4) (Buffer A), at 4°C. Alternatively, cells were switched to DMEM F12 media without FBS and treated for 6 h with cycloheximide (CHM) (18 ug/mL) with either NH_4Cl (25 mM) or lactacystin (25 uM). Cells were collected in Buffer A + 0.5% Triton X-100 +0.5% NP-40 and sonicated for further analysis. MLE cells were also exposed to human KGF (20ng/mL) for 24 h prior to harvest. Rat type II cells were transduced for 48 h with lentivirus, constructed at the University of Iowa gene transfer vector core, containing LPCAT1 in a pLenti6/V5-Dest vector.

Phospholipid analysis

Lipids were extracted from equal amounts of membrane protein and levels of the individual phospholipids quantitated with a phosphorus assay [103]. DPPtdCho was assayed as before[8]. For PtdCho *de novo* synthesis, cells were pulsed with 1 µCi of [*methyl*-^{3}H]choline chloride (85 Ci/mmol) during the final 2 h of incubation with choline-depleted medium. For remodeling activity, cells were labeled with 1.75 nM of [^{14}C] LysoPtdCho (55mCi/mmol) for 3 h. Total cellular lipids were extracted, resolved using thin layer chromatography (TLC), and processed for scintillation counting [8].

LPCAT activity

Cells were harvested in lysis buffer (250mM sucrose, 10mM Tris-HCl at pH=7.4), and equal amounts of microsomal cellular protein or cell lysate were used in the assay. One nmole of 1-palmitoyl-*sn*-glycero-3-phosphocholine was added for every µL of 5x assay buffer (final working concentration 65mM Tris-HCl, pH 7.4, 10mM $MgCl_2$, 12.5 mM fatty acid free BSA, 2mM EDTA) sonicated. 35 µL of H_2O and cellular protein was added to 10 µL sonicated assay buffer containing 5 µL of [1-^{14}C]acyl-CoA (0.1µCi, 1.8nmole) for a total assay volume of 50 µL. Upon addition of [1-^{14}C] acyl-CoA, samples were incubated at 30^{o}C for 10 min, after which the reaction was terminated by addition of chloroform/methanol/H_2O (1:2:0.70 vol/vol). Total cellular lipids from

reaction mixtures were extracted by the method of Bligh and Dyer [104], spotted on LK5D plates, and PtdCho was resolved using TLC and detected using a Bioscan AR-2000 scintillation plate reader.

KGF treatment of MLE cells

MLE cells were treated with HITES medium or with medium containing 20ng/mL KGF. Twenty-four hours after treatment cells were harvested and cell lysates were used for LPCAT and CPT activity assays. Cell lysates were also separated by SDS-PAGE, transferred to nitrocellulose, and LPCAT1 and β-actin immunoblot analyses were performed

Mechanical ventilation of mice

C57B1 mice were mechanically ventilated with a tidal volume of 20mL/Kg for 15 min or were left unventilated. After 18 h mice were anesthetized, sacrificed, lungs harvested, and heart perfused to remove red blood cells. Lungs were then homogenized in Buffer A and lysates were separated by SDS-PAGE, transferred to nitrocellulose, and LPCAT1 and β-actin immunoblot analyses were performed. Cell homogenates were also used in CPT activity assays.

De novo enzyme activities

The activity of CK was assayed as described [8]. CCT activity was determined by using a charcoal extraction method [110]. CPT activity was assayed as described [111]. Each reaction mixture contained 50 mM Tris ·HCl buffer (pH 8.2), 0.1 mg/ml Tween 20, 1 mM 1,2-dioleoylglycerol, 0.8 mM phosphatidylglycerol, 0.5mM [^{14}C]-CDP-choline (specific activity 1,110 dpm/nmol), 5 mM dithiothreitol, 5 mM EDTA, 10mM $MgCl_2$, and 30–40 μg of protein. The lipid substrate was prepared by combining appropriate amounts of 1,2-dioleoylglycerol (1 mM) and phosphatidylglycerol (0.8 mM) in a test

tube, drying under nitrogen gas, and brief sonication before addition to the assay mixture to achieve the final desired concentration. The reaction proceeded for 1h at 37°C and terminated with 4 ml of methanol-chloroform-water (2:1:7, vol/vol). The remainder of the assay was performed exactly as described [111]. A Bioscan AR-2000 plate reader was used for detection of radiolabeled PtdCho on LK5D TLC plates with data quantified using WinScan software. PtdCho bands on the LK5D silica plates were also scraped and quantified by liquid scintillation counting.

Immunoblot analysis

Immunoblotting was performed as described [100, 112]. Antibodies were diluted as follows: LPCAT1 1:2000, V5 1:2000, Flag 1:5000, and
β-actin 1:10000.

Immunofluorescence microscopy

MLE cells were plated at 30% confluence on 35mm MetTek glass-bottom culture dishes, and transfected with individual CFP plasmids. Cells were washed with PBS and fixed with 4% paraformaldehyde for 20min, then exposed to 15% BSA, 1:200 β-1, 3-galactosyltransferase 2 primary goat antibody and 1:200 Fluorescein (FITC)-conjugated AffiniPure Donkey anti-goat IgG (H+L) (Jackson Immunoresearch) to visualize the trans-Golgi; cells were also incubated with Rab5 rabbit primary antibody and Alexa568-labeled goat anti-rabbit secondary antibody to visualize the early endosomal compartments. Nuclei were visualized using To-Pro-3 (1:2000, dilution). Immunofluorescent cell imaging was performed on a Zeiss LSM 510 confocal microscope using the 458nm, 568nm or 615nm wavelength. All experiments were done with a Zeiss x63 or x100 oil differential interference contrast objective lens. The 458nm wavelength was used to excite the CFP-CPT1 fusion proteins, with fluorescence emission collected through a 475nm filter. A 488nm wavelength was used to excite Fluorescein

dye, with fluorescence emission collected through a 505-530nm filter. A 488nm wavelength was used to excite βGT-YFP, with fluorescence emission collected through a 530-600nm filter. A 613nm wavelength was used to excite To-Pro-3 dye, with fluorescence emission collected through a 633nm filter. Scanning was bidirectional at the highest possible rate measurement using a digital 1X zoom.

Statistical analysis

Statistical analysis was performed by two-way analysis of variance or Student's *t* test. Data are presented as mean ± S.E or mean ± S.D.

Figure 3. Pulmonary expression of LPCAT isoforms

Primary murine lung type II cells, alveolar macrophages, and fibroblasts were isolated and total cellular RNA reversed transcribed to cDNA for quantitative Real Time PCR (qRT-PCR). The mRNA levels of each LPCAT were measured and normalized to GAPDH mRNA. The data represent cells isolated from at least five mice/group. *$p<0.05$ versus type II cells.

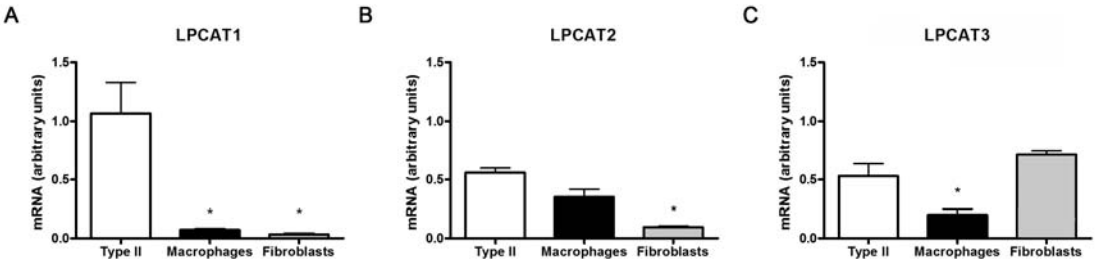
A
LPCAT1
mRNA (arbitrary units)
1.5
1.0
0.5
0.0
*
*
Type II
Macrophages
Fibroblasts
B
LPCAT2
mRNA (arbitrary units)
1.5
1.0
0.5
0.0
*
Type II
Macrophages
Fibroblasts
C
LPCAT3
mRNA (arbitrary units)
1.5
1.0
0.5
0.0
*
Type II
Macrophages
Fibroblasts

Figure 4. LPCAT1 expression and activity in MLE cells

MLE cells were transfected with a plasmid encoding LPCAT1 or an empty (E) vector. After 24h, cells were collected and lysates were used in (A) the quantitation of LPCAT1 mRNA (measured and normalized relative to S18 mRNA) by qRT-PCR, or (B) cell lysates where separated by SDS-PAGE, transferred to nitrocellulose, and LPCAT1 and β-actin immunoblot analyses were performed (B [inset]), or cell lysates were use for LPCAT1 enzyme activity assays (B).

A

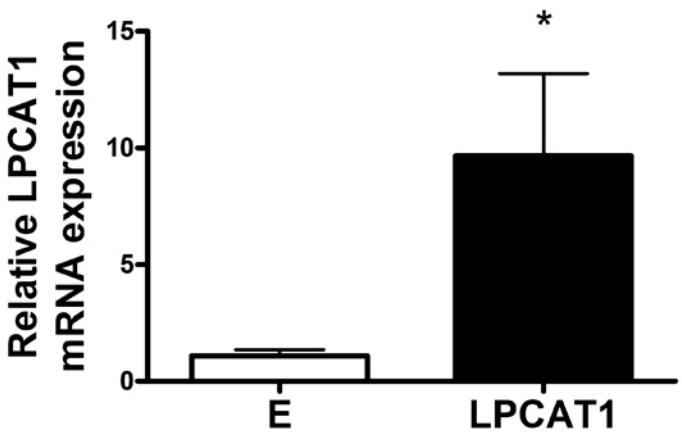
Relative LPCAT1 mRNA expression
15
10
5
0
*
E
LPCAT1

B

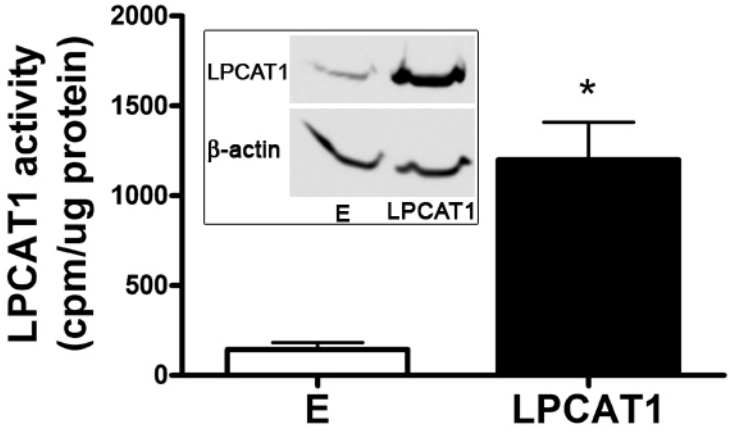
LPCAT1 activity (cpm/ug protein)
2000
1500
1000
500
0
LPCAT1
β-actin
E
LPCAT1
*
E
LPCAT1

Figure 5. LPCAT1 expression regulates surfactant metabolism

MLE cells were transfected with a plasmid encoding LPCAT1 or an empty (E) vector. After 24h, cells were (A) labeled with [^{14}C] LysoPtdCho for 3 h prior to collection. DPPtdCho lipid was isolated by thin layer chromatography (TLC) and the resolved radio labeled phospholipid was isolated from plates, and counted using liquid scintillation. (B) Cells were transfected as above and lipid extraction and TLC analysis were performed to isolate PtdCho, DPPtdCho, PI, and PG. Phospholipid mass was measured by inorganic $P0_4^{3-}$ determination. (A-B) were normalized for cellular protein. (C) Surfactant secretion was measured by ^{3}[H] palmitic acid labeling of cells. Activities were assayed in medium by lipid extraction of medium and isolation by TLC as above. Data is expressed as cpm medium/ml/total cellular DPPtdCho phospholipid phosphorus/mg protein. Results are mean ± S.E. from at least three individual. *$p<0.05$ or ^$p<0.076$ versus empty construct.

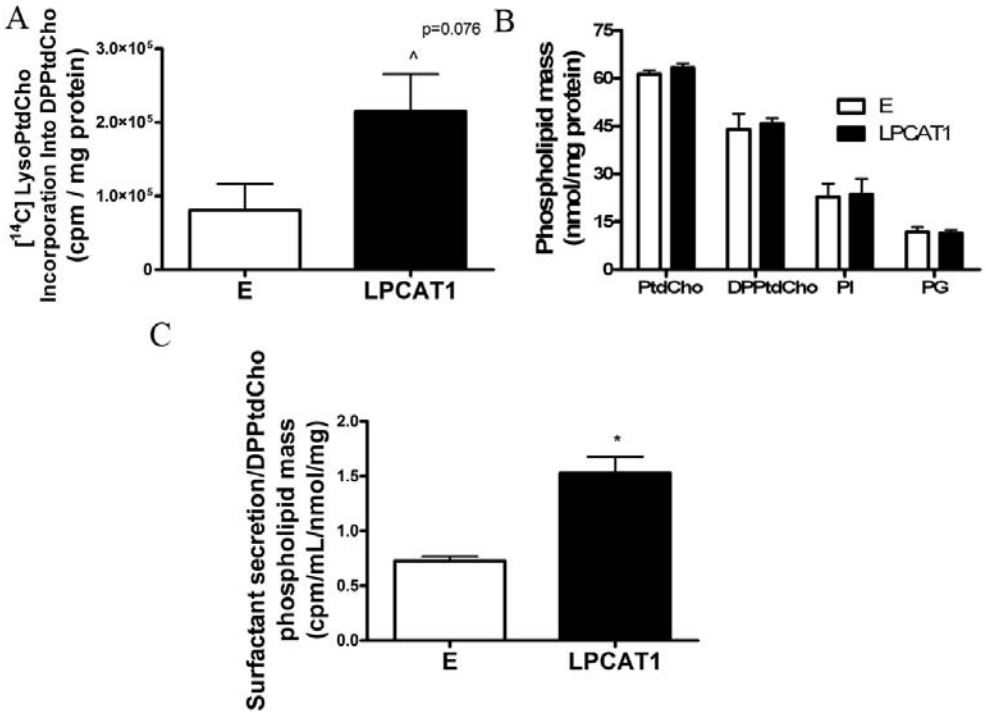
A
[14C] LysoPtdCho Incorporation Into DPPtdCho (cpm / mg protein)
3.0×10^5
2.0×10^5
1.0×10^5
0
p=0.076
^
E
LPCAT1
B
Phospholipid mass (nmol/mg protein)
75
60
45
30
15
0
E
LPCAT1
PtdCho
DPPtdCho
PI
PG
C
Surfactant secretion/DPPtdCho phospholipid mass (cpm/mL/nmol/mg)
2.0
1.5
1.0
0.5
0.0
*
E
LPCAT1

Figure 6. LPCAT1 expression inhibits the *de novo* (CDP-choline) pathway

MLE cells were transfected with a plasmid encoding LPCAT1 or an empty (E) plasmid. (A) Cells were labeled with ^{3}[H] choline and after 2 h cells were harvested. Lipids from lysates were extracted prior to resolution using TLC. PtdCho was isolated from TLC plates and activity counted using liquid scintillation. ^{3}[H] choline into PtdCho is a measure of *de novo* synthesis. (B) Cell lysates were used for determination of CK, (C) CCT, and (D) CPT activity assays. Results are mean ± S.E. from at least three individual experiments. *$p<0.05$ versus empty construct.

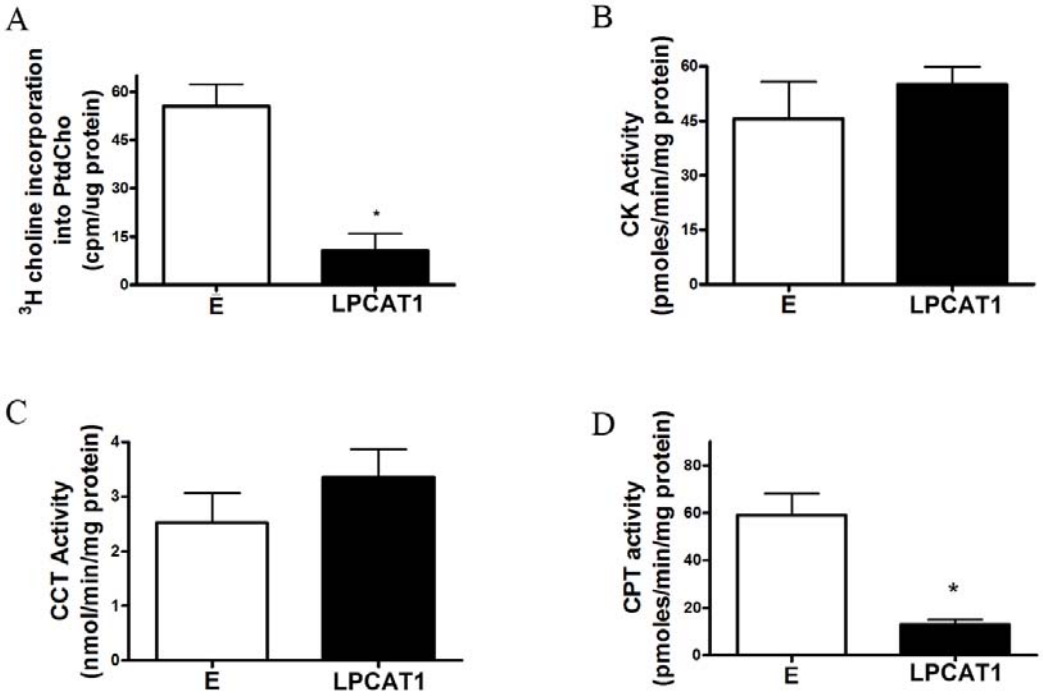
A
^{3}H choline incorporation into PtdCho (cpm/ug protein)
60
45
30
15
0
*
E
LPCAT1
B
CK Activity (pmoles/min/mg protein)
60
45
30
15
0
E
LPCAT1
C
CCT Activity (nmol/min/mg protein)
4
3
2
1
0
E
LPCAT1
D
CPT activity (pmoles/min/mg protein)
80
60
40
20
0
*
E
LPCAT1

Figure 7. LPCAT1 expression in primary type II cells inhibits the *de novo* (CDP-choline) pathway

(A-B) Primary rat type II cells were isolated, cultured, and infected with a plasmid construct encoding LPCAT1-V5 packaged in lentivirus. (A) 24 h after infection cells were labeled with ^{3}[H] choline for 2 h prior to cell harvest for the measure ^{3}[H] choline incorporation into PtdCho (the *de novo* PtdCho activity assay). Cell lysates were also separated by SDS-PAGE, transferred to nitrocellulose, and V5 and LPCAT1 immunoblot analyses were performed (B [inset]), cell lysates were used in CPT1 activity assays (B). Results are from at least three individual experiments and mean ± S.E. was calculated when appropriate. *$p<0.05$ versus empty construct.

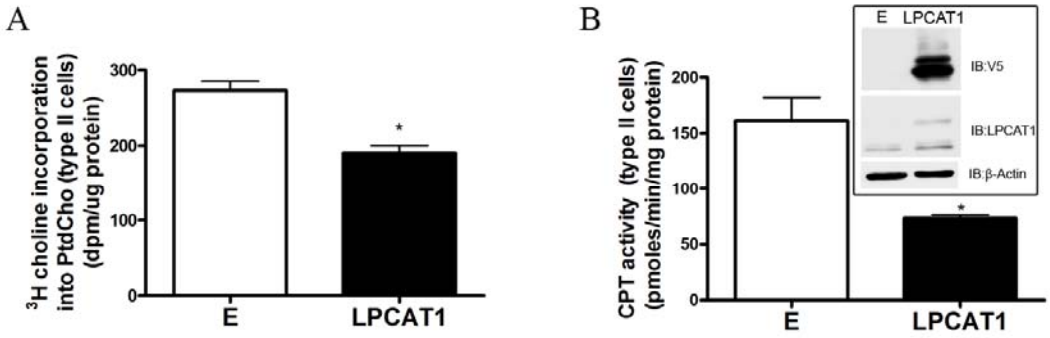
A
^{3}H choline incorporation into PtdCho (type II cells) (dpm/ug protein)
300
200
100
0
*
E
LPCAT1
B
CPT activity (type II cells) (pmoles/min/mg protein)
200
150
100
50
0
E
LPCAT1
E LPCAT1
IB:V5
IB:LPCAT1
IB:β-Actin
*
E
LPCAT1

Figure 8. Physiologic factors that increase LPCAT1 levels reduce CPT activity

(A-B) Cells were left untreated or treated with KGF (20ng/mL) and 24 h post-treatment cells were harvested and cell lysates were separated by SDS-PAGE, transferred to nitrocellulose, and LPCAT1 immunoblot analyses were performed (A [inset]) and cell lysates were used in LPCAT activity assays (A). (B) Cell lysates were also used in CPT activity assays. (C) C57Bl/6 mice (3 mice/group) were ventilated with a tidal volume of 20mL/Kg for 15 min or were left unventilated (control). Following an 18 h recovery, lung homogenates were immediately separated by SDS-PAGE, transferred to nitrocellulose, and LPCAT1and β-actin immunoblot analyses were performed (A [inset]) or cell homogenates were used in CPT activity assays (B). Results are from at least three individual experiments and mean ± S.E. was calculated when appropriate. *$p<0.05$ versus empty construct.

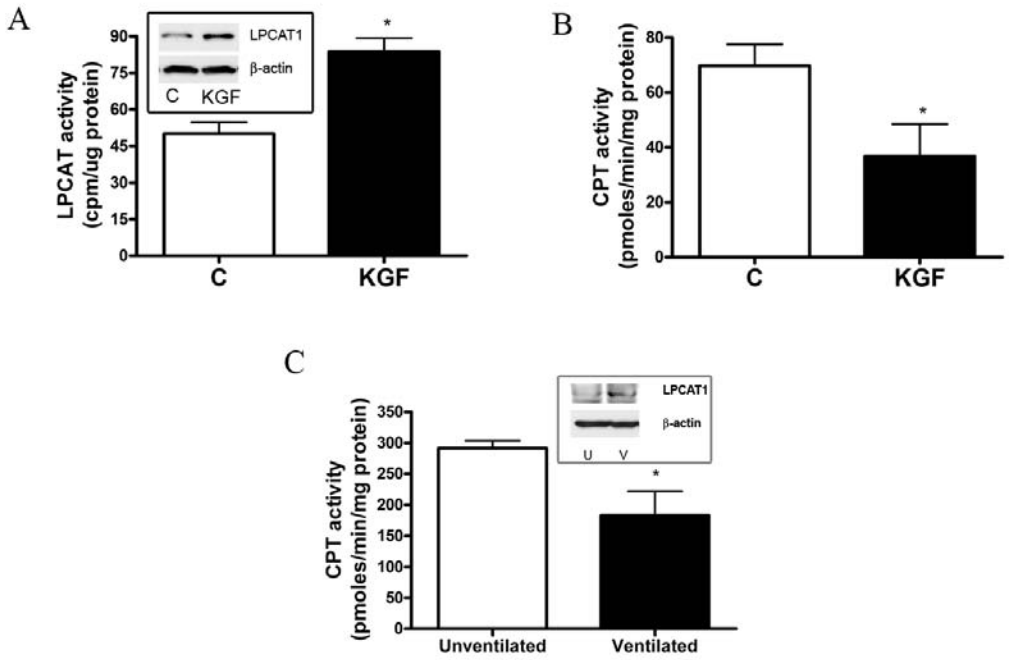
A
LPCAT activity (cpm/ug protein)
90
75
60
45
30
15
0
LPCAT1
β-actin
C KGF
*
C
KGF
B
CPT activity (pmoles/min/mg protein)
80
60
40
20
0
*
C
KGF
C
CPT activity (pmoles/min/mg protein)
350
300
250
200
150
100
50
0
LPCAT1
β-actin
U V
*
Unventilated
Ventilated

Figure 9. LPCAT1 expression promotes CPT1 degradation

(A) MLE cells were transfected with empty, CPT1 or CEPT1 coding plasmids and cell lysates were used in CPT activity assays. (B) Cells were transfected with empty (E), LPCAT1 (L), CPT1 (C) coding plasmids alone or in combination with empty or LPCAT1 coding plasmids and after 16 h cell lysates were separated by SDS-PAGE, transferred to nitrocellulose, and CPT1 (V5), LPCAT1, and β-actin immunoblot analyses were performed. (C) Experiments similar to (B) were performed except CEPT1 was over-expressed instead of CPT1. (D) Cells were transfected with empty (E) or LPCAT1 expression vectors and relative mRNA levels of CPT1, CEPT1, and CCT in cells were assayed using qRT-PCR. The lower graphs in (B, C) show densitometric values of bands from respective immunoblots. Data in each panel represent three individual experiments and mean ± S.E. was calculated when appropriate. * $p<0.05$ versus empty group.

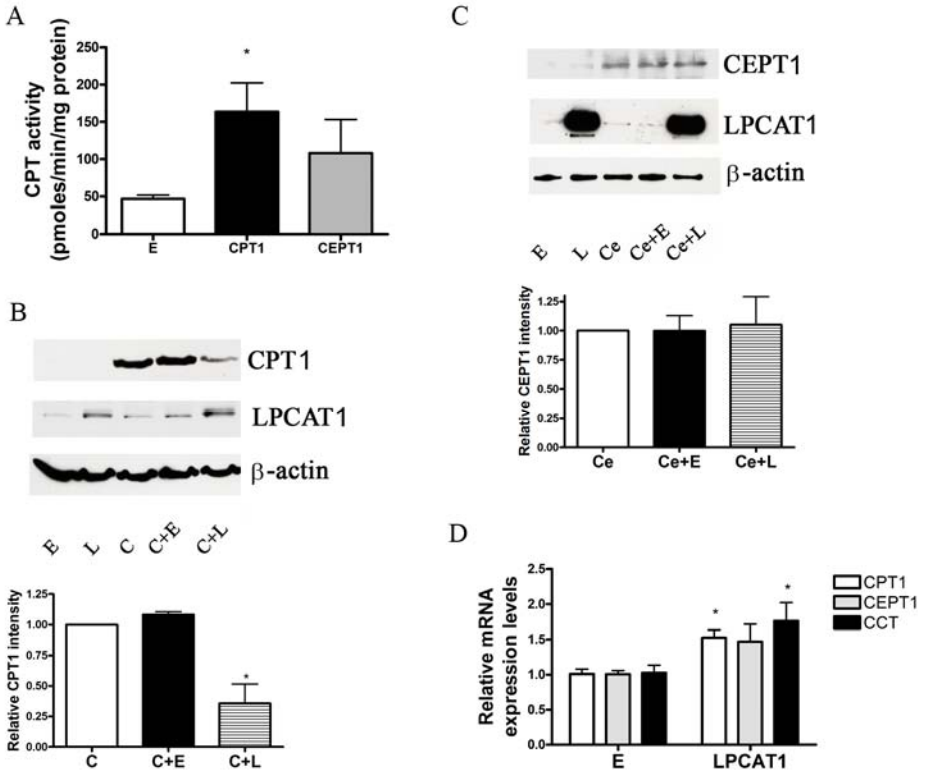
A
CPT activity
(pmoles/min/mg protein)
250
200
150
100
50
0
*
E
CPT1
CEPT1
B
CPT1
LPCAT1
β-actin
E
L
C
C+E
C+L
Relative CPT1 intensity
1.25
1.00
0.75
0.50
0.25
0.00
*
C
C+E
C+L
C
CEPT1
LPCAT1
β-actin
E
L
Ce
Ce+E
Ce+L
Relative CEPT1 intensity
1.25
1.00
0.75
0.50
0.25
0.00
Ce
Ce+E
Ce+L
D
Relative mRNA
expression levels
2.5
2.0
1.5
1.0
0.5
0.0
*
*
CPT1
CEPT1
CCT
E
LPCAT1

Figure 10. CPT1 degradation is attenuated by lysosomal inhibitors

(A) Empty (E), LPCAT1 (L), or CPT1 (C) encoding plasmids were transfected in cells alone or in combination and after 12 h cells were exposed to cycloheximide (CHM) (18μM) with or without either NH_4Cl (25mM), or lactacystin (Lac) (10μM). After an additional 6 h, cells were harvested and cell lysates were separated by SDS-PAGE, transferred to nitrocellulose, and V5 (CPT1), LPCAT1, and β-actin immunoblot analyses were performed (upper). (A [lower panel]) Densitometric analysis of band intensities from respective immunoblots is shown. (B) Cells were transfected with plasmids encoding empty vector (E), CPT1 and/or LPCAT1 or treated with NH_4Cl. As a positive control, cells were also treated with NP-40 for 15 min. Medium was collected and analyzed for LDH activity units. Data represent at least two individual experiments and mean ± S.D. was calculated when appropriate

A

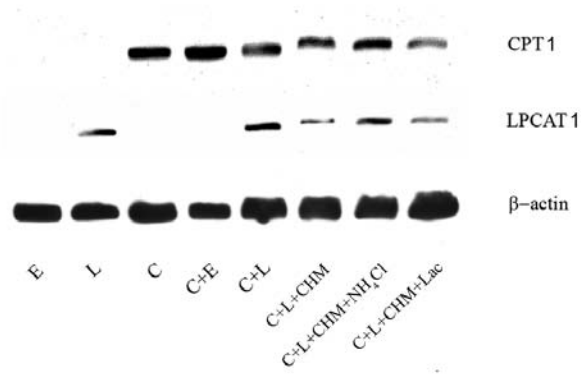
CPT1
LPCAT1
β−actin
E
L
C
C+E
C+L
C+L+CHM
C+L+CHM+NH4Cl
C+L+CHM+Lac

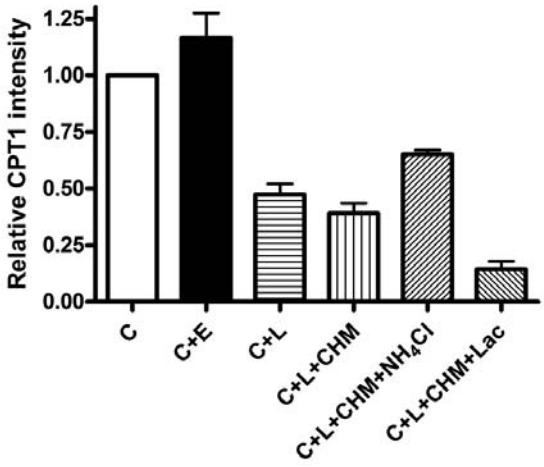
Relative CPT1 intensity
1.25
1.00
0.75
0.50
0.25
0.00
C
C+E
C+L
C+L+CHM
C+L+CHM+NH4Cl
C+L+CHM+Lac

B

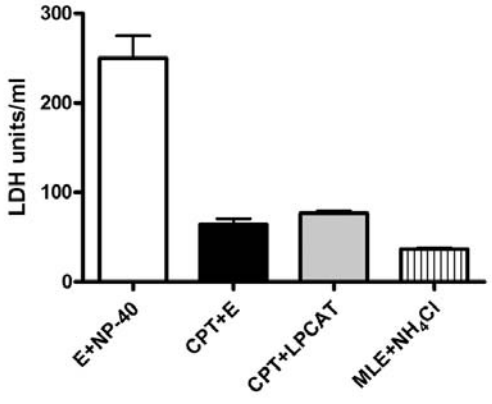
LDH units/ml
300
200
100
0
E+NP-40
CPT+E
CPT+LPCAT
MLE+NH4Cl

Figure 11. CPT1 is localized to the Golgi but degraded within the lysosomes

MLE cells were transfected with CFP-CPT1, βGT-YFP, and/or LPCAT1 encoding plasmids. (A) (Upper) Cells were fixed and stained using a β-1,3-Gal-T2 (αβ-GT) primary antibody and Fluorescein (FITC)-conjugated AffiniPure Donkey anti-goat IgG to visualize the trans-Golgi. To-pro-3 was used to visualize nuclei. (Lower) Cells were co-transfected with plasmids coding for CFP-CPT1 and βGT-YFP and processed for imaging. The white bar represents a 20 nm scale. (B) Transfected cells were exposed to NH_4Cl for 24 h as indicated. Cells were allowed to recover (without NH_4Cl) for 2 h prior to incubation with Lyso-Tracker dye for 1h. Cells were then fixed and visualized using confocal microscopy. Arrows in merged panels represent co-localization with Lyso-Tracker.

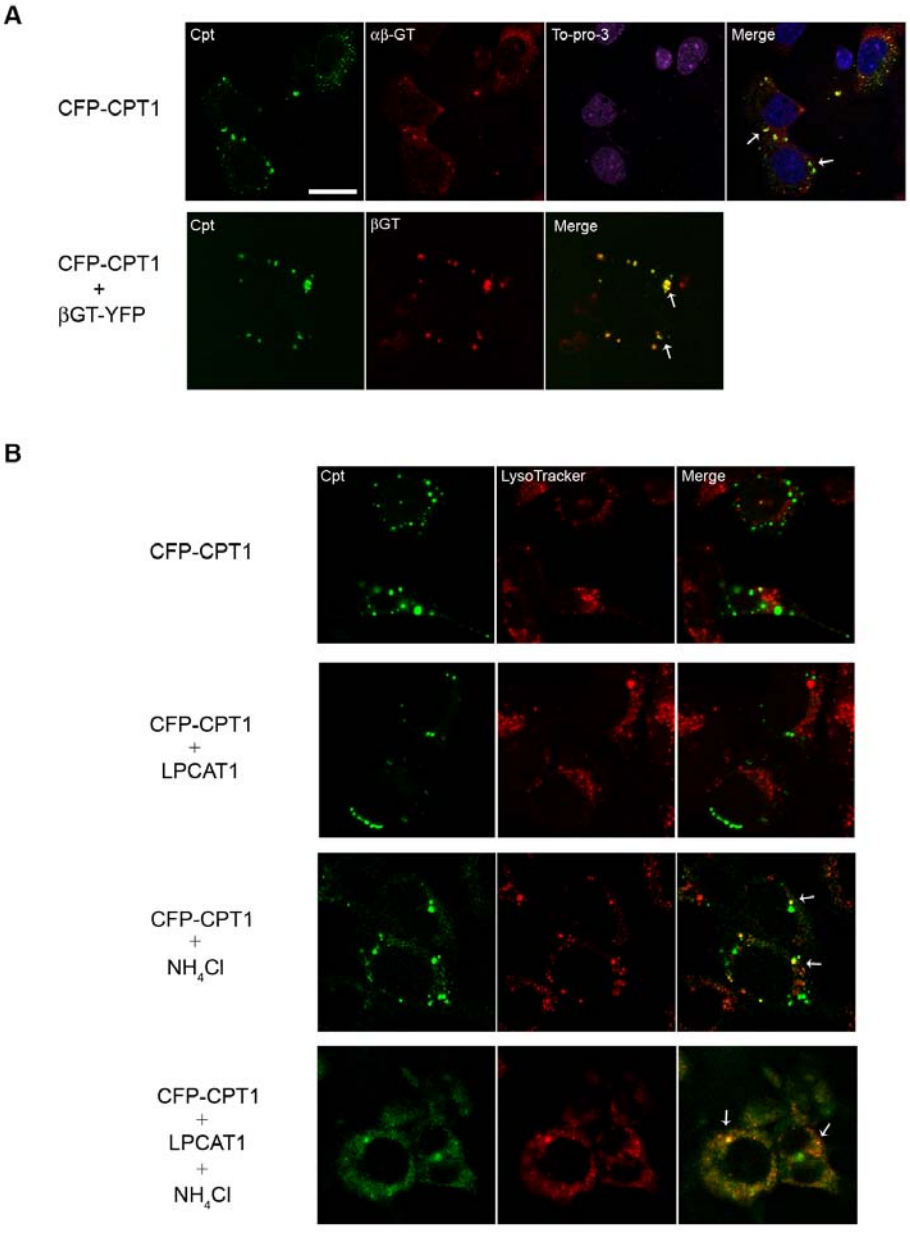
A
CFP-CPT1
Cpt
αβ-GT
To-pro-3
Merge
CFP-CPT1
+
βGT-YFP
Cpt
βGT
Merge
B
CFP-CPT1
Cpt
LysoTracker
Merge
CFP-CPT1
+
LPCAT1
CFP-CPT1
+
NH4Cl
CFP-CPT1
+
LPCAT1
+
NH4Cl

Figure 12. CPT1 localization is disrupted by nocodazole treatment

MLE cells were transfected with CFP-CPT1 and βGT-YFP coding plasmids. After 18h cells were treated with 20μM nocodazole (lower) or DMSO control (upper) for 4h. Cells were then fixed and visualized using confocal microscopy. Left panels show CFP signals (CPT1), middle panels represent YFP signals (βGT), and right panels represent a merged image of YFP and CFP signals (Merge).

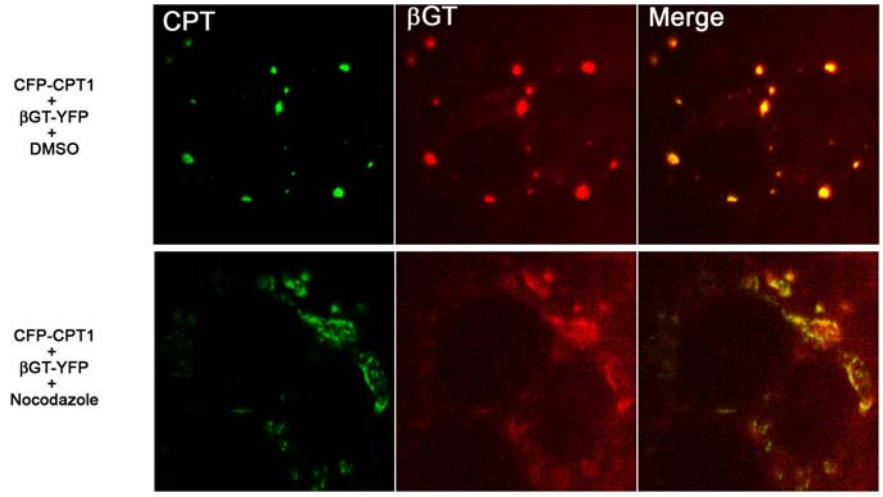
CPT
βGT
Merge
CFP-CPT1
+
βGT-YFP
+
DMSO
CFP-CPT1
+
βGT-YFP
+
Nocodazole

Figure 13. CPT1 is trafficked though the endosomes

(A) MLE cells were transfected with plasmids encoding CFP-CPT1 alone or in combination with LPCAT1 and were exposed to NH_4Cl for 24 h as indicated. Cells were fixed and stained using a Rab5 rabbit primary antibody and alexa568-labeled goat anti-rabbit secondary antibody to visualize the early endosomal compartments using confocal microscopy. Arrows in merged panels represent co-localization with Rab5.

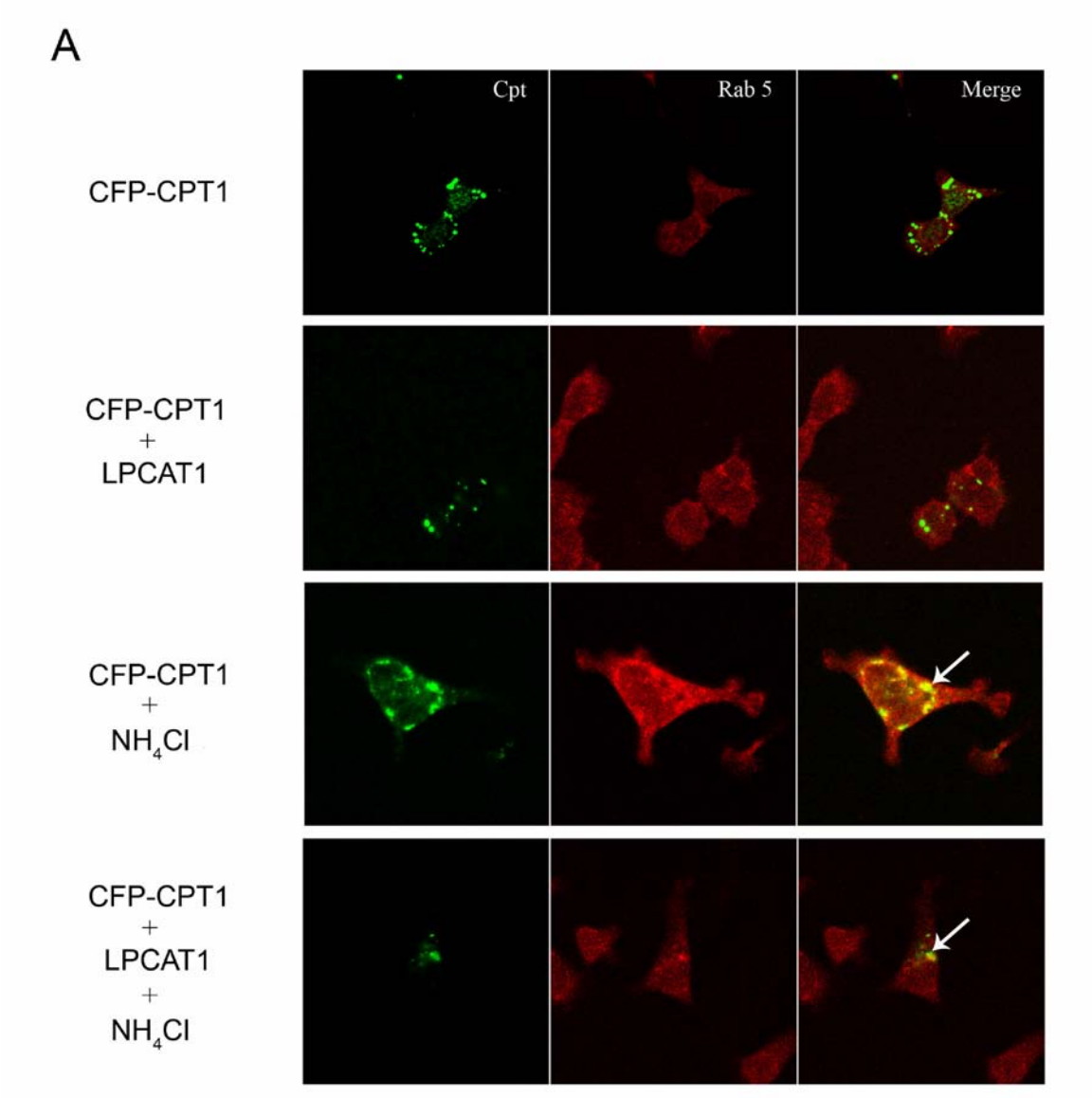
A
Cpt
Rab 5
Merge
CFP-CPT1
CFP-CPT1
+
LPCAT1
CFP-CPT1
+
NH4Cl
CFP-CPT1
+
LPCAT1
+
NH4Cl

Figure 14. Effects of a catalytically-inactive acyltransferase on CPT1

(A-B) Cells were transfected with empty plasmid, or transfected with a plasmid encoding CPT1 in combination with either LPCAT1, or an enzymatically inactive LPCAT1 (LPCAT1 H135N or LPCAT1 H135Q). (A) After 18h, cells were labeled with ^{3}[H] choline for 2h prior to harvest. Cell lysates were then processed for *de novo* PtdCho activity analysis after extracting cellular lipids, resolution of lipids by TLC, and scintillation counting. (B) Cell lysates were separated by SDS-PAGE, transferred to nitrocellulose, and V5 (CPT1) and β-actin immunoblot analyses were performed. Results are from least two individual experiments and mean ± S.D. was calculated in panel (A). *$p<0.05$ versus a paired control.

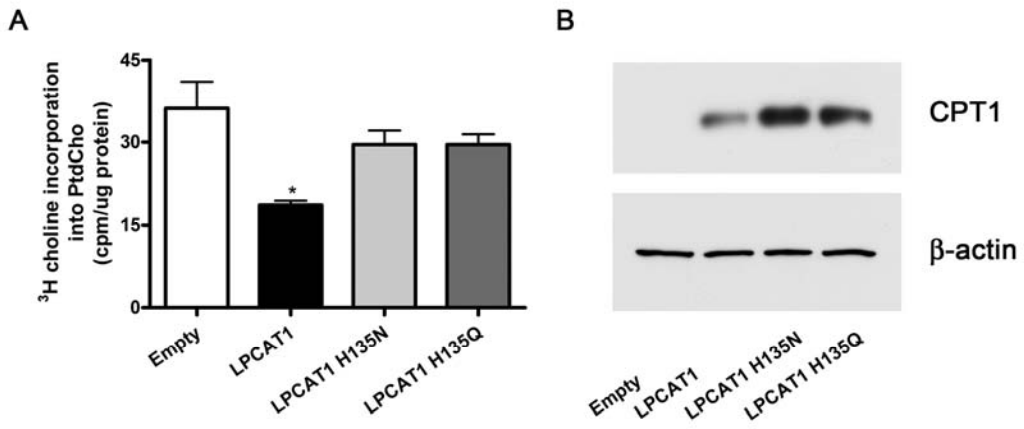
A
B
^{3}H choline incorporation into PtdCho (cpm/ug protein)
45
30
15
0
*
Empty
LPCAT1
LPCAT1 H135N
LPCAT1 H135Q
CPT1
β-actin
Empty
LPCAT1
LPCAT1 H135N
LPCAT1 H135Q

Figure 15. Specificity of acyltransferase-dependent degradation of CPT1

(A-B) Cells were transfected with plasmid encoding empty (E), LPCAT2-V5his (L2), LPCAT3-V5his (L3), CPT1 (C), CPT1+Empty (C+E), CPT1+LPCAT2-V5his (C+L2), or CPT1+LPCAT3-V5his (C+L3). Cell lysates were separated by SDS-PAGE, transferred to nitrocellulose and (upper) V5 and β-actin (lower) immunoblot analysis was performed. Lower graphs: densitometry was performed on CPT1 immunoreactive bands and normalized for β-actin. Immunoblots are indicative of at least two experiments. (C-D) LPCAT1, LPCAT2, and LPCAT3 coding plasmids were expressed in cells and lysates were separated by SDS-PAGE, transferred to nitrocellulose, and V5 and β-actin immunoblot analysis was performed (C). In (D), cells transfected as above were also incubated for 2 h with ^{3}[H] choline and lysates were used for *de novo* PtdCho synthesis assays. Results are from at least two individual experiments and mean ± S.D. was calculated and presented in bar graphs. *$p<0.05$ versus paired controls.

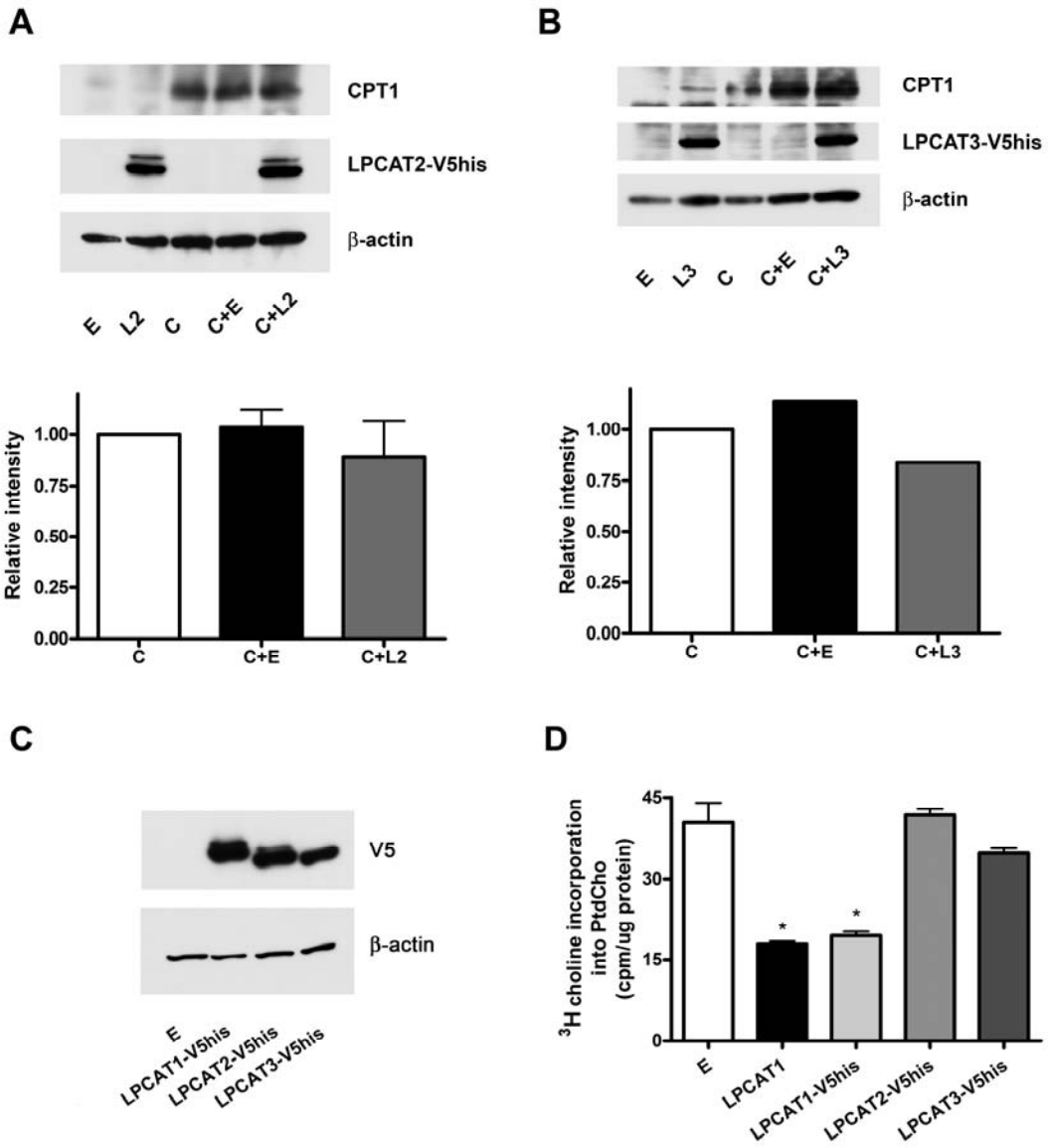
A
CPT1
LPCAT2-V5his
β-actin
E
L2
C
C+E
C+L2
Relative intensity
1.00
0.75
0.50
0.25
0.00
C
C+E
C+L2
B
CPT1
LPCAT3-V5his
β-actin
E
L3
C
C+E
C+L3
Relative intensity
1.00
0.75
0.50
0.25
0.00
C
C+E
C+L3
C
V5
β-actin
E
LPCAT1-V5his
LPCAT2-V5his
LPCAT3-V5his
D
3H choline incorporation into PtdCho (cpm/ug protein)
45
30
15
0
*
*
E
LPCAT1
LPCAT1-V5his
LPCAT2-V5his
LPCAT3-V5his

Figure 16. LPCAT1 knockdown regulates *de novo* PtdCho synthesis enzymes

LPCAT1 or scrambled siRNA was incubated with a viral expression system, HJV; cells were incubated with virus/siRNA mixture for 72h, and cells were collected. (A) LPCAT1 activity, (A, inset, LPCAT1 immunoblot), (B) CPT activity, and (C) CCT activity were measured from lysates. Results are from at least two individual experiments and mean ± S.D. are shown in bar graphs. *$p<0.05$ versus paired controls.

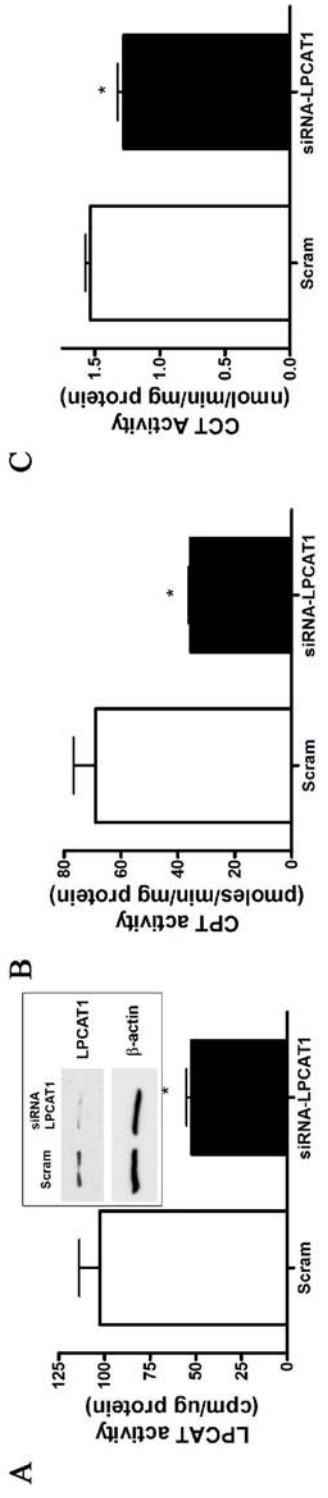
A
LPCAT activity
(cpm/ug protein)
125
100
75
50
25
0
Scram
siRNA-LPCAT1
*
Scram
siRNA LPCAT1
LPCAT1
β-actin
B
CPT activity
(pmoles/min/mg protein)
80
60
40
20
0
Scram
siRNA-LPCAT1
*
C
CCT Activity
(nmol/min/mg protein)
1.5
1.0
0.5
0.0
Scram
siRNA-LPCAT1
*

CHAPTER III

UBIQUITINATION OF CPT1 REGULATES PHOSPHOLIPID PRODUCTION IN LUNG EPITHELIAL CELLS

Abstract

CPT1, an enzyme first cloned from yeast roughly 25 years ago, is indispensible for *de novo* synthesis of PtdCho in the lung, yet poorly studied. Studies presented in chapter II suggest CPT1 degradation involves its processing through the endosome/lysosome pathway. Traditionally, mono- or multi-ubiquitin modification of enzymes has been associated with trafficking through the endosomal compartments and degradation within the lysosome. In these studies I have discovered that CPT1 mutants harboring arginine substitutions at multiple carboxyl-terminal lysine residues exhibited proteolytic resistance to effects of LPCAT1 overexpression. Cellular expression of these CPT1 mutants also restores *de novo* PtdCho synthesis to levels normally observed in lung epithelia. Further studies involved overexpression of β-TrCP that lead to CPT1 degradation, suggesting a role for an E3 ubiquitin ligase as a possible direct regulator of terminal *de novo* enzyme. CPT1 is a transmembrane protein that has not been purified to homogeneity nor has a crystal structure been obtained; however, a proposed membrane orientation model allows for the possibility of several lysine residues located in the enzyme's carboxyl-terminal end are spatially exposed within the cytosol. It is possible that the lysine residues within the carboxyl-terminus of the enzyme may be unmasked and nonspecifically ubiquitinated leading to CPT1 degradation. This mechanism would explain the inability of single lysine mutants to prevent LPCAT1-dependent degradation. Thus, ubiquitin lysosomal processing of CPT1 at multiple lysine residues by an SCF member (β-TrCP) subunit appears to partake in the mechanistic regulation of cellular PtdCho content.

Introduction

PtdCho is a lipid unique to eukaryotic organisms and comprises ~50-80% of phospholipids of mammalian cell membranes. In lung epithelia, however, PtdCho has a more substantial role than just as a major component of the plasma membranes and cellular organelles. Surfactant is the tension-lowering substance present at the air-liquid interface of the lung that prevents lung collapse (atelectasis). The main component of surfactant is a specific disaturated form of PtdCho, or termed DPPtdCho [27]. Although other surfactant proteins are also important to surfactant function, the lipid composition of surfactant is vital to its ability to lower surface tension at the air-surface interface. Because of the unique requirements of the lung due to a very large surface-area and attendantly high surface-tension, specialized type II lung epithelial cells residing in the distal lung tissue constitutively secrete surfactant DPPtdCho necessary to preserve lung structure and function. Two major pathways are responsible for PtdCho synthesis in type II cells: the *de novo* CDP-choline pathway and the PtdCho remodeling pathway.

The *de novo* pathway requires three enzymes: CK, CCT, and CPT1. CCT is the rate-regulatory enzyme in the *de novo* synthesis pathway and has been extensively studied. My studies presented in Chapter II, however, suggest that total lipid homeostasis may depend on the ability of the LysoPtdCho remodeling pathway to regulate the *de novo* synthesis pathway at the terminal enzyme CPT1, in surfactant-producing cells. Although regulation at the CPT1 step is not rate-regulatory, CPT1 dysregulation has been previously described to be sufficient to alter total cellular PtdCho synthesis [89, 113]. Genetic inactivation of CPT1 genes results in reduced phospholipid synthesis, and its inhibition by isoprenoids and ceramides triggers apoptosis, underscoring CPT1 as a key regulator of PtdCho synthesis [89, 114, 115]. The enzyme responsible for PtdCho remodeling in lung epithelial is LPCAT1, which is abundant in type II lung epithelia. Overexpression of LPCAT1 increases surfactant production while total cellular lipid levels remain constant, therefore preserving cellular lipid composition. LPCAT1 targets

CPT1 for trafficking and degradation through the endosome/lysosome pathway that inhibits cellular *de novo* synthesis of PtdCho.

Unlike CCT, there is limited information on the molecular control of CPT1. Farnesol and argininosuccinate potently induce apoptosis in lymphoid human leukemic CEM-C1 or hamster liver cells, respectively, by inhibiting CPT1 function through a yet undescribed mechanism [114, 115]. The primary structures of mammalian CPT1 enzymes are known and secondary structures predicted [80]. Primary structural analyses of CPT1 reveal a carboxyl-terminus containing eleven lysine residues. Predicted secondary structures suggest the presence of seven membrane-spanning domains [80]. Biochemical fractionation and immunolocalization studies suggest CPT1 resides either in the endoplasmic reticulum or the Golgi apparatus [82, 116, 117]. Previous studies presented in Chapter II of this thesis are the first to demonstrate altered trafficking of CPT1 to the lysosome. The lysosomal trafficking of transmembrane proteins has been well described and is often a result of ubiquitination [118, 119]. I therefore considered CPT1 as a candidate for ubiquitination.

Protein ubiquitination is a key post-translational modification that regulates diverse physiologic processes. The conjugation of ubiquitin to a target protein is orchestrated by a series of enzymatic reactions involving an E1 ubiquitin-activating enzyme, ubiquitin transfer from an E1-activating enzyme to an E2-ubiquitin conjugating enzyme, and lastly, generation of an isopeptide bond between the substrate's lysine ε-amino group and the carboxyl-terminus of ubiquitin catalyzed by an E3-ubiquitin ligase. The behavior of ubiquitinated proteins within cells depends, in part, upon ubiquitin chain length and the lysine residue upon which additional ubiquitin moieties are conjugated (K48 or K63 lysine-lysine conjugation) [45]. Ubiquitin modification of a single lysine residue by a ubiquitin chain with K48 linkages is often a signal for proteasomal degradation [120, 121]. At present, most other ubiquitin modifications involving mono-, multi-, and poly-ubiquitin chains linked at the K63 ubiquitin residue result in trafficking

and degradation through the lysosome [45]. Studies on tyrosine receptor kinases, such as epidermal growth factor receptor (EGFR), have shown ubiquitination to be an important modification responsible for trafficking of membrane-bound proteins to the endosomal compartments with subsequent trafficking back to the cell surface or further movement to the lysosome for degradation [122, 123]. Although ubiquitin is not always necessary for receptor protein internalization, ubiquitination is often required for protein degradation and transmembrane protein trafficking. As like most membrane bound proteins, CPT1 is likely trafficked through the lysosomes for its degradation. While data presented in chapter II of this thesis support this mechanism for CPT1 disposal, the role of ubiquitination in this model has not been fully elucidated.

Herein, I hypothesized that LPCAT1 of the PtdCho remodeling pathway regulates CPT1 by targeting the enzyme for degradation within the lysosome after CPT1 ubiquitination. Overexpression of the remodeling enzyme, LPCAT1, in lung epithelia significantly decreased CPT1 protein levels by increasing the enzyme's degradation though the lysosomal pathway. Through the use of CPT1 lysine substitution mutants, I determined that the degradation of CPT1 though the endosome/lysosome pathway resulted from ubiquitination of lysine residues within the carboxyl-terminus of the enzyme. The data provide new insight into of the lifespan of CPT1 and its control by this post-translational event in eukaryotic cells.

Results

CPT1 is ubiquitinated

Generally, mono-ubiquitinated or multi-ubiquitinated proteins are sorted and degraded in the lysosome, whereas poly-ubiquitinated (K48) proteins are degraded in the 26S proteasome [124]. Since it has been previously described that the use of proteasome or lysosome inhibitors can decrease the available ubiquitin pool necessary for proper sorting or degradation of ubiquitinated proteins [77, 125, 126], I first co-transfected a

plasmid containing the ubiquitin coding sequence with a plasmid encoding Flag-CPT1, or Flag-luciferase (as a nonspecific control), in an attempt to maintain a sufficient ubiquitin pool size during the experiment. Assuming ubiquitin was expressed, I observed that levels of CPT1 decreased with ubiquitin co-expression compared to the control. This effect was lessened after exposing co-transfected cells to the lysosomal inhibitor, NH_4Cl (Fig. 17A). Densitometric analyses were performed (Fig. 17A, lower) on signals obtained from Flag and β-actin immunoblot analysis, except for Flag-Luc (Fig. 17A, upper). Although an immunoreactive band was present at around the size of Flag-CPT1 in the control Flag-Luciferase lane, it accounts for only about 10% of the intensity of the Flag-CPT1 signal, which may be a result of non-specific association of primary antibody to a protein expressed in MLE cells. Alternatively, it is possible that sample from the adjacent lane may have overflowed into the control lane before SDS-PAGE was performed. At about 75kDa, the expected Flag-Luciferase signal appears, so it is also possible that the recombinant luciferase is degraded under the experimental conditions to yield the observed ~35kDa band. To examine association, cells were co-transfected with a HA-ubiquitin and Flag-CPT1 plasmids and cells exposed to NH_4Cl (Fig. 17B). Cells were transfected with plasmids encoding Flag-CPT1 or HA-ubiquitin and CPT1-V5his, with or without LPCAT1 and cell lysates were separated by SDS-PAGE, transferred to nitrocellulose; Flag immunoblot analyses was performed to serve as an input for subsequent immuneprecipitations. Interestingly, an immunoreactive signal was observed at about twice the size of Flag-CPT1 indicated as non-specific (NS) (Fig. 17B upper) that may also represent a Flag-CPT1 dimer that was not fully reduced before or during SDS-PAGE. Next, HA-ubiquitin was immunoprecipitated from cells and elutants were separated by SDS-PAGE, transferred to nitrocellulose, and processed for Flag immunoblotting. Here, LPCAT1 expression increased detectable CPT1 of both unmodified and higher molecular weight species (Fig. 17B, lower panel, arrows). Surprisingly, bands at ~35 kDa were also visualized, again suggesting that full-length

CPT1 might aggregate with ubiquitinated CPT1 during immunoprecipitation, but dissociated during SDS-PAGE. It is also possible that under the native conditions of the immunoprecipitation, unmodified CPT1 is binding another ubiquitinated protein.

To complement the above studies, an alternate method was used to enrich ubiquitinated CPT1. I expressed a plasmid encoding CPT1-V5his or CCT-V5his in MLE cells and partially purified protein from cellular lysates using Ni^{2+} chromatography. Chromatographic elutants were separated by SDS-PAGE, transferred to nitrocellulose, and V5 immunoblotting was performed (Fig. 18A). I observed several slower migrating immunoreactive bands after CPT1-V5his expression; these results differ from CCT where a single mono-ubiquitinated band at ~ 50 kDa and dimeric species was recently detected [108]; untransfected cell lysates applied and eluted on these columns served as a negative control.

Multiple CPT1 ubiquitination sites are responsible for trafficking through the endosomal pathway

As ubiquitination of proteins commonly occurs on one or multiple lysine residues, I chose to construct and express CPT1 mutant plasmids coding for CPT1 protein harboring mutations at several lysine residues to determine the extent of CPT1 ubiquitination. Final expression plasmids encoded either four or six K→R mutations, termed $CPT1_{K4R}$ and $CPT1_{K6R}$, respectively (Fig. 18B). Specific candidate lysine residues were mutated based on the enzyme's proposed secondary structure where these residues are likely exposed to the cytosol and conserved between mouse and human sequences [80]. Cells were first transfected with plasmids coding for CPT1-V5his, $CPT1_{K4R}$, $CPT1_{K6R}$ or a luciferase-V5 negative control. After 18 h, transfected cells were treated with NH_4Cl for 24h. Cells were then collected, and cell lysates were applied to ubiquitin capture columns, where agarose was complexed to ubiquitin-binding domain peptides. After washing and elution from the matrix using the suggested manufacture

protocol, elutants were separated by SDS-PAGE, transferred to nitrocellulose, and V5 immunoblotting was performed (Fig. 18C) [127]. Comparable levels of the ~35kDa CPT1 were detected before resin loading (Fig. 18C, [Input]). Multiple high molecular weight bands were observed in immunoblot lanes of cells transfected with plasmid coding for CPT1-V5his in a pattern similar to immunoblots of Fig. 18A. These bands were only visualized after prolonged exposure of autoradiograms. As explained above and observed in ubiquitin immunoprecipitation experiments presented in Fig. 17B, ~35kDa immunoreactive bands are once again present. Importantly, the intensity of several higher molecular weight immunoreactive V5 bands was reduced, some to undetectable levels, in immunoblot lanes that were analyzed from preparations using $CPT1_{K4R}$ and $CPT1_{K6R}$ mutant elutants (Fig. 18C, lower panel, arrows). Cells transfected with plasmid coding for CPT1-V5his with or without plasmid coding for LPCAT1 were also processed similarly as in left panel (Fig. 18C, far right panel). After immunoblots were briefly exposed to film, LPCAT1 co-expression increased the appearance of slower migrating CPT1 bands.

$CPT1_{K6R}$ may be resistant to LPCAT1-dependent degradation

To address the ability of LPCAT1 expression to cause reduction in CPT1 protein, cells were transfected with plasmids coding for CPT1-V5his or $CPT1_{K6R}$ in combination with an empty vector control or with plasmid coding for LPCAT1. Eighteen hours post transfection, cycloheximide (CHM), a inhibitor of protein synthesis, was added to the medium to a final concentration of 18μM. Thirty minutes after CHM treatment, either 0, 0.5, 1, 2, 3, 4, 8, or 12 h time point cells were harvested, and cell lysates were separated by SDS-PAGE, transferred to nitrocellulose, and V5 and β-actin immunoblot analyses were performed.(Fig. 19A, B). Densitometry analyses were performed on immunoblots and plotted relative to t=0. Phase exponential decay line fitting was performed by

graphing software based on densitometric data (Fig. 19A, B, left) from immunoblots (Fig. 19A, B, right). Cells transfected with plasmid coding for CPT1-V5his and empty vector plasmid displayed extended protein stability verses cells transfected with plasmids coding for CPT1-V5his and LPCAT1 (Fig. 19A). Furthermore, a similar approach was used for Fig. 19B where observed stability of $CPT1_{K6R}$ remains constant despite LPCAT1 overexpression. To address statistical significance; I performed two-way Student's *t* test analyses of individual time points comparing data at specific time points. First, I observed statistically significant reductions of wild-type CPT1 levels after co-expression of LPCAT1 over a broad range of time points analyzed as shown in Fig. 19A (upper and lower panels). $CPT1_{K6R}$ stability appeared not to be altered by LPCAT1 co-transfection (Fig. 19, panel B). Data analyzed using one phase exponential decay curves (Fig. 19B lower panel) indicate no significant difference in protein half-life. I have further analyzed the data by performing two-way Student's *t* test analyses of individual time points that also indicate no significant difference between these data (except at t=4 in (Fig. 19B upper graph)). Interestingly, different relative levels of protein were detected at the plateau of the curves (Fig. 19A). There are several possible explanations for the retention of CPT1 or CPT1 mutants at constant levels during the experimental time frame. It is possible that cycloheximide concentrations were not sufficient to comparably affect all cells, leading to a subpopulation of cells still synthesizing protein, and thus a basal plateau CPT1 protein level is observed. It is also possible that after ~4 h, when CPT1 and $CPT1_{K6R}$ lysate protein levels appeared to remain constant for the duration of the experiment, ubiquitin concentration within cells was not sufficient to support proper ubiquitination and trafficking within cells. Finally, there may also be several pools of CPT1 within the cell that are resistant to degradation within the time period of analysis; thus, the stability curve would then reflect degradation of the susceptible CPT1 pool while the protected CPT1 enzyme pool would remain constant. This also might account for the final extent of plateau between expressed proteins. To address the latter

assumption that different pools of CPT1 exist, I further analyzed the data (Fig. 19A lower), by normalization to respective pseudo end plateau points and renormalization to set the beginning time points to value of 1. This analysis suggests that the stability of CPT1 is not significantly different with or without LPCAT1 transfection (Fig. 19C). The validity of this conclusion drawn from Figure 19C depends on the mechanism of the plateau present in the upper panel of Figure 19A. If the cause of the plateau is a result of different pools of CPT1 within cells, which is neither supported nor excluded by immunofluorescence co-localization studies (Fig. 11), then the normalized data suggest a similar CPT1 protein stability in cells co-expressing either with CPT1 and Empty or CPT1 and LPCAT1. However, if the plateau observed is the result of insufficient ubiquitin trafficking caused by extended cycloheximide treatment, then the data would suggest that LPCAT1 expression does alter CPT1 protein stability. Therefore, without currently being able to determine the cause of the flattening of decay curves in CPT1 and $CPT1_{K6R}$ protein degradation at 4 h, it is reasonable to suggest that specific ubiquitination acceptor sites within CPT1 may regulate its stability while CFP-$CPT1_{K6R}$ stability appears not to be altered by LPCAT1. Finally, a plasmid coding for CFP-$CPT1_{K6R}$ was expressed in cells and used for subcellular localization studies. Unlike CFP-CPT1, CFP-$CPT1_{K6R}$ failed to co-localize with Lyso-Tracker Red despite overexpression of LPCAT1 or treatment with NH_4Cl (Fig. 20A, B). CFP-$CPT1_{K6R}$ does, however, co-localize with βGT-YFP, similar to CFP-CPT1 (Fig 20A, white arrows).

Because CPT1 appears to be modified by ubiquitin at multiple sites, I determined if a CFP-CPT1-ubiquitin fusion protein would localize differently than CFP-CPT1 in cells (Fig. 21). Cells were transfected with a plasmid encoding CFP-CPT1 or a carboxyl-terminal ubiquitin linked to CFP-CPT1 (CFP-CPT1x1Ub). Eighteen hours after transfection cells were treated with Lyso-Tracker for 1 h and fixed. Confocal microscopy was then used to observe immunofluorescent fixed cells. The merged images obtained from CFP and Lyso-Tracker signals suggest co-localization of CFP-CPT1 to lysosomal

compartments (Lyso-Tracker) as evidenced by increases in punctate yellow signals. It is an important note that CFP-CPT1x1Ub contains ubiquitin at the carboxyl end of the protein. Since ubiquitin is conjugated to substrates using the carboxyl-terminal end of the ubiquitin peptide, it is possible that CFP-CPT1x1Ub acts as an 'extended ubiquitin peptide' that is conjugated to other ubiquitinated proteins within the cell. Therefore, CFP-CPT1x1Ub immunofluorescence data are considered supportive and not confirmatory of altered localization caused by ubiquitin modification of CPT1. Further studies may include mutation to the carboxyl-terminal G75 and G76 residues as demonstrated by Urbanowski et al. [128].

CPT1 mutants are functional and restore de novo PtdCho synthesis

Previous experiments suggest that CPT1 mutants are less ubiquitinated than CPT1 (Fig. 18). To further determine the activity and effect of the CPT1 K4R and K6R mutants on *de novo* PtdCho synthesis, cells were co-transfected with CPT1-V5his alone or together with a plasmid encoding LPCAT1. Transfected cells were harvested after 18 h, and cell lysates were separated by SDS-PAGE, transferred to nitrocellulose, and LPCAT1, V5, and β-actin immunoblot analyses were performed (Fig. 22A). For CPT activity, cells were transfected as above (Fig. 22A) and, after 18 h, cell lysates were used for functional assays (Fig. 22B). Cells were also transfected as above (Fig. 22A), but at 18 h ^{3}[H] choline was added to medium for 2 h to assess *de novo* PtdCho synthesis (Fig. 22C). While LPCAT1 overexpression decreased immunoreactive levels of CPT1-V5his and $CPT1_{K4R}$, levels were comparable to control levels in cells co-expressing the $CPT1_{K6R}$ mutant and LPCAT1 (Fig. 22A). Overexpression of each construct led to a robust increase in CPT activity indicating that proteins were functional (Fig. 22B). Cells co-expressing recombinant $CPT1_{K4R}$ and LPCAT1 exhibited a ~45% reduction in CPT activity versus cells transfected with $CPT1_{K4R}$ alone; nevertheless, cells from the former

group exhibited greater CPT activity than untransfected cells or cells co-transfected with wild-type CPT1 and LPCAT1 (Fig. 22C). Compared to CPT1-V5his, overexpression of $CPT1_{K6R}$ restored both CPT activity and PtdCho synthesis despite LPCAT1 expression (Fig. 22B, C). As a whole, the data supports CPT1 ubiquitination at highly conserved lysine residues, and that the CPT1 lysine mutants are resistant or partially resistant to the inhibitory actions of LPCAT1 within the phospholipid pathway.

E3 ubiquitin ligase (β-TrCP) degrades CPT1

To determine the identity of possible ubiquitin E3 ligases responsible for ubiquitination of CPT1, I transfected a CPT1-V5his construct with plasmids coding for one of the following E3 ubiquitin ligases: β-TrCP, FbxW4, Fbxo4, Fbxo15, or FbxL2. Cells were collected 18 h post-transfection, and cell lysates were separated by SDS-PAGE, transferred to nitrocellulose, and V5 immunoblot analyses was performed (Fig. 23). Of the E3 ligases expressed, only β-TrCP resulted in a detectable decrease in CPT1 protein levels. Thus, β-TrCP is one potential CPT1 ubiquitin ligase that targets CPT1 for its ubiquitination and processing.

Discussion

The PtdCho remodeling pathway is important for enrichment of disaturated lipid (DPPtdCho) within the surfactant secreted from alveolar epithelial cells. Additionally, the acyltransferase activity of the remodeling enzyme, LPCAT1, is linked to *de novo* PtdCho synthesis that produces a higher fraction of unsaturated PtdCho phospholipid often destined for incorporation into cell membranes (Fig. 5). LPCAT1 overexpression selectively reduced CPT activity, immunoreactive protein levels, and shortened CPT1 stability in lung epithelia (Figs. 6, 9, 19). Exogenously expressed CPT1 also appears to have extended stability that exceeds other lipogenic enzymes including hydroxymethylglutaryl-CoA reductase or CCT suggestive of stabilizing ligands or post-

translational modifications within its primary structure; a recently studied potential glycosylation site within LPCAT1 was not found to harbor such a modification [100, 129] . A reduced life-span of CPT1 may be an indirect result of increased sorting from the Golgi to endosomal/lysosomal organelles, compartments known to promote enzyme degradation. Co-localization of CPT1 with Lyso-Tracker Red was limited and only observed after simultaneous treatment with NH_4Cl consistent with the demonstration that acidic compartments limit fluorescence of CFP-tagged constructs much like other GFP fusion proteins [130]. These results suggest that LPCAT1 overexpression leads to increased CPT1 trafficking to the endosome/lysosomal compartments, where the protein is rapidly degraded. A key aspect of this processing may involve CPT1 ubiquitination, as this modification serves as a sorting signal for regulatory molecules, transmembrane proteins, and cell surface receptors [131].

Ubiquitin can divert proteins either from the cell surface, endosomes, or trans-Golgi network to lysosome compartments [131]. Much debate exists as to the role of mono-, multi-, and poly-ubiquitination modifications as a cellular signal, and the molecular acceptor site of ubiquitin linkage (such as the common K48 or K63) appears to be just as important if not more important than ubiquitin chain size [47]. Mono-ubiquitination has been extensively studied as a marker of trafficking and removal of membrane proteins [132], but in subsequent years the importance and increased effectiveness of ubiquitin chains for endosomal sorting has emerged [133]. Ubiquitin K63 linkages are involved in ubiquitination of a yeast plasma membrane protein [133, 134]. There are, however, differential roles of poly/multi-ubiquitination over mono-ubiquitination of targets. Adaptor molecules or binding partners may associate with differently formed ubiquitin chains (K63 or K48) or may have varying affinities for ubiquitin chains allowing for a time-delayed effect for sorting or protein degradation [135]. For instance, some ubiquitin-binding motifs may show increased affinity for ubiquitin chains as opposed to a single ubiquitination modification [135].

Several proteins containing ubiquitin-binding domains comprise the machinery to assist in the trafficking of ubiquitinated cargos to lysosomes. These cargos may be mono-ubiquitinated or multi-ubiquitinated, but less often poly-ubiquitinated. Evidence in support of CPT1 ubiquitination include our observations that (i) CPT1 cellular levels accumulate after treatment with NH_4Cl, which impairs the degradation of ubiquitinated substrates, (ii) overexpression of ubiquitin decreases CPT1 levels, (iii) CPT1 effectively binds a ubiquitin-binding domain peptide, (iv) LPCAT1-dependent reduction in $CPT1_{K6R}$ stability is not observed, and (v) ubiquitin fusion to CPT1 is sufficient for lysosomal targeting. Last, expression of CPT1 mutants harboring multiple Lys-Arg substitutions at candidate ubiquitin acceptor sites led to reduced binding to ubiquitin-binding domain peptide and resulted in proteolytic resistance to actions of LPCAT1. However, LPCAT1 might still act through nonubiquitin-dependent mechanisms or even indirectly to alter CPT1 stability. CPT1 mutants still, however, show some degree of residual binding to ubiquitin-binding domain peptide, suggesting that several yet unidentified lysine residues partake as ubiquitin acceptor sites when some sites are mutated (Fig. 18C). It is likely that other downstream events are activated (e.g. E3 ligases) or inhibited (DUBs) after LPCAT1 overexpression to modulate CPT1 protein stability. Furthermore, expression of a catalytically inactive LPCAT1 protein containing amino acid substitution at His^{135} does not alter CPT1 levels or significantly reduce *de novo* PtdCho synthesis (Fig. 14). This suggests a mechanism involving lipid-dependent signaling. Ongoing studies suggest that beta-transducin repeat containing protein (β-TrCP) might serve as a putative E3 ligase targeting CPT1 for its degradation (Fig. 23).

CPT1 targeting to the endosome/lysosome pathway may also involve GGA (Golgi-localized, gamma-ear-containing, Arf-binding) proteins that specifically target Golgi-localized ubiquitinated proteins to lysosomes through the GGA protein GAT domain [136]. This interaction has been primarily described in yeast but may also occur in mammalian cells, requiring phosphatidylinositol-4-phosphate kinase IIa for optimal

sorting [137]. Thus, it is possible that LPCAT1-directed CPT1 ubiquitination and lysosomal targeting requires these GGA-like adaptor molecules for its cellular trafficking/elimination.

These results do not exclude the possibilities that LPCAT1 triggers poly-ubiquitination or even mono-ubiquitination of CPT1 as a means to regulate phospholipid metabolism. In this manner, CPT1 would be modified and processed similarly to receptor tyrosine kinases that appear covalently attached at multiple or single sites to ubiquitin [64]. However, it is often difficult to detect mono-ubiquitinated proteins in cells because the subpopulation of select proteins that are ubiquitinated at any given time is extremely small [138]. Detection of ubiquitinated proteins also depend on optimal exposure of autoradiograms. Levels of these ubiquitinated cargos are also regulated by activities of DUBs, making detection difficult. The use of new approaches, such as ubiquitin-mediated fluorescence complementation, may aid in resolving detection difficulties in future studies (54). One intriguing possibility that deserves further study is the hypothesis that a subpopulation of ubiquitinated CPT1 traffics to lysosomes independently of Golgi-localized ubiquitin-binding proteins, and through autophagy. This mechanism has recently been described for lysosomal degradation of long-lived mono-ubiquitinated proteins during cell stress, requiring the ubiquitin-binding protein p62 [139]. Another alternative, yet interesting, possibility is the method by which cells dispose of protein by the use of aggresome formation which delivers proteins to the lysosome using an endocytic-independent mechanism. Although aggresome cargo is usually comprised of misfolded cytosolic proteins undergoing endoplasmic associated degradation (ERAD) [140, 141], evidence of membrane protein aggregation and eventual degradation has been documented[142].

Experimental procedures

Materials

The source of murine lung epithelial (MLE) cells, culture medium, immunoblotting materials and radiochemicals were described previously [8]. Mouse monoclonal ubiquitin antibody was purchased from Cell Signaling (Danvers, MA). The pAmCyan1-C1 and pZsYellow-C1 vector was purchased from Clontech (Mountain view, CA). Lyso-Tracker Red, mouse monoclonal V5 antibody, the To-Pro-3 nuclear staining kit, the PCRTOPO4.1 cloning kit, pcDNA-DEST40, pcDNA3.1/nV5-DEST, and pLenti6/V5-Dest cloning vectors, *E. coli* One Shot competent cells, the pENTR Directional TOPO cloning kits, LR clonase II recombinase, Superscript III RT kit, and the Gateway mammalian expression system were purchased from Invitrogen (Carlsbad, CA). Ni^{2+} resin, HIS-select Nickel Affinity gel, Tri Reagent, human KGF, and β-actin primary mouse monoclonal antibody were obtained from Sigma (St. Louis, MO). LPCAT1 antibody was generated by Covance (Princeton, NJ). Amicon Ultra-4 centrifugal filter devices were from Millipore (Billerica, MA). The QuickChange site-directed mutagenesis kit, XL-gold cells, and pCMV-Tag1 vector were from Stratagene (La Jolla, CA). A ubiquitin plasmid was constructed as described [108]. The gel extraction kit and QIAprep Spin Miniprep kits were from Qiagen (Valencia, CA). NucleoBond Xtra Maxi prep kits were obtained from Macherey-Nagel (Bethlehem, PA). Cycloheximide (CHM) and UbiQapture-Q (Ub Capture) matrix was from Biomol (Plymouth Meeting, PA). HA-tagged ubiquitin was a gift from Dr. Peter Snyder (U. of Iowa). β1,3-galactosyltransferase 2 goat polyclonal primary antibody was purchased from Santa Cruz Biotechnology (Santa Cruz, CA). Power CYBR Green PCR master mix was from Applied Biosystems (Carlsbad, California). All restriction enzymes and ligases were purchased from New England Biolabs (Ipswich, MA). The TNT coupled reticulocyte lysate system and RQ1 DNase kit was purchased from Promega (Madison, WI). All DNA sequencing was performed by the University of Iowa DNA Core Facility.

Cloning primers were purchased from IDT (Coralville, IA). The Zeiss LSM 510 confocal microscope is part of the University of Iowa Central Microscopy Research Facility.

Expression plasmids

The coding sequence available for LPCAT1, CPT1 and CEPT1 on the NCBI website (NM_145376, NM_144807, NM_133869) were used to construct primers for cloning of genes from cDNA from mRNA via reverse transcriptase PCR from murine liver and kidney tissues. Amplified fragments were subcloned into PCRTOPO4.1, and sequenced, where it was identical to the deposited NCBI LPCAT1 sequence. The resulting PCRTOPO4.1 vector served as a source for cloning into pacAd5 CMV IRES eGFP pA (University of Iowa DNA core) using ClaI and BamHI restriction sites. For CPT1 and CEPT1, the Invitrogen® Gateway System was used. Primers constructed containing CACC overhangs upstream of the 5' ATG and antisense sequence with (V5-CEPT1) or without (CPT1-V5his) a stop codon were used for amplification using a blunt end polymerase and pENTR/D-TOPO per manufacturers' instruction. LR clonase II recombinase was used for cloning of CPT1 and CEPT1 sequences into pcDNA-DEST40 or pcDNA3.1/nV5-DEST gateway vectors, respectively (CPT1-V5his, V5-CEPT1). $CPT1_{K4R}$ and $CPT1_{K6R}$ were constructed by performing site-directed mutagenesis on CPT1-V5his at K^{254}, K^{282}, K^{283}, K^{292}, ($CPT1_{K4R}$) and additionally K^{307} and K^{311} for $CPT1_{K6R}$ using the QuickChange II XL Site-Directed Mutagenesis (Stratagene) kit. CFP-CPT1 was generated similar to CFP-CCT [100]. The CPT1 construct $CPT1_{K6R}$ was digested with BgIII and SalI, purified, and ligated into pAmCyan-C1 as described, generating CFP-$CPT1_{K6R}$ [108]. Flag-CPT1 was constructed by amplification of CPT1 and ligation into pCMV-Tag1. A βGT-YFP (carboxyl-terminal YFP tag) plasmid was constructed by amplifying or digesting three separate fragments for ligation. First, a human cDNA was used as a template to amplify the first 249 base pairs of UDP-

Gal: βGlcNAc β 1,4-galactosyltransferase gene (B4GALT1) (gene bank number BC045773) with flanking ClaI/EcoRV restriction sites. Fragment two was an EcoRV/EcoRI YFP fragment amplified from pZsYellow-C1. Finally, a pacAd5 CMV IRES eGFP pA vector and the two amplified fragments were digested with appropriate restriction enzymes and gel extracted. The B4GALT1 and YFP fragments were ligated into pacAd5 CMV IRES eGFP pA to generate βGT-YFP. Tandem Ubi-CFP-CPT fusion constructs were generated by cloning the ubiquitin coding sequence at the carboxyl-terminus of CFP-CPT1 using SalI and ApaI sites to generate CFP-CPT1xUb.

Cell isolation, culture, and transient transfection

Alveolar macrophages, primary type II cells, and fibroblasts were isolated as previously described [109]. MLE cells were maintained in HITES medium (DMEM F12) with 2% fetal bovine serum at 37^{o}C in 5% CO_2. After reaching 80% confluency, the cells were harvested using 0.25% trypsin and 0.1% EDTA and resuspended in medium, and plated onto appropriate culture dishes containing a 3 ul per 1ug DNA ratio of FuGENE6 lipofection reagent and appropriate expression vector. After incubation overnight, the medium was replaced with HITES medium with 2% fetal bovine serum for 8 h before cell harvesting. In some studies, an Amaxa electroporation device with program T-013 and solution L was used for plasmid transfection of cells. Cells were maintained as described as above, except, after trypsinization, cells were resuspended in a small volume of solution L per manufacturer's directions. Plasmids were transfected into cells or cells were left untransfected. Medium was aspirated 24 h post-transfection and cells were treated an additional 24 h with 0% FBS DMEM F12 medium supplemented with or without NH_4Cl (25 mM). Cell lysates were harvested by brief sonication in 150 mM NaCl, 50 mM Tris-HCl, 1 mm EDTA (no EDTA if Ni^{2+} purification was performed), 2 mM dithiotreitol, 0.025% sodium azide, and 1 mM phenylmethylsulfonyl fluoride (pH 7.4) (Buffer A), at 4°C. Alternatively, cells were switched to DMEM F12 media without

FBS and treated for 6 h with cycloheximide (CHM) (18 ug/mL) with either NH_4Cl (25 mM) or lactacystin (25 uM). Cells were collected in Buffer A + 0.5% Triton X-100 + 0.5% NP-40 and sonicated for further analysis. MLE cells were also exposed to human KGF (20ng/mL) for 24 h prior to harvest. Rat type II cells were transduced for 48h with lentivirus containing LPCAT1 in a pLenti6/V5-Dest vector, constructed at the University of Iowa Gene Transfer Vector Core.

Isolation of microsome fractions

Cells were resuspended in Buffer A and samples first centrifuged at 16,000 x g for 10 min at 4^{o}C. The resulting supernatant was centrifuged at 100,000 x g for 60 min at 4°C. The resulting microsomal pellet was resuspended in a solution containing 250mM sucrose and 10mM Tris-HCl at pH=7.4 using a 25 G needle.

Phospholipid analysis

Lipids were extracted from equal amounts of membrane protein and levels of the individual phospholipids quantitated with a phosphorus assay [103]. DPPtdCho was assayed as before [8]. For PtdCho *de novo* synthesis, cells were pulsed with 1 µCi of [*methyl*-^{3}H]choline chloride during the final 2 h of incubation with choline deplete medium. For remodeling activity, cells were labeled with 1.75 nM of [^{14}C] LysoPtdCho (55mCi/mmol) for 3 h. Total cellular lipids were extracted, resolved using thin layer chromatography (TLC), and processed for scintillation counting [8].

LPCAT activity

Cells were harvested in lysis buffer (250mM sucrose, 10mM Tris-HCl at pH=7.4), and equal amounts of microsomal cellular protein or cell lysate were used in the assay. One nmole of 1-palmitoyl-*sn*-glycero-3-phosphocholine was added for every µL of 5x assay buffer (final working concentration 65mM Tris-HCl, pH 7.4, 10mM $MgCl_2$, 12.5

mM fatty acid free BSA, 2mM EDTA) sonicated. 35 µL of H_2O and cellular protein was added to 10 µL sonicated assay buffer containing 5 µL of [1-^{14}C]acyl-CoA (0.1µCi, 1.8nmole) for a total assay volume of 50 µL. Upon addition of [1-^{14}C] acyl-CoA, samples were incubated at 30^{o}C for 10 min after which the reaction was terminated by addition of chloroform/methanol/H_2O (1:2:0.70 vol/vol). Total cellular lipids from reaction mixtures were extracted by the method of Bligh and Dyer [104], spotted on LK5D plates, and PtdCho was resolved using TLC and detected using a Bioscan AR-2000 scintillation plate reader.

De novo enzyme activities

CPT activity was assayed as described [111]. Each reaction mixture contained 50 mM Tris ·HCl buffer (pH 8.2), 0.1 mg/ml Tween 20, 1 mM 1,2-dioleoylglycerol, 0.8 mM phosphatidylglycerol, 0.5mM [^{14}C]-CDP-choline (specific activity 1,110 dpm/nmol), 5 mM dithiothreitol, 5 mM EDTA, 10mM $MgCl_2$, and 30–40 µg of protein. The lipid substrate was prepared by combining appropriate amounts of 1,2-dioleoylglycerol (1 mM) and phosphatidylglycerol (0.8 mM) in a test tube, drying under nitrogen gas, and brief sonication before addition to the assay mixture to achieve the final desired concentration. The reaction proceeded for 1 h at 37°C and was terminated with 4 ml of methanol-chloroform-water (2:1:7, vol/vol). The remainder of the assay was performed exactly as described [111]. A Bioscan AR-2000 plate reader was used for detection of radiolabeled PtdCho on LK5D TLC plates with data quantified using WinScan software. PtdCho bands on the LK5D silica plates were also scraped and quantified by liquid scintillation counting.

Immunoblot analysis

Immunoblotting was performed as described [100, 112]. The dilution factor for the LPCAT1, V5, Flag, and β -actin antibodies were 1:2000, 1:2000, 1:5000, and 1:10,000 respectively.

Immunoprecipitation

Cell lysates were also incubated with 3 μL HA antibody (Sigma) at 4°C overnight, incubated with 20 μL Pierce protein A/G matrix for 2h, eluted with protein sample buffer (40% Glycerol, 240 mM Tris/HCl pH 6.8, 8% SDS, 0.04% bromophenol blue, 2% beta-mercaptoethanol, 1% DTT) prior to immunoblot analysis
[100, 112].

Immunofluorescence microscopy

MLE cells were plated at 30% confluency on 35mm MetTek glass-bottom culture dishes, and transfected with individual CFP plasmids. Cells were washed with PBS and fixed with 4% paraformaldehyde for 20min., then exposed to 15% BSA, 1:200 β-1, 3-galactosyltransferase 2 primary goat antibody and 1:200 Fluorescein (FITC)-conjugated AffiniPure Donkey anti-goat IgG (H+L) (Jackson Immunoresearch) to visualize the trans-Golgi; cells were also incubated with an alexa568-labeled goat anti-rabbit secondary antibody. Nuclei were visualized using To-Pro-3 (1:2000, dilution). Immunofluorescent cell imaging was performed on a Zeiss LSM 510 confocal microscope using the 458nm, 568nm or 615nm wavelength. All experiments were done with a Zeiss x63 or x100 oil differential interference contrast objective lens. The 458nm wavelength was used to excite the CFP-CPT1 fusion proteins, with fluorescence emission collected through a 475nm filter. A 488nm wavelength was used to excite Fluorescein dye, with fluorescence emission collected through a 505-530nm filter. A 488nm wavelength was used to excite βGT-YFP, with fluorescence emission collected through a 530-600nm filter. A 613nm

wavelength was used to excite To-Pro-3 dye, with fluorescence emission collected through a 633nm filter. Scanning was bidirectional at the highest possible rate measurement using a digital1X zoom.

UbiQapture-Q matrix pulldown

Cell lysates were incubated with 40μL (this symbol did not show up on my computer) of agarose beads complexed to ubiquitin-binding domain peptide over night at 4^{o}C. An aliquot of pre-bound lysate was also resolved by 10% SDS-PAGE to determine loading onto the resin. The matrix resin was washed with 5x1 volume of 9:1 PBS to lysis buffer as described in the Biomol protocol and protein sample buffer was used to elute bound protein.

Ni^{2+} resin purification

Cell lysates were incubated with 40 mL of His-select nickel affinity gel resin overnight at 4^{o}C. The matrix resin was washed sequentially with a 3x3 bead volume of Buffer A without EDTA and 0.05% Triton X and 0.05% NP-40, a 2x3 bead volume of Buffer A without EDTA, 0.005% Triton X, 0.005% NP-40, 500mM NaCl, and 6mM Imidizole, and finally 1 volume of Buffer A without EDTA, 0.005% Triton X, 0.005% NP-40, 500mM NaCl, and 200mM imidazole. After 30min, protein sample buffer was added to the resin/buffer mixture, samples were incubated at 25^{o}C overnight, and proteins visualized by immunoblot analysis.

Statistical analysis

Statistical analysis was performed by two-way analysis of variance or Student's *t* test. Data are presented as mean ± S.E.

Figure 17. CPT1 is ubiquitinated

(A) Cells were co-transfected with ubiquitin, Flag-luciferase (Luc) or Flag-CPT1 expression plasmids with or without NH_4Cl treatment (25 mM) for 24 h. Total cell lysates were separated by SDS-PAGE, transferred to nitrocellulose, and Flag and β-actin immunoblot analyses were performed (upper). The lower graph represents densitometric analysis of two Flag immunoblots that are normalized for β-actin immunoreactive levels, and the value of Flag-CPT1 signal transfected alone (far left lane). Flag-Luc is not represented in the graph. (B) Cells were transfected with plasmids coding for Flag-CPT1, HA-ubiquitin, CPT1-V5his, with or without LPCAT1. Transfected cells were incubated for 18 h and then treated with NH_4Cl (25mM) for 24h using methods previously described. Cell lysates were separated by SDS-PAGE, transferred to nitrocellulose, and Flag immunoblot analysis was performed (Input). Cell lysates from above were also incubated with HA antibody/protein A/G matrix, eluted, and separated by SDS-PAGE, transferred to nitrocellulose, and Flag immunoblot analysis performed (lower). NS=nonspecific bands; arrows denote CPT1 or higher migrating CPT1-Ub conjugates. Results are from at least two individual experiments. Mean ± S.D. was calculated in panel (A), lower bar graph.

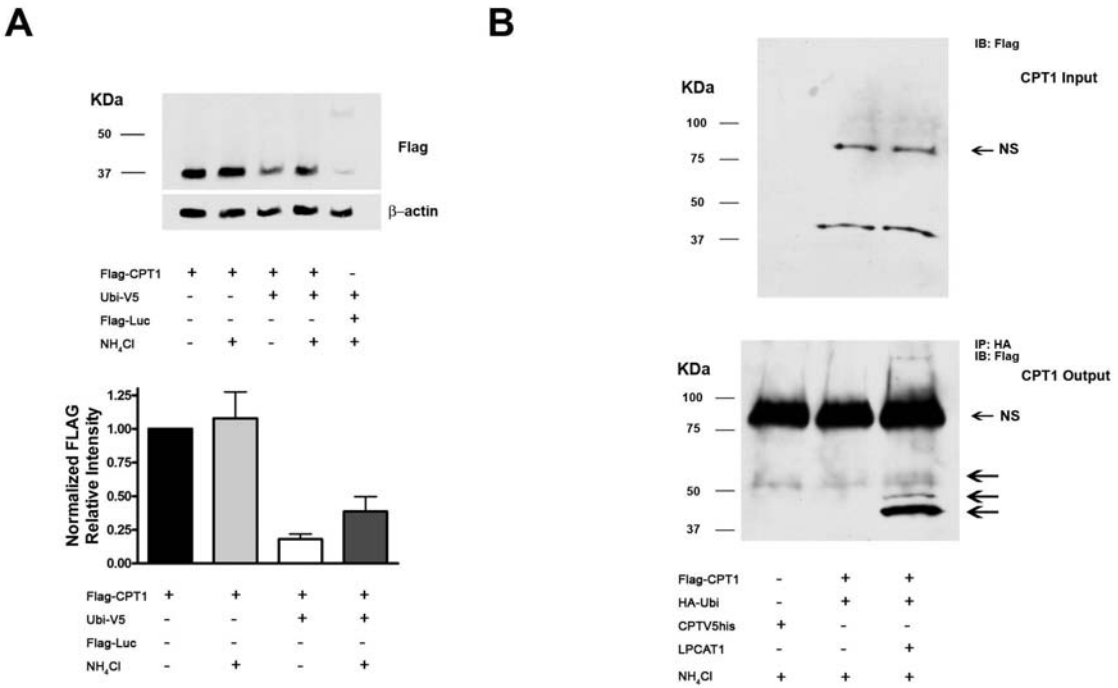
A
KDa
50
37
Flag
β–actin
Flag-CPT1 + + + + -
Ubi-V5 - - + + +
Flag-Luc - - - - +
NH4Cl - + - + +
Normalized FLAG Relative Intensity
1.25
1.00
0.75
0.50
0.25
0.00
Flag-CPT1 + + + +
Ubi-V5 - - + +
Flag-Luc - - - -
NH4Cl - + - +
B
KDa
100
75
50
37
IB: Flag
CPT1 Input
NS
KDa
100
75
50
37
IP: HA
IB: Flag
CPT1 Output
NS
Flag-CPT1 - + +
HA-Ubi - + +
CPTV5his + - -
LPCAT1 - - +
NH4Cl + + +

Figure 18. Slower migrating CPT1 is conjugated to ubiquitin

(A) Cells were transfected with plasmid coding for CPT1-V5his (CPT1) or CCT-V5 (CCT) or left untransfected (MLE) and after 18 h, cells were treated with NH_4Cl (25mM) for an additional 6 h. Cells were harvested and cell lysates were incubated with Ni^{2+} resin at 4^{o}C for 4 h. Ni^{2+} resin bound protein was eluted separated by SDS-PAGE, transferred to nitrocellulose, and V5 immunoblot analysis was performed. (B) Schematic of candidate ubiquitin acceptor sites targeted for generation of multiple K-R CPT1-V5his mutants. The $CPT1_{K4R}$ mutant harbors mutations at K^{254}, K^{282}, K^{283}, K^{292}, and the $CPT1_{K6R}$ construct also harbors substitutions at these sites and K^{307} and K^{311}. (C) (left blot) CPT1, $CPT1_{K4R}$, $CPT1_{K6R}$, and luciferase-V5 (Luc) coding plasmids were transfected into cells; after 18 h cells were exposed to NH_4Cl (25mM) for 24 h and cells were harvested. Cell lysates were separated by SDS-PAGE, transferred to nitrocellulose and V5 immunoblot analyses performed (Input). Cell lysates were also incubated with Ub Capture matrix (4^{o}C for 4 h), eluted, and elutants were separated by SDS-PAGE, transferred to nitrocellulose and V5 immunoblot analyses performed (lower). Arrows indicate slower migrating bands that exhibit differential levels of intensities between recombinant CPT1 and mutant constructs. Right blot: untransfected cells, or cells transfected with plasmids coding for CCT, CPT1 alone, or co-transfected with LPCAT1 coding plasmid. Cell lysates were subjected to the same protocol as above using the Ub Capture matrix. All panels were exposed extensively to detect ubiquitinated products except the far right panel. Results are representative of at least three individual experiments.

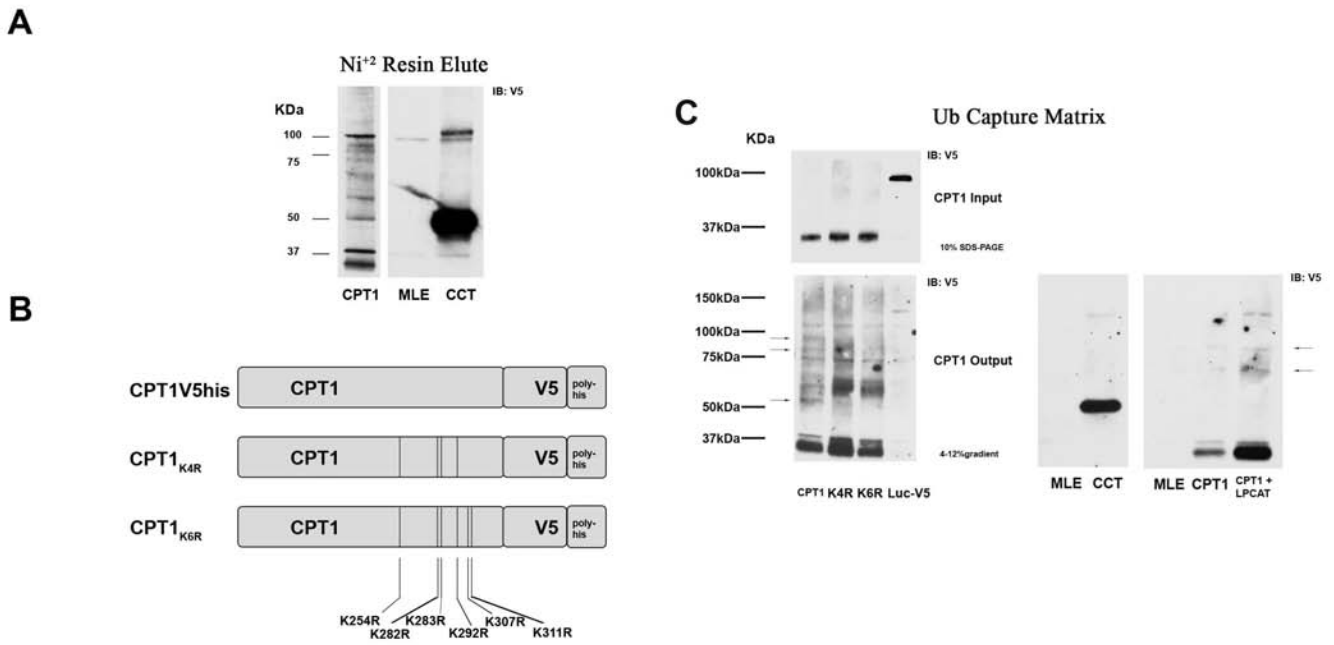
A
Ni+2 Resin Elute
KDa
100
75
50
37
IB: V5
CPT1
MLE
CCT
B
CPT1V5his
CPT1
V5
poly-his
CPT1K4R
CPT1K6R
K254R
K282R
K283R
K292R
K307R
K311R
C
Ub Capture Matrix
KDa
100kDa
37kDa
IB: V5
CPT1 Input
10% SDS-PAGE
150kDa
100kDa
75kDa
50kDa
37kDa
CPT1 Output
4-12%gradient
CPT1 K4R K6R Luc-V5
MLE CCT
MLE CPT1 CPT1 + LPCAT

Figure 19. LPCAT1 does not alter $CPT1_{K6R}$ stability

(A-B) Cells were co-transfected with plasmid coding for CPT1 or $CPT1_{K6R}$ with either an empty (E) or LPCAT1 coding plasmid and incubated in medium containing CHM (18μM). Cells from each group were harvested at times after CHM treatment and cell lysates were separated by SDS-PAGE, transferred to nitrocellulose, and V5 immunoblot analyses performed (right) and densitometric analyses of autoradiograms were performed (left). Separate experiments were performed as above analyzing additional time points (A-B, lower). The starting (0) hr time point was normalized to equal 1 for each test group. Results are from at least two separate (upper) or at least three (lower) individual experiments. Best-fit lines are a result of one phase exponential decay line fitting performed by Prism graphing software. Two-way Student's *t* test analyses were also performed on individual time points comparing data. . (C) Data represented in panel A (lower) were normalized against either group's respective protein plateau value. This value was then normalized for a starting (0) hr time point equal to 1. Mean ± S.D. (upper graphs) or mean ± S.E (lower graphs and C) was calculated. *$p<0.05$ versus controls.

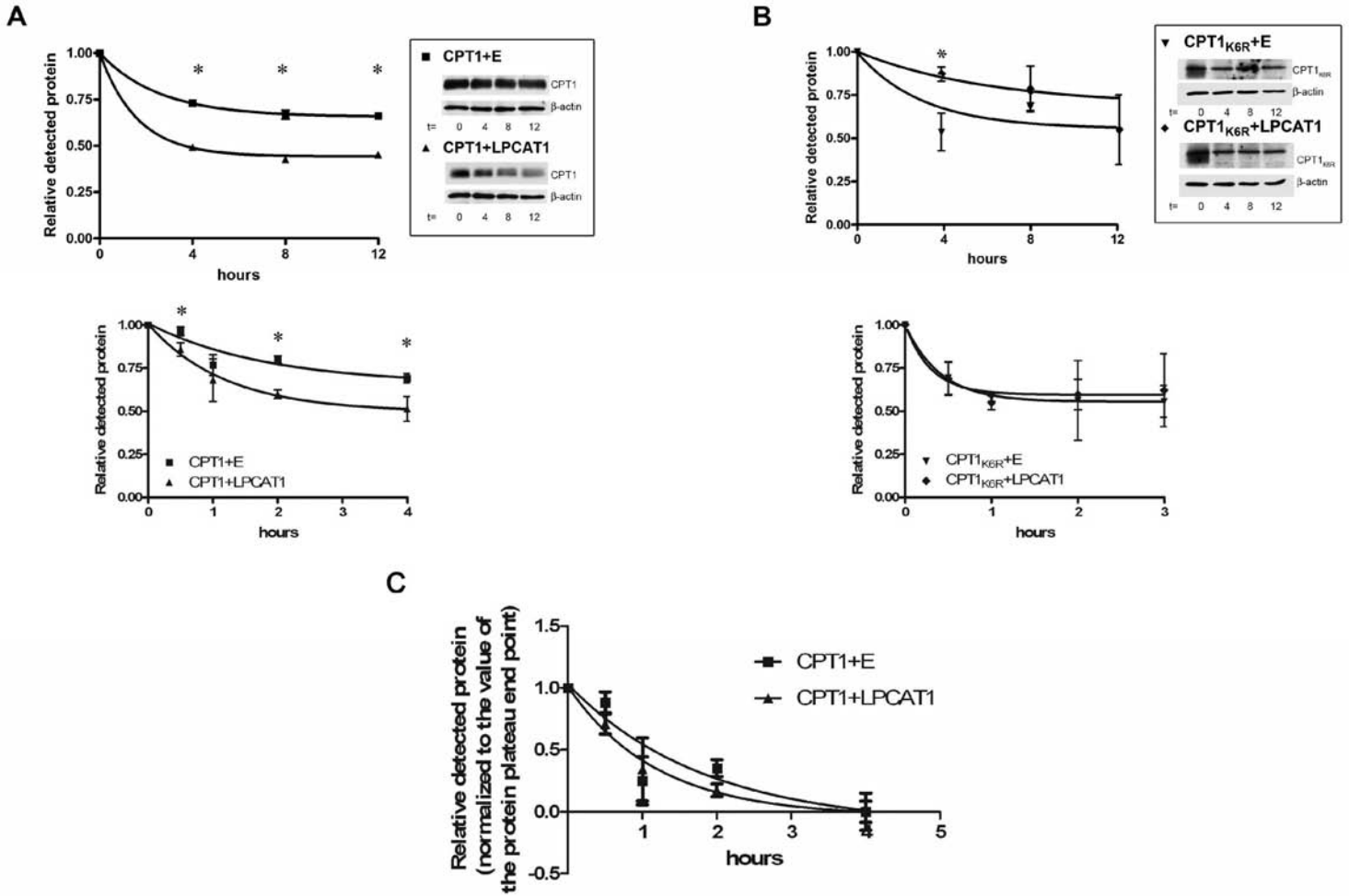
A
Relative detected protein
1.00
0.75
0.50
0.25
0.00
0
4
8
12
hours
*
*
*
CPT1+E
CPT1
β-actin
t= 0 4 8 12
CPT1+LPCAT1
CPT1
β-actin
t= 0 4 8 12
Relative detected protein
1.00
0.75
0.50
0.25
0.00
0
1
2
3
4
hours
*
*
*
CPT1+E
CPT1+LPCAT1
B
Relative detected protein
1.00
0.75
0.50
0.25
0.00
0
4
8
12
hours
*
CPT1K6R+E
CPT1K6R
β-actin
t= 0 4 8 12
CPT1K6R+LPCAT1
CPT1K6R
β-actin
t= 0 4 8 12
Relative detected protein
1.00
0.75
0.50
0.25
0.00
0
1
2
3
hours
CPT1K6R+E
CPT1K6R+LPCAT1
C
Relative detected protein
(normalized to the value of
the protein plateau end point)
1.5
1.0
0.5
0.0
-0.5
1
2
3
5
hours
CPT1+E
CPT1+LPCAT1

Figure 20. $CPT1_{K6R}$ is not trafficked to the lysosome upon LPCAT1 overexpression

(A-B) Cells were transfected with plasmid coding for CFP-$CPT1_{K6R}$ alone or in combination with βGT-YFP or LPCAT1 coding plasmids. Cells expressed (A) CFP-$CPT1_{K6R}$ and βGT-YFP, were fixed, and immunofluorescence analyses were performed using a confocal microscope. Arrows indicate co-localization of CFP-$CPT1_{K6R}$ with βGT-YFP. In (B), transfected cells were exposed to medium containing NH_4Cl (25mM) for 24 h. Cells were allowed to recover (no NH_4Cl) for 2 h prior to incubation with Lyso-Tracker dye for 1h. Cells were then fixed and visualized by confocal microscopy.

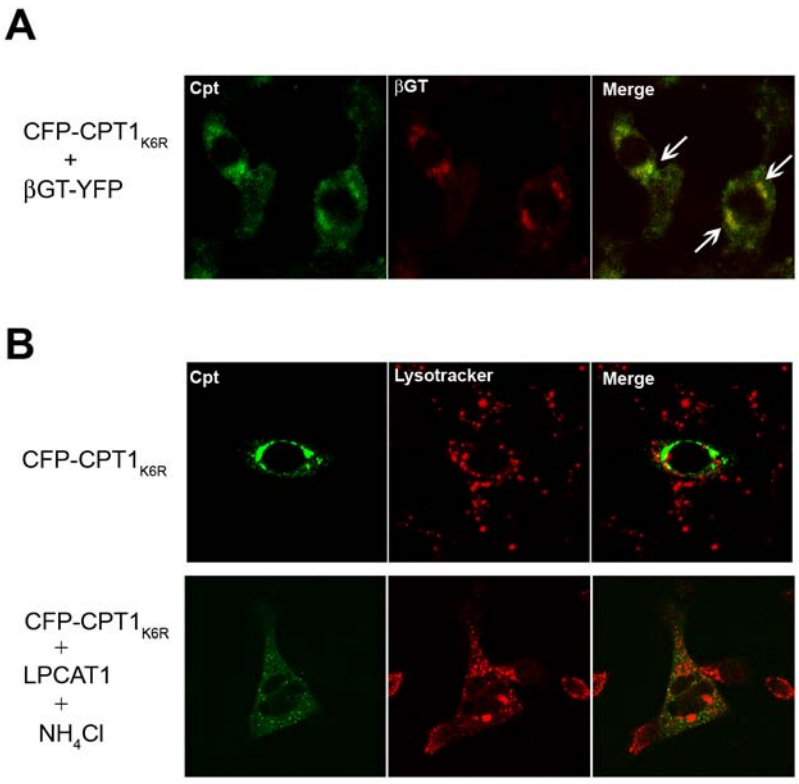
A
CFP-CPT1K6R
+
βGT-YFP
Cpt
βGT
Merge
B
CFP-CPT1K6R
Cpt
Lysotracker
Merge
CFP-CPT1K6R
+
LPCAT1
+
NH4Cl

Figure 21. CPT1 ubiquitin fusion proteins target to the lysosome

MLE cells were transfected with plasmids coding for CFP-CPT1 and CFP-CPT1-1xUb (schemes upper). After 18 h, cells were incubated with Lyso-Tracker dye for 1h. Cells were then fixed and visualized using confocal microscopy.

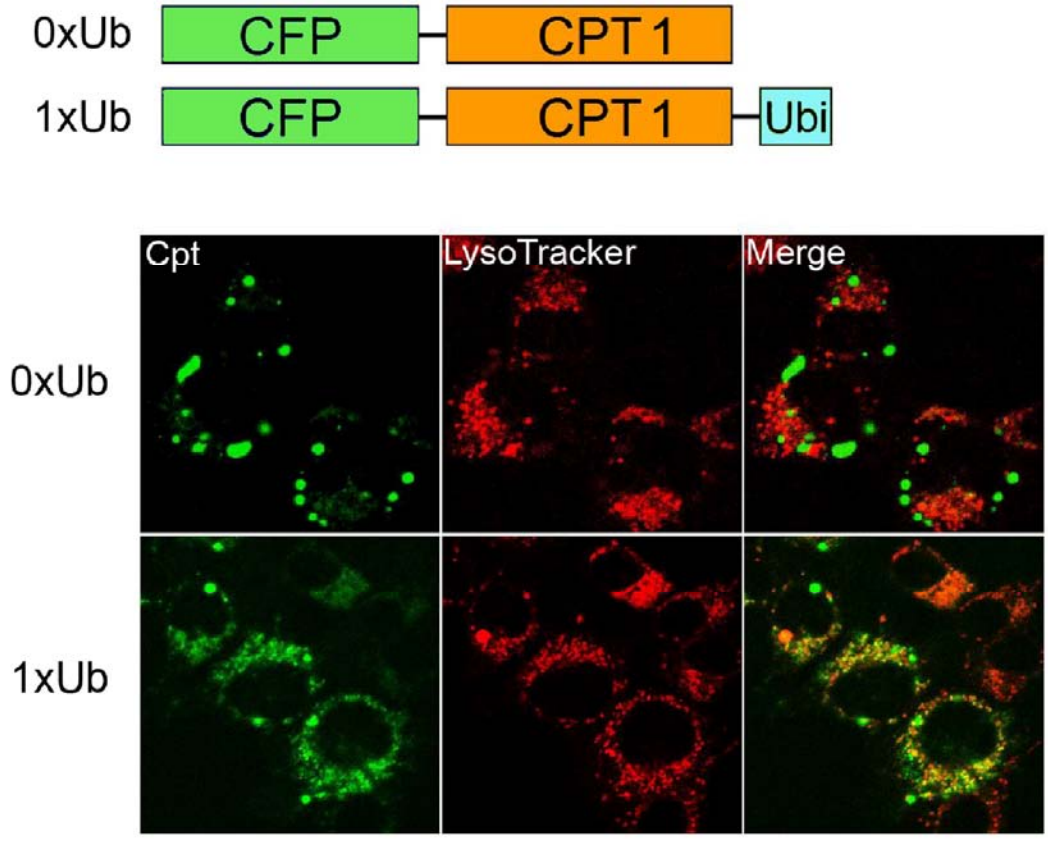
0xUb
CFP
CPT1
1xUb
CFP
CPT1
Ubi
Cpt
LysoTracker
Merge
0xUb
1xUb

Figure 22. CPT1 K→R mutants are resistant to LPCAT1-induced degradation

(A) MLE cells were un-transfected or transfected with plasmid coding for CPT1-V5his, $CPT1_{K4R}$, or $CPT1_{K6R}$ alone or in combination with LPCAT1 coding plasmid, and cell lysates were separated by SDS-PAGE, transferred to nitrocellulose, and LPCAT1, V5 (CPT1), and β-actin immunoblot analyses were performed (A). CPT activity assays were performed on above lysates (B). Cells were transfected as described above and, after 18 h, were treated with ^{3}[H] choline for 2 h. Cell lysates were harvested, and *de novo* PtdCho synthesis assays were performed. (C). Results are from at least three individual experiments, and mean ± S.E. was calculated in panels B-C. *$p<0.05$ versus paired controls.

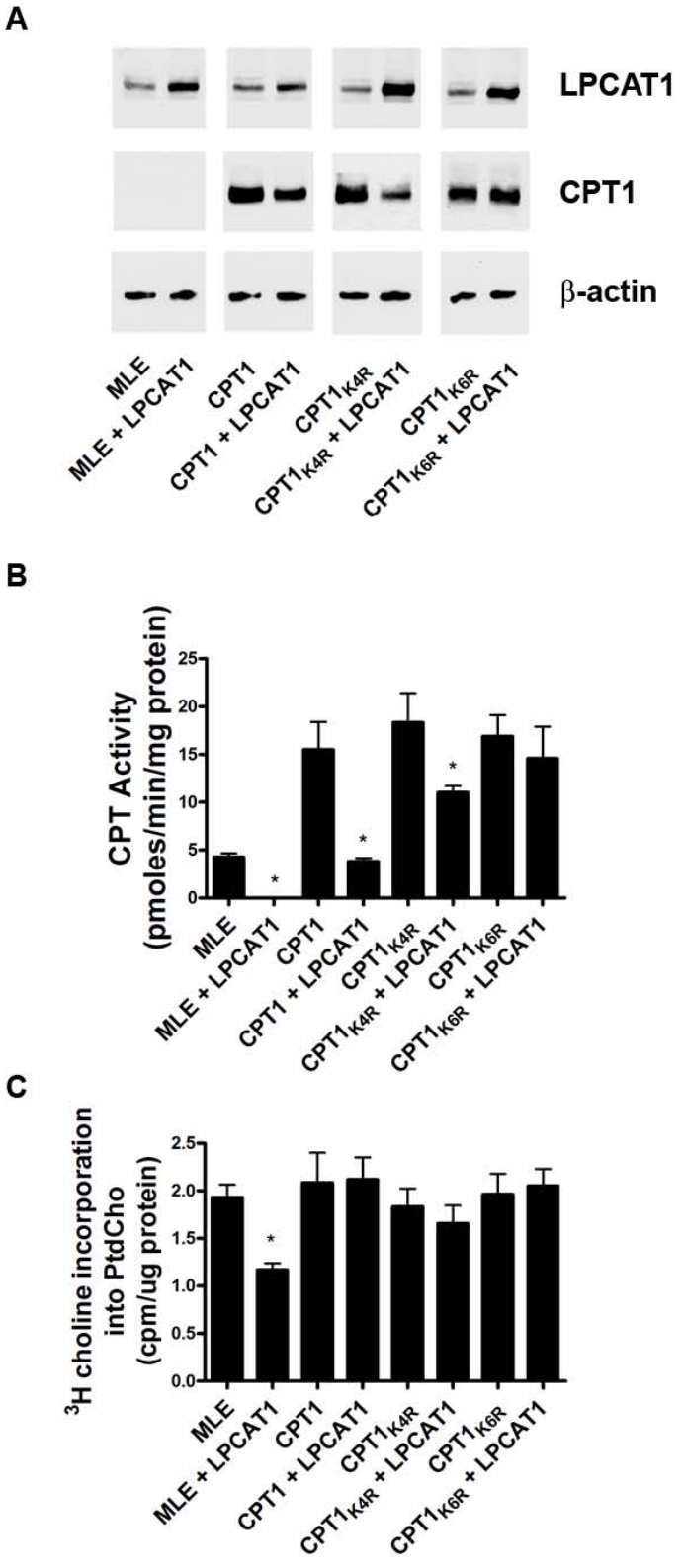
A
LPCAT1
CPT1
β-actin
MLE
MLE + LPCAT1
CPT1
CPT1 + LPCAT1
CPT1K4R
CPT1K4R + LPCAT1
CPT1K6R
CPT1K6R + LPCAT1
B
CPT Activity
(pmoles/min/mg protein)
25
20
15
10
5
0
*
*
*
MLE
MLE + LPCAT1
CPT1
CPT1 + LPCAT1
CPT1K4R
CPT1K4R + LPCAT1
CPT1K6R
CPT1K6R + LPCAT1
C
3H choline incorporation
into PtdCho
(cpm/ug protein)
2.5
2.0
1.5
1.0
0.5
0.0
*
MLE
MLE + LPCAT1
CPT1
CPT1 + LPCAT1
CPT1K4R
CPT1K4R + LPCAT1
CPT1K6R
CPT1K6R + LPCAT1

Figure 23. E3 Ubiquitin ligase (β-TrCP) overexpression causes CPT1 degradation

Cells were transfected with plasmid encoding CPT1-V5his and a plasmid coding for one of the following E3 ubiquitin ligases: no ligase (NT), β-TrCP, FbxW4, Fbxo4, Fbxo15, or FbxL2. Cells were collected 18h post-transfection. Cell lysates were separated by SDS-PAGE, transferred to nitrocellulose, and V5 immunoblot analyses were performed. Results are representative of at least three individual experiments.

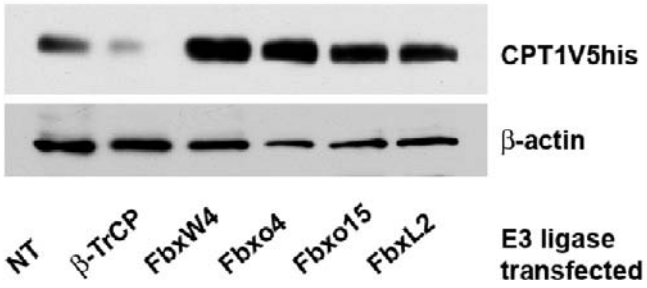
CPT1V5his
β-actin
NT
β-TrCP
FbxW4
Fbxo4
Fbxo15
FbxL2
E3 ligase transfected

CHAPTER IV

β-TrCP TARGETS LPCAT1 FOR POLYUBIQUITINATION

Abstract

A recently discovered acyltransferase, LPCAT1, has been implicated as the key enzyme responsible for PtdCho remodeling in lung epithelia [10, 11]. Substrate specificity, enzymatic cation requirements, and binding affinities have been measured for this enzyme, but cellular and physiologic responses to possible protein modifications such as phosphorylation have not been investigated. LPCAT1 has been described as a membrane-associated enzyme, similar to other lipogenic enzymes. Because, ubiquitin modification is a common modification regulating the behavior and fate of membrane-associated lipid synthesizing enzymes, I pursued studies on LPCAT1 protein stability. I confirmed the ability of recombinant ubiqutin-HA to become attached to LPCAT1, suggesting LPCAT1 is ubiquitinated *in vivo.* Through the use of transient transfection of multiple candidate E3 ubiquitin ligases into lung cells, my analyses suggest that β-TrCP is an E3 ubiquitin ligase potentially responsible for LPCAT1 ubiquitination. Preliminary data suggest LPCAT1 is phosphorylated *in vitro,* consistent with the known ability of β-TrCP to bind phosphorylated substrates. Decreased LPCAT1 activity and reduced [^{14}C] palmitate incorporation into cellular PtdCho (a marker of lipid synthesis) were observed in LPCAT1/ β-TrCP co-transfected cells. Using β-TrCP as a probe to trigger LPCAT1 degradation, MG-132 (a proteasomal inhibitor) was found to prevent LPCAT1 degradation. LPCAT1 degradation was not prevented in cells treated with NH_4Cl or leupeptin (acidifies lysosomal compartments or inhibits serine and cystine proteases, respectively). Other work shows immunoprecipitation of LPCAT1, followed by immunoblotting with anti-Ub antibodies, results in accumulation of high molecular weight ubiquitin conjugates. To further map ubiquitin acceptor sites within LPCAT1, I

constructed multiple carboxyl-terminal truncation mutants. Research in progress examines the ability of overexpressed β-TrCP to degrade mutants, and maps the β-TrCP binding site within LPCAT1. Overall, these preliminary observations indicate that LPCAT1 is ubiquitinated by the E3 ubiquitin ligase, β-TrCP, and subsequently processed for degradation within the 26S proteasome.

Introduction

Surfactant PtdCho is relatively unique because it is selectively enriched with 16:0/16:0 molecular species (DPPtdCho) on the phospholipid glycerol backbone and this species of DPPtdCho is not the primary product of the remodeling lipid synthesis pathway in lung type II cells. Indeed, perhaps ~55-75% of surfactant PtdCho is synthesized by the remodeling pathway with the remainder generated by *de novo* synthesis [17, 18, 143]. This pathway involves first cleavage of unsaturated PtdCho at the *sn*-2 position by a calcium-independent phospholipase A_2 generating LysoPtdCho and then re-acylation by an acyltransferase with a palmitate (16:0) fatty acid species, generating DPPtdCho. It is known that the calcium-independent phospholipase A2 is indispensable for surfactant homeostasis during lung development [90]. Relative to the *de novo* pathway, however, very limited data is available about the molecular and biochemical regulation of the remodeling pathway.

Until recently, the identity of the acyltransferase with substrate specificity for 16:0 palmitate remained elusive. In chapter II, I performed qrt-PCR experiments with specific primers detecting LPCAT1, and the two related species LPCAT2 and LPCAT3, to determine relative expression of these candidate acyltransferases (Fig. 3). The qrt-PCR data suggest LPCAT1 may be the acyltransferase important for surfactant synthesis because it is most abundant in mouse type II cells, the cells responsible for surfactant production, compared to nonsurfactant-secreting cells. Indeed, our results are consistent

with recent studies that have identified LPCAT1 as the putative acyltransferase responsible for lipid remodeling in lung type II cells [10, 11].

I have previously described the cellular consequences of the overexpression of LPCAT1 and its ability to down-regulate *de novo* PtdCho synthesis. Because PtdCho, and specifically DPPtdCho, is critical for lung cell survival and some lipogenic enzymes are regulated at the level of protein stability [81, 100], I investigated the cellular mechanism for LPCAT1 degradation. In chapter II, I have demonstrated the ability of keratinocyte growth factor (KGF) to stimulate an increase in LPCAT1 activity and protein levels. Although LPCAT1 activity and LPCAT1 mRNA transcript levels increase almost 10-fold in response to glucocorticoids [10], almost nothing is known about this enzyme's post-translational regulation. The lung must have intrinsic control mechanisms at the molecular level to rapidly increase levels of LPCAT1 at times when the need for surfactant DPPtdCho increases. Although transcriptional control, mRNA translational efficiency, or mRNA stability are attractive mechanisms for LPCAT1 control, these processes may be delayed and not rapidly responsive in times of cellular stress. Thus, it is possible that post-translational control also plays a role as an early event in controlling levels or functionality of LPCAT1. In this regard, my *in vitro* data indicate that LPCAT1 is a substrate for phosphorylation. LPCAT1 phosphorylation increases its activity; this mechanism might also modify LPCAT1 vulnerability to proteolysis, change localization, or allow for binding to different partners as described elsewhere [144-146].

Herein, I hypothesized that the PtdCho remodeling enzyme LPCAT1 is regulated by protein ubiquitination. Consistent with this hypothesis, my preliminary data showing that LPCAT1 is phosphorylated makes it a potential target for several E3 ubiquitin ligases. My studies indicate that β-TrCP may be one E3 ubiquitin ligase involved in recognition of LPCAT1 for subsequent degradation within the proteasome. Investigations on the protein stability of LPCAT1 will provide new insight into the

molecular apparatus involved in control of the enzymatic behavior of this key protein in surfactant lipid homeostasis.

Results

LPCAT1 is phosphorylated in vitro

Phosphorylation is a modification common to many membrane-bound enzymes and receptors, most notably receptor tyrosine kinases. Our laboratory has studied PtdCho enzymes that are phosphorylated (CCT) by proline-directed kinases. As most phosphorylated proteins have tyrosine, serine, or threonine residues as acceptor sites, I first determined if LPCAT1 is phosphorylated *in vitro*. First, MLE cells were transfected with plasmid coding for LPCAT1-V5. Cells were then harvested after 18 h, and cell lysates de-phosphorylated with λ phosphatase (PPase) (Fig. 24A) or left untreated with phosphatase (Fig. 24B). Then, lysates were treated with sodium orthovanadate to inhibit PPase activity (Fig. 24A), and lysates were phosphorylated using protein kinase C (PKC) in the presence of ^{32}P-γ-ATP (Fig. 24A, B). A LPCAT-V5 V5 immunoprecipitation was performed, and elutants were separated by SDS-PAGE, transferred to nitrocellulose, and blots exposed to X-ray films for detection of ^{32}P incorporation (Fig. 24A, B upper) followed by LPCAT1 immunoblot analyses (Fig. 24A, B lower). Data presented in the upper panels of Figure 24A and 24B do show non-specific signals in the lanes not treated with PKC. Non-specific signals may be the result of insufficient washing of the protein A/G matrix used for immunoprecipitation, or endogenous kinase activity.

Microsomal fractions (ER and Golgi sub-fractions of cell lysate obtained from centrifugation) were also collected from untransfected cells incubated for 1.5h with buffer alone (CON) or with 10 or 15 units of alkaline phosphatase (AP) or with heat-denatured AP (dCON) as a control. Samples were then separated by SDS-PAGE, transferred to nitrocellulose, and LPCAT1 immunoblot analysis performed (Fig. 24C) or lysates were assayed for LPCAT enzyme activity (Fig. 24D). Immunoblot analysis

reveals that phosphatase treatment alters the migration of a subpopulation of detectable LPCAT1 (Fig. 24C). The altered LPCAT1 population migrates more slowly by SDS-PAGE and phosphatase treatment decreases the prevalence of the slowest migrating detectable band, which is consistent with phosphorylation. Interestingly, the phosphatase treated microsome fractions also display decreased LPCAT activity, suggesting that phosphorylated LPCAT1 may be more enzymatically active (Fig 24D). These results demonstrate for the first time that LPCAT1 may be regulated by phosphorylation and that LPCAT1 is phosphorylated in response to the addition of PKC *in vitro*.

LPCAT1 is ubiquitinated in vivo

LPCAT1 is a transmembrane protein, associated with the endoplasmic reticulum (ER) that harbors from 1-3 transmembrane domains within its amino-terminus and contains a KKXX di-lysine ER retention signal at its carboxyl-terminus. It is common for transmembrane proteins to be trafficked through the endocytic pathway via their ubiquitination [127, 131, 147]. It is also possible that LPCAT1 could be proteolytically cleaved and degraded within the cytosol by the proteasome or degraded while still attached to the ER membrane [148]. To determine if LPCAT1, similar to CCT or CPT1, is ubiquitinated, I transfected MLE cells with plasmids coding for LPCAT1, LPCAT1-V5his, or Flag-his-LPCAT1 in combination with or without HA-ubiquitin plasmid (Fig. 25 A and B). Cells were harvested and cell lysates was separated by SDS-PAGE, transferred to nitrocellulose, and V5 and LPCAT1 immunoblot analyses were performed. Immunoblot analyses revealed the presence of several higher molecular weight forms of LPCAT1 that were enriched in cells co-expressing HA-ubiquitin (Fig. 25A, * indicate distinct band). The co-expression of HA-ubiquitin allowed for the detection of higher molecular weight forms of ubiquitin that are conjugates of modified proteins. Cell lysates used in Fig. 25A were also used in HA immunoprecipitation experiments (Fig 25B). After HA immunoprecipitation, elutants were separated by SDS-PAGE,

transferred to nitrocellulose, and V5 immunoblot analyses were performed. Immunoblot analysis for detection of LPCAT1-V5his suggests the enzyme is associated with HA-ubiquitin by detection of several conjugates of LPCAT1-V5his with a ladder banding pattern indicative of poly-ubiquitination chains (Fig. 25B, * indicates distinct band). Thus, these observations, though preliminary, suggest that LPCAT1 may be ubiquitinated.

β-TrCP E3 ubiquitin ligase regulates LPCAT1 ubiquitination

The recognition of substrates by some SCF E3 ubiquitin ligases is dependent upon phosphorylation [83-86]. One such E3 ubiquitin ligase, termed beta-transducin repeat-containing protein (β-TrCP), was thus a candidate for LPCAT1 ubiquitination because primary targets of β-TrCP-mediated ubiquitination are phosphorylated. Therefore, I chose to transfect several plasmids encoding candidate SCF ubiquitin E3 ligases into cells to determine the identity of a putative LPCAT1 E3 ubiquitin ligase. I transfected MLE cells with plasmid coding for β-TrCP and other plasmids coding for candidate SCF E3 ligases: FbxW4, Fbxo4, Fbxo15, or FbxL2; untransfected MLE cells served as a negative control. Eighteen hours later, cells were harvested and cell lysates were separated by SDS-PAGE, transferred to nitrocellulose, and LPCAT1 and β-actin immunoblot analyses were performed (Fig. 26A, upper). The data suggest that endogenous levels of LPCAT1 decrease significantly with co-transfection of β-TrCP when compared to control and other candidate E3 ubiquitin ligases. Preliminary data show that endogenous LPCAT activity after β-TrCP transfection also decreases (Fig. 26A, lower). To further determine the effects of β-TrCP overexpression on LPCAT activity and PtdCho synthesis, LPCAT1-V5his coding plasmid was expressed in cells with or without overexpressed β-TrCP coding plasmid. Cells were harvested, cell lysates were separated by SDS-PAGE, transferred to nitrocellulose, and V5 and β-actin immunoblot analyses were performed

(Fig. 26B). Cell lysates were also used in LPCAT activity assays (Fig. 26C). Cells transfected as above (Fig. 26C) and were labeled with ^{3}[H] palmitate for 5 h and cell lysates were collected. Lipid extractions were performed on lysates and TLC analysis separated radio-labeled PtdCho for measurement (Fig 26D), a marker of phospholipid synthesis and remodeling. Data presented in Fig. 26 show that both endogenous and recombinantly expressed LPCAT1 protein are reduced in cells overexpressing β-TrCP when compared to controls. Also, down-regulation of LPCAT1 protein levels relates to an observed decrease in cellular LPCAT and palmitate incorporation into PtdCho.

Finally, cells transfected with plasmid coding for LPCAT1 with or without β-TrCP coding plasmid were exposed to MG-132 (proteasome inhibitor), leupeptin (lysosome inhibitor), or no inhibitor followed by lysates separation by SDS-PAGE, transfer to nitrocellulose, and LPCAT1 immunoblotting or LPCAT1 immunoprecipitation followed by separation of elutants by SDS-PAGE, transfer to nitrocellulose, and ubiquitin immunoblotting (Fig. 27A, B). In experiments presented in panel A and B, inhibitors were added individually 18h post-transfection and incubated with cells for 18h. It is therefore possible that earlier application of agents or longer exposure to the inhibitors would enhance appearance of ubiquitinated LPCAT1. Higher molecular weight bands of LPCAT1 appear in MG-132-treated cells overexpressing β-TrCP and are more apparent after prolonged exposure of immunoblots (Fig. 27A, lower). LPCAT1 immunoblots from immunoprecipitation experiments show significant smearing in the lane containing MG-132-treated cells overexpressing β-TrCP (Fig. 27B). Cells treated with leupeptin did not show LPCAT1-Ub conjugates; however these species may be less prevalent and masked by the non-specific heavy chain signal. As a whole, these results suggest that the proteasomal pathway may contribute to LPCAT1 degradation. Importantly, although Fig. 27B does not support the hypothesis that LPCAT1 accumulates upon lysosome inhibition, Fig. 27A appears to support this hypothesis suggesting that different

immunoprecipitation conditions may be necessary to detect LPCAT1 that is trafficked though the lysosome.

β-TrCP E3 ubiquitin ligase may bind LPCAT1 at its amino-terminus

I next began to investigate where LPCAT1 may be ubiquitinated and where β-TrCP may be bound to LPCAT1. By constructing and transfecting expression plasmids encoding truncated LPCAT1 in MLE cells, I assessed the ability of β-TrCP to cause downregulation of LPCAT1 and LPCAT1 truncation mutants. Figure 28A represents a diagram of LPCAT1 with numerical labels for molecular sites corresponding to LPCAT1 truncation mutants. The diagram also highlights major domains within LPCAT1. First, LPCAT1, $LPCAT1_{1193\Delta}$, $LPCAT1_{968\Delta}$, or $LPCAT1_{728\Delta}$ coding plasmids were overexpressed with or without plasmid coding for β-TrCP. Following an 18 h incubation post-transfection, cell lysates were separated by SDS-PAGE, transferred to nitrocellulose, and V5 and β-TrCP immunoblot analyses were performed (Fig. 28B). β-TrCP seems to be overexpressed in all cases except for the $LPCAT1_{968\Delta}$ group, which would account for the unchanged levels of immunoreactive $LPCAT1_{968\Delta}$ in the pictured immunoblot. In another experiment, the three LPCAT1 truncation mutants were again overexpressed with β-TrCP and treated with MG-132 (Fig. 28C). In all cases, MG-132 triggered accumulation of V5 signal, suggesting that the mutants are still regulated by ubiquitination. I would like to note that the immunoblot shown in Figure 28C is overexposed to emphasize the accumulation of higher molecular weight conjugates which makes it is difficult to determine if β-TrCP effectively triggered LPCAT1 degradation. Furthermore, very few if any detectable higher molecular weight conjugates were identified for $LPCAT1_{728\Delta.}$ The data are preliminary but of interest because they demonstrate for the first time that LPCAT1 may be ubiquitinated by β-TrCP and this process likely occurs within a series of acceptor sites within a yet undefined amino-

terminal region of the enzyme. I am currently mapping these LPCAT1 ubiquitination sites with better precision; I will also map a possible β-TrCP binding site within LPCAT1.

Discussion

Until recently, enzymatic studies relating to PtdCho synthesis have centered on the rate-limiting enzyme, CCT, in the CDP-choline or *de novo* pathway because of its pivotal role in biosynthesis of this important phospholipid. Various groups, including our own, have discovered a new class of proteins exhibiting acyltransferase activities with varying substrate requirements for acyl-CoA and LysoPtdCho. I have previously shown in chapter II and III of this thesis that, for the first time, LPCAT1 is an acyltransferase that regulates the enzymatic behavior of CPT1 within the *de novo* pathway to maintain lipid homeostasis in lung epithelia. This "cross-talk" occurs through ubiquitination of CPT1 carboxyl-terminal lysine residues leading to enzyme degradation. The biological importance of this discovery is that lung cells harbor an exquisite mechanism to shift the type of phospholipids from "nonsurfactant" to "surfactant" (DPPtdCho) under conditions when LPCAT1 mass is increased to preserve lung structure and function by increasing surfactant secretion into airways. The observation that CPT1 [82] and CCT [149] are highly regulated at the level of protein stability suggest a central role of the ubiquitin modification system in potentially governing the life-span of many lipogenic regulatory enzymes. Thus, the overall goal of the studies outlined within chapter IV is to examine the molecular mechanisms whereby LPCAT1 is regulated by protein ubiquitination within the cellular degradation pathway. My studies have attempted to determine the functional consequences of LPCAT1 modification within lung epithelial cells as it pertains to phospholipid (specifically surfactant) homeostasis.

Prior studies suggest that LPCAT1 is critical for DPPtdCho production and surfactant secretion in cells, as targeted deletion results in lethality and disrupted

surfactant balance [150]. To further investigate LPCAT1 regulatory networks involved in its disposal in cells, I determined enzyme protein stability. Because of the similarity of enzymatic products, substrates and the proposed membrane-bound nature of LPCAT1 and CPT1, I explored ubiquitination as one cellular mechanism for regulation. Interestingly, both enzymes appear to be regulated by a putative E3 ubiquitin ligase, β-TrCP. The discovery of LPCAT1 modification by ubiquitin conjugation is significant in the fact that none of the currently discovered lipid recycling acyltransferases have been shown to be regulated in this manner.

Thus far I have not been able to detect altered ubiquitination or susceptibility to β-TrCP overexpression in the LPCAT1 truncation mutants studied. Current mutants, $LPCAT1_{1193\Delta}$, $LPCAT1_{968\Delta}$, and $LPCAT1_{728\Delta}$, all appear to be ubiquitinated and degraded with β-TrCP overexpression. Truncation analysis has its limitations, as there is no argument that protein structure is altered which may activate other methods of mutant degradative clearance of a misfolded protein or a buried degradation signal could be exposed, for instance. A more precise method of determining molecular interaction sites, within enzymes, involves amino acid substitution mutants. Primary structural analysis of LPCAT1 has revealed two potential β-TrCP binding sites, one residing within the amino-terminal half and another located near the carboxyl-terminal end. Current studies are focusing on Ser→Arg mutants to inhibit phosphorylation at a likely phosphorylation-dependent motif –S-X-X-X-S- whereby β-TrCP binds LPCAT1; further testing will involve the use of various mutants containing substitutions of several lysine residues in the region of the proposed binding site to also determine a putative lysine ubiquitination site. One potential limitation is that proposed truncation mutations within LPCAT1 might alter enzymatic catalytic behavior or topology. Thus, the determination of the mechanism of LPCAT1 regulation will be based on truncation studies but will be complemented with internal and point mutants with the aim of minimizing the effect on overall LPCAT1 structure. Nevertheless, the hypothesis that critical serine residues

within this motif are important for β-TrCP docking to LPCAT1 is consistent with ability of β-TrCP to associate directly with phosphoserine-enriched binding motifs within its targets. I will also attempt to determine if β-TrCP binding is required for ubiquitination and proteasomal degradation of LPCAT1.

Unlike CPT1 ubiquitination, LPCAT1 is ubiquitinated and may be processed though the proteasome. Classically, membrane proteins are cleared and degraded through the lysosomal pathway. It is believed that LPCAT1 is bound to the ER membrane, but with fewer membrane-spanning domains than CPT1. As LPCAT1 contains transmembrane domains only within the amino-terminus, it may be degraded differently than proteins containing membrane-spanning domains throughout their sequences. For instance, it is possible that the enzyme is proteolytically cleaved and escorted to the proteasome or degraded while still attached to the ER membrane. Recent studies and reviews suggest a role for ubiquitination in Endoplasmic Reticulum associated degradation (ERAD) which may yield information regarding ubiquitination of ER-associated proteins in general [85, 151]. By extension, ER proteins may be ubiquitinated, treated as if misfolded, translocated, and degraded by the proteasome in a process similar to the ERAD [151]. I would like to note that there are inherent problems associated with long term inhibition of the proteasome pathway which lead to low availability of ubiquitin peptide, since the proteasome is unable to cleave many of its products and recycle conjugated ubiquitin. Inhibition of the proteasome can also arrest the cell cycle and cause cell death [152].

Phosphorylation is necessary for many SCF complexes to bind and ubiquitinate their substrates [153]. Future studies will explore the role of reversible phosphorylation of LPCAT1 with respect to ubiquitination, in response to specific kinases (e.g. PKC). One method I may utilize will involve the incubation of PPase in cells expressing LPCAT1 or LPCAT1 mutants in combination with or without β-TrCP, prior to cell lysis. After treatment, LPCAT1 protein levels and cellular activity will be measured; LPCAT1

will be immunoprecipitated, and relative β-TrCP binding will be assessed. I hypothesize that de-phosphorylation would negatively affect LPCAT1/β-TrCP binding and would therefore also protect LPCAT1 from degradation. As a complementary approach, LPCAT1-transfected cells could be harvested and treated with PPase before or after LPCAT1 immunoprecipitation. If β-TrCP binding to LPCAT1 is phosphorylation-dependent, then PPase treatment would effectively de-phosphorylate LPCAT1, leaving β-TrCP unbound to its substrate. If necessary, LPCAT1 phosphorylation mimetics could be used as controls in these experiments. Such studies will help elucidate the molecular signatures required for LPCAT1 ubiquitination by β-TrCP.

When I searched for potential phosphorylation sites within LPCAT1, NetPhos 2.0 server database analysis suggested that several signatures were present in the β-TrCP binding site. The major predictor of a β-TrCP binding site is the presence of two serine residues with three to four intervening amino acids. Although original β-TrCP binding was described as having a flexible glycine residue between the serine residues, that is no longer considered a prerequisite for a β-TrCP binding motif [153]. Interestingly, one article suggests it is the charge of the substrate binding site and not necessarily phosphorylated serine residues that are sufficient to allow for β-TrCP binding [154]. LPCAT1 contains a potential β-TrCP binding site in a conserved region of the enzyme at S^{178} and S^{182}. Thus, mutation of these residues will allow us to potentially describe the docking site within LPCAT1 utilized by β-TrCP.

Although the kinase(s) responsible for LPCAT1 phosphorylation is/are not known, prediction programs can aid in the identification of phosphorylation sites and potential kinase phosphorylation motifs. Prediction programs such as the internet based *Calmodulin Target Database*, although only suggestive, describe LPCAT1 as a potential calmodulin binding partner based upon several factors known to contribute to calmodulin binding (hydropathy, alpha-helical propensity, residue charge, and other characteristics). Calmodulin binding could be a potentially interesting method of LPCAT1 regulation

related to its phosphorylation and degradation by ubiquitination. It has been described that calmodulin recruits calmodulin kinase to various substrates for their phosphorylation [155]. In this manner, LPCAT1 may be phosphorylated by calmodulin kinase before β-TrCP is able to bind LPCAT1.

Interestingly, LPCAT1 may also be negatively regulated by cations, but results in the literature are conflicting. Some initial studies included Mg^{2+} in activity assays, and others described activity as Mg^{2+} and Ca^{2+}-independent [10, 11]. Although LPCAT1 activity was described as Ca^{2+}-independent, after careful analysis, cations may be inhibitory to LPCAT1 enzymatic activity [94]. The study of cation regulation of LPCAT1 was proposed because of the prediction of EF-hand-like motifs present in the carboxyl- terminus of LPCAT1. These motifs may bind Ca^{2+} and inhibit activity. Many mechanisms may account for increased intracellular Ca^{2+} concentration in cells undergoing apoptosis such as: i) Ca^{2+} release from organelles into the cytosol, ii) increased Ca^{2+} influx, or iii) decreased Ca^{2+} efflux. These mechanisms, alone, or in concert, lead to the increase of cytosolic Ca^{2+} above the normally observed lower μM range in the cytosol or ~1-2mM concentrations present in surfactant [156-158]. The increase of calcium ion concentration causes cytosolic phospholipase and protease enzymes to be activated, and when coupled with several signaling responses, leads to the demise of epithelia [156]. Strains of bacteria involved in pneumonia have also been implicated in the increase of cellular Ca^{2+} levels, which cause topographical changes in another lipogenic enzymes such as CCT [155]. Further studies are necessary before the Ca^{2+}-dependent localization change of LPCAT1 is confirmed, but this observation will eventually determine if LPCAT1 enzyme localization change is inhibitory or destructive to LPCAT1 or lung surfactant in general. Interestingly, β-TrCP has at least two known isoforms, one of which is located in the nucleus[102]. It would indeed be intriguing to determine if, by a novel mechanism, LPCAT1 is trafficked to the nucleus in times of Ca^{2+} influx leading to its ubiquitination by β-TrCP. Thus, cytosolic Ca^{2+} increase during

apoptosis appears to serve as an intrinsic signal that could also inhibit LPCAT1 function, limiting PtdCho remodeling.

The studies in this chapter begin to address the lack of biochemical information available in the field of phospholipid biochemistry as they relate to the molecular regulation of acyltransferases (LPCAT1), the major enzyme involved in surfactant phospholipid remodeling. Determining the molecular factors that govern LPCAT1 protein stability by ubiquitination provides a new model for cellular control of lipid remodeling. Further studies will need to assess this mechanism using more sophisticated *in vivo* systems (conditional-regulated E3 ligase components in murine systems, knockouts, etc.) to assess apoptotic cellular responses and surfactant in the context of lung injury. Inhibition of LPCAT1 degradation by use of small molecule (e.g. β-TrCP) antagonists may prove to be a more viable strategy of surfactant supplementation in patients with critical illness.

Experimental procedures

Materials

The source of murine lung epithelial (MLE) cells, culture medium, immunoblotting materials and radiochemicals were described previously [8]. Mouse monoclonal ubiquitin antibody was purchased from Cell Signaling (Danvers, MA). PCRTOPO4.1 cloning kit and pcDNA-DEST40 cloning vector, *E. coli* One Shot competent cells, the pENTR Directional TOPO cloning kits, LR clonase II recombinase, Superscript III RT kit, and the Gateway mammalian expression system were purchased from Invitrogen (Carlsbad, CA). Ni^{2+} resin, HIS-select Nickel Affinity gel, Tri Reagent, human KGF, and β-actin primary mouse monoclonal antibody were obtained from Sigma (St. Louis, MO). LPCAT1 antibody was generated by Covance (Princeton, NJ). Amicon Ultra-4 centrifugal filter devices were from Millipore (Billerica, MA). The QuickChange site-directed mutagenesis kit, XL-gold cells, and pCMV-Tag1 vector were from

Stratagene (La Jolla, CA). A ubiquitin plasmid was constructed as described [108]. The gel extraction kit and QIAprep Spin Miniprep kits were from Qiagen (Valencia, CA). NucleoBond Xtra Maxi prep kits were obtained from Macherey-Nagel (Bethlehem, PA). Cycloheximide (CHM) and UbiQapture-Q matrix was from Biomol (Plymouth Meeting, PA). HA-tagged ubiquitin was a gift from Dr. Peter Snyder (U. of Iowa). All restriction enzymes and ligases were purchased from New England Biolabs (Ipswich, MA). RQ1 DNase kit was purchased from Promega (Madison, WI). All DNA sequencing was performed by the University of Iowa DNA Core Facility. Cloning primers were purchased from IDT (Coralville, IA).

Expression plasmids

The coding sequence available for LPCAT1 on the NCBI website (NM_145376), was used to construct primers for cloning of genes to cDNA from mRNA via reverse transcriptase PCR from murine liver and kidney tissues. Amplified fragments were subcloned into PCRTOPO4.1, and sequenced, confirming identity to the deposited NCBI LPCAT1 sequence. The resulting PCRTOPO4.1 vector served as a source for cloning into pacAd5 CMV IRES eGFP pA, (University of Iowa DNA core) using ClaI and BamHI restriction sites. For LPCAT1-V5his and $LPCAT1_{1193\Delta}$, $LPCAT1_{968\Delta}$, and $LPCAT1_{728\Delta}$ (truncation numbers represent LPCA1 base pairs), the Invitrogen® Gateway System was used. Primers containing CACC overhangs upstream of the 5' ATG and antisense sequence without a stop codon were used for amplification using a blunt end polymerase and pENTR/D-TOPO per manufacturers' instruction. LR clonase II recombinase was used for cloning into a pcDNA-40 gateway vector. $LPCAT1_{K154R}$, $LPCAT1_{S177A}$, $LPCAT1_{S181A}$ and $LPCAT1_{S177\text{-}181A}$ were constructed by performing site-directed mutagenesis on LPCAT1 in the pacAd5 CMV IRES eGFP pA using the QuickChange II XL Site-Directed Mutagenesis (Stratagene) kit. Flaghis-LPCAT1 was

constructed by primer insertion amplifying LPCAT1 in the pacAd5 CMV IRES eGFP pA.

Cell isolation, culture, and transient transfection

Alveolar macrophages, primary type II cells, and fibroblasts were isolated as previously described [109]. MLE cells were maintained in HITES medium (DMEM F12) with 2% fetal bovine serum at 37^{o}C in 5% CO_2. After reaching 80% confluency, the cells were harvested using 0.25% trypsin and 0.1% EDTA, resuspended in medium, and plated onto appropriate culture dishes containing a 3 μl per 1μg DNA ratio of FuGENE6 lipofection reagent and appropriate expression vector. After incubation overnight, the medium was replaced with HITES medium with 2% fetal bovine serum for 8 h before cell harvesting. In some studies, an Amaxa electroporation device with program T-013 and solution L was used for plasmid transfection of cells. Cells were maintained as described as above, except after trypsinization, cells were resuspended in a small volume of solution L per manufacturer's directions. Plasmids were transfected into cells or cells were left untransfected. Medium was aspirated 24 h post-transfection, and cells were treated an additional 24 h with 0% FBS DMEM F12 medium supplemented with or without NH_4Cl (25 mM). Cells lysates were harvested by brief sonication in 150 mM NaCl, 50 mM Tris-HCl, 1 mm EDTA (no EDTA if Ni^{2+} purification performed), 2 mM dithiotreitol, 0.025% sodium azide, and 1 mM phenylmethylsulfonyl fluoride (pH 7.4) (Buffer A), at 4°C. Alternatively, cells were switched to DMEM F12 media without FBS and treated for 6 h with cycloheximide (CHM) (18 μg/mL) with either MG-132 (10 μM) or leupeptin (20 μM). Cells were collected in Buffer A + 0.5% Triton X-100 +0.5% NP-40 and sonicated for further analysis.

Isolation of microsome fractions

Cells were resuspended in Buffer A, and samples first centrifuged at 16,000 x g for 10 min at 4^{o}C. The resulting supernatant was centrifuged at 100,000 x g for 60 min at 4°C. The resulting microsomal pellet was resuspended in The resulting microsomal pellet was resuspended in a solution containing 250mM sucrose and 10mM Tris-HCl at pH=7.4 using a 25 G needle.

LPCAT1 phosphorylation and phosphorylation activity assays

MLE cells were transfected with plasmid coding for LPCAT1-V5. Cells were then harvested after 18 h, and cell lysates were subjected to de-phosphorylation with 1000 U of λ phosphatase (PPase) at 30°C for 1h. Then, lysates were treated with sodium orthovanadate (10mM in final lysate solution) to inhibit PPase activity, and lysates were phosphorylated using 0.1 µg protein kinase C (PKC) for 1h at 30°C in the presence of 12.5 µCi of ^{32}P-γ-ATP (30Ci/mmol). LPCAT1-V5 was immunoprecipitated with V5 antibody, was separated by SDS-PAGE, transferred to nitrocellulose, and blots exposed to X-ray films for detection of ^{32}P incorporation followed by LPCAT1 immunoblotting using rabbit antiserum. Lysates were de-phosphorylated with protein phosphatase (PPase) or left untreated with PPase. LPCAT1 protein and activity studies involved the collection of microsome fractions from untransfected cells incubated at 37°C for 1.5h with buffer alone (CON) or with 10 or 15 units of alkaline phosphatase (AP) or with denatured AP (dCON) as a control. Samples were then used in an LPCAT activity assay or separated by SDS-PAGE, transferred to nitrocellulose, and LPCAT1 immunoblot analysis performed.

Phospholipid analysis

Lipids were extracted from equal amounts of membrane protein, and levels of the individual phospholipids were quantitated with a phosphate assay [103]. DPPtdCho was assayed as before[8]. For PtdCho *de novo* synthesis, cells were pulsed with 1 µCi of [*methyl*-^{3}H]choline chloride during the final 2 h of incubation with choline- depleted medium. For remodeling activity, cells were labeled with 1.75 nM of [^{14}C] LysoPtdCho (55mCi/mmol) for 3 h. Total cellular lipids were extracted, resolved using thin layer chromatography (TLC), and processed for scintillation counting [8].

LPCAT activity

Cells were harvested in lysis buffer (250mM sucrose, 10mM Tris-HCl at pH=7.4), and equal amounts of microsomal cellular protein or cell lysate were used in the assay. One nmole of 1-palmitoyl-*sn*-glycero-3-phosphocholine was added for every µL of 5x assay buffer (final working concentration 65mM Tris-HCl, pH 7.4, 10mM $MgCl_2$, 12.5 mM fatty acid free BSA, 2mM EDTA) sonicated. 35 µL of H_2O and cellular protein was added to 10 µL sonicated assay buffer containing 5 µL of [1-^{14}C]acyl-CoA (0.1µCi, 1.8nmole) for a total assay volume of 50 µL. Upon addition of [1-^{14}C] acyl-CoA, samples were incubated at 30^{o}C for 10 min after which the reaction was terminated by addition of chloroform/methanol/H_2O (1:2:0.70 vol/vol). Total cellular lipids from reaction mixtures were extracted by the method of Bligh and Dyer [104], spotted on LK5D plates, and PtdCho was resolved using TLC and detected using a plate reader.

Immunoblot analysis– Immunoblotting was performed as described [100, 112]. The dilution factor for the LPCAT1, V5, and β-actin antibodies were 1:2000, 1:5000, and 1:10,000 respectively.

Immunoprecipitation

Cell lysates were incubated with 3 μL HA antibody (Sigma) at 4°C overnight. Next, 20 μL of Pierce protein A/G matrix was added and incubation continued for an additional 2h. The matrix was eluted with denaturing protein sample buffer prior to SDS-PAGE, transfer to nitrocellulose, and immunoblot analysis [100, 112].

Statistical analysis

Statistical analysis was performed by two-way analysis of variance or Student's *t* test. Data are presented as mean ± S.E.

Figure 24. LPCAT1 is a substrate for phosphorylation

(A,B) MLE cells were transfected with a plasmid coding for LPCAT1-V5, 200 µg of cell lysates were subjected to de-phosphorylation with λ phosphatase (PPase) (1000 U, 1 h at 30°C). Next, sodium orthovanadate (10mM) was added to inhibit PPase activity. Then, proteins were phosphorylated using PKC (0.1 µg, 1 h at 30°C) in the presence of 12.5 µCi of ^{32}P-γ-ATP (30Ci/mmol). LPCAT-V5 was immunoprecipitated with V5 antibody, elutants were separated by SDS-PAGE, transferred to nitrocellulose and blots were exposed to film (^{32}P, at top) followed by LPCAT1 immunoblotting (IB, bottom panels). (A) Cell lysates were de-phosphorylated, or (B) cell lysates were not de-phosphorylated by addition of PPase. NO represents no PKC addition. (C,D) Microsome fractions (10ug protein) from cells were incubated (90 min, 37°C) with buffer alone (CON) or with 10 or 15 units of alkaline phosphatase (AP) or with denatured AP (dCON) as a control. Samples were then separated by SDS-PAGE, transferred to nitrocellulose, and LPCAT1 immunoblot analysis performed (C) using rabbit antiserum (diluted 1:1,000) or assayed for LPCAT enzyme activity (D). Values are mean ± SD, from two separate experiments.

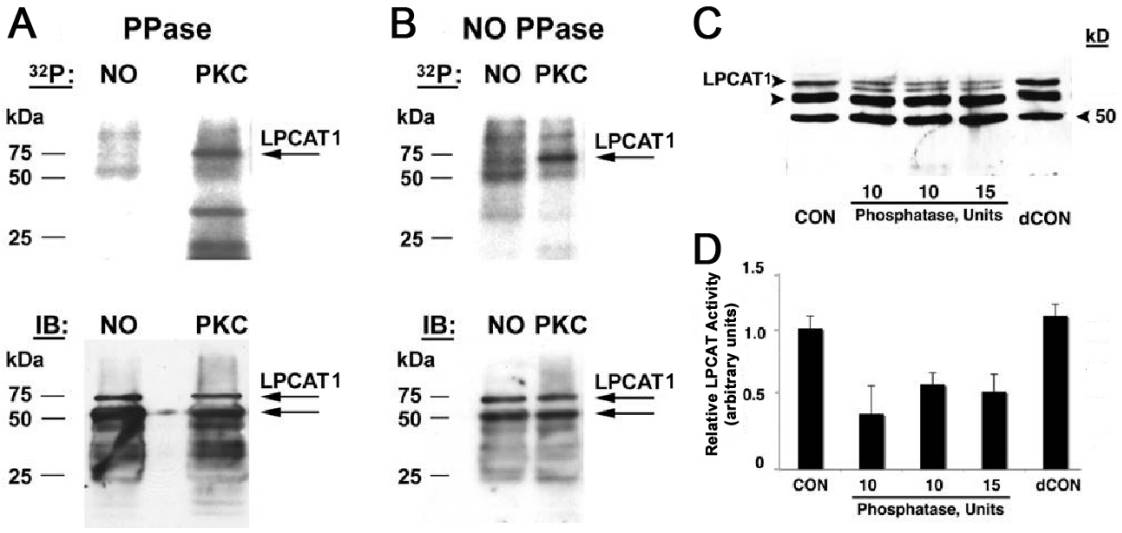
A
PPase
32P: NO PKC
kDa
75
50
25
LPCAT1
IB: NO PKC
kDa
75
50
25
LPCAT1
B
NO PPase
32P: NO PKC
kDa
75
50
25
LPCAT1
IB: NO PKC
kDa
75
50
25
LPCAT1
C
kD
LPCAT1
50
10 10 15
CON
Phosphatase, Units
dCON
D
Relative LPCAT Activity (arbitrary units)
1.5
1.0
0.5
0
CON
10 10 15
Phosphatase, Units
dCON

Figure 25. LPCAT1 is ubiquitinated

MLE cells were transfected with a plasmid coding for LPCAT1, LPCAT1-V5his, or Flag-his-LPCAT1 with or without HA-ubiquitin coding plasmid. Transfected cells were harvested and (A) separated by SDS-PAGE, transferred to nitrocellulose, and V5 and LPCAT1 immunoblot analysis was performed. (B) Cell lysates were incubated with HA antibody/protein A/G matrix, eluted, and elutants were separated by SDS-PAGE, transferred to nitrocellulose, and V5 immunoblot analysis was performed. Using these methods, as shown by *, slower migrating LPCAT1 species accumulate with HA-ubiquitin co-transfection and LPCAT1 was detected in association with HA-ubiquitin. HC= heavy chain immunoglobulins. Immunoblots are indicative of at least two experiments.

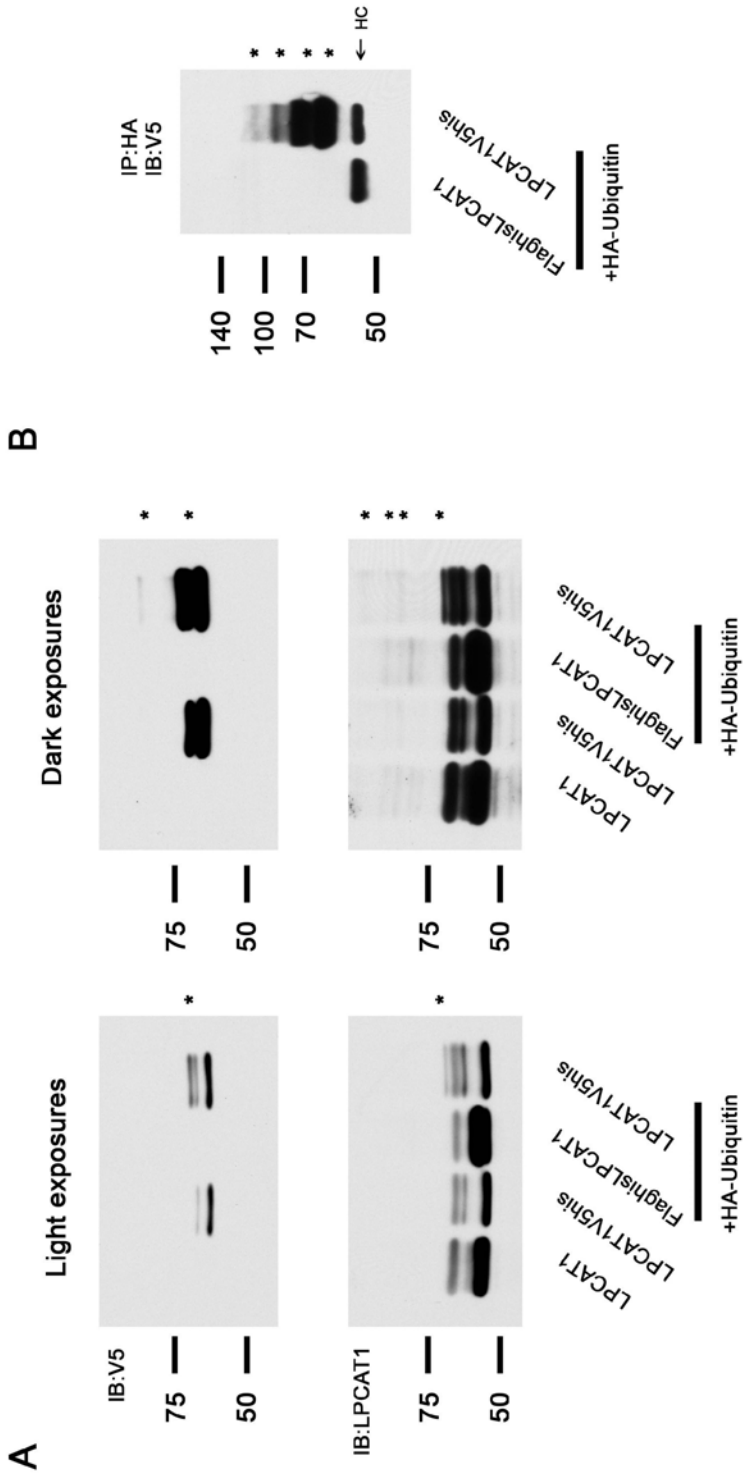
A
Light exposures
Dark exposures
IB:V5
IB:LPCAT1
75
50
LPCAT1
LPCAT1V5his
FlagHisLPCAT1
LPCAT1V5his
+HA-Ubiquitin
B
IP:HA
IB:V5
140
100
70
50
HC
FlagHisLPCAT1
LPCAT1V5his
+HA-Ubiquitin

Figure 26. E3 ubiquitin ligase β-TrCP causes LPCAT1 degradation

(A) MLE cells were transfected with plasmids coding for one of the following E3 ubiquitin ligases: no ligase (NT), β-TrCP, FbxW4, Fbxo4, Fbxo15, or FbxL2. Cells were collected 18h post-transfection and cell lysates were separated by SDS-PAGE, transferred to nitrocellulose, and LPCAT1 and β-actin immunoblot analysis was performed (upper). Cell lysate from NT or b-TrCP transfected cells were used in LPCAT activity assays (lower). (B) Cells were transfected with no plasmid (MLE) or a plasmid encoding for LPCAT1 alone or in combination with a plasmid encoding β-TrCP. Cell lysates were separated by SDS-PAGE, transferred to nitrocellulose, and V5 and β-actin immunoblot analyses was performed. (C) LPCAT1 activities were measured in the above cell lysates. (D) Cells transfected as above were treated with [^{3}H]-palmitate. 5 h post-transfection radiolabeled PtdCho was measured. (A-D) Data are indicative of at least two experiments.

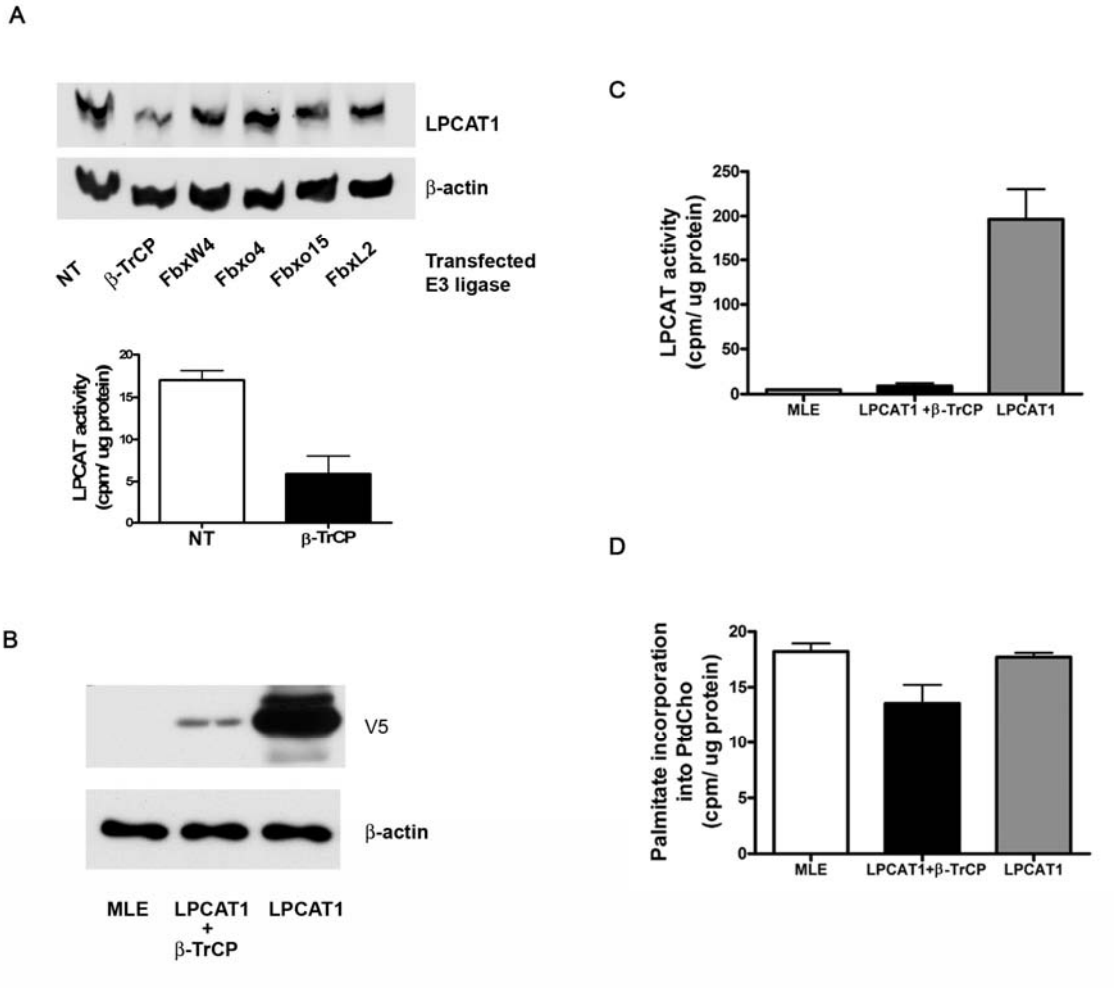
A
LPCAT1
β-actin
NT
β-TrCP
FbxW4
Fbxo4
Fbxo15
FbxL2
Transfected
E3 ligase
LPCAT activity
(cpm/ ug protein)
NT
β-TrCP
B
V5
β-actin
MLE
LPCAT1
+
β-TrCP
LPCAT1
C
LPCAT activity
(cpm/ ug protein)
MLE
LPCAT1 +β-TrCP
LPCAT1
D
Palmitate incorporation
into PtdCho
(cpm/ ug protein)
MLE
LPCAT1+β-TrCP
LPCAT1

Figure 27. LPCAT1 may be degraded through the proteasome pathway

MLE cells were transfected with or without a plasmid coding for β-TrCP and after 18h were incubated with no inhibitor (NT), MG-132 proteasomal inhibitor (10uM), or leupeptin lysosomal inhibitor (20uM) for an additional 18h. Treated cells were harvested and (A) separated by SDS-PAGE, transferred to nitrocellulose, and LPCAT1 immunoblot analyses was performed. (B) The above cell lysates were incubated with LPCAT1 antibody/protein A/G matrix, eluted, elutants were separated by SDS-PAGE, transferred to nitrocellulose, and ubiquitin immunoblot analysis was performed. As shown by *, slower migrating LPCAT1 species accumulate with MG-132 and leupeptin inhibitor exposure and a smear of LPCAT1 conjugates appears after immunoprecipitation of LPCAT1 and immunoblotting of ubiquitin when cells were treated with MG-132+β-TrCP. HC= heavy chain immunoglobulins. Immunoblots are indicative of at least two experiments.

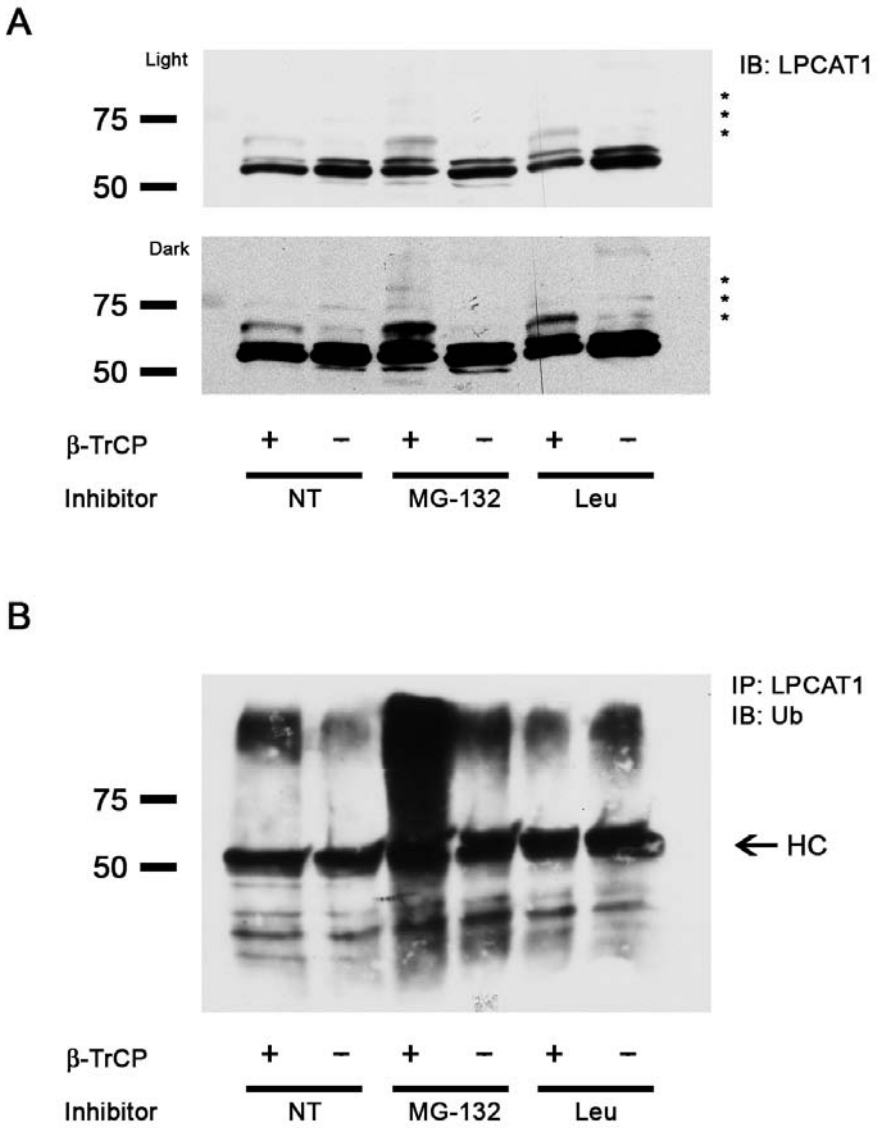
A
Light
75
50
IB: LPCAT1
Dark
75
50
β-TrCP
+ − + − + −
Inhibitor
NT
MG-132
Leu
B
75
50
IP: LPCAT1
IB: Ub
HC
β-TrCP
+ − + − + −
Inhibitor
NT
MG-132
Leu

Figure 28. LPCAT1 degradation may require ubiquitination of a lysine residue at the amino-terminal half of LPCAT1

(A) Diagram of LPCAT1 with labels for molecular sites corresponding to truncation mutants used in this figure. LPCAT1, $LPCAT1_{1193\Delta}$, $LPCAT1_{968\Delta}$, or $LPCAT1_{728\Delta}$ coding plasmids were transfected in MLE cells and were co-expressed with or without a plasmid coding β-TrCP. (B) After 18 h, cells were harvested and lysates were separated by SDS-PAGE, transferred to nitrocellulose, and V5 and β-TrCP immunoblot analyses were performed. (C) Similar to (B) except cells were treated for 18 h with or without the MG-132 proteasome inhibitor after an initial 18 h incubation post-transfection. Immunoblots are indicative of at least two experiments.

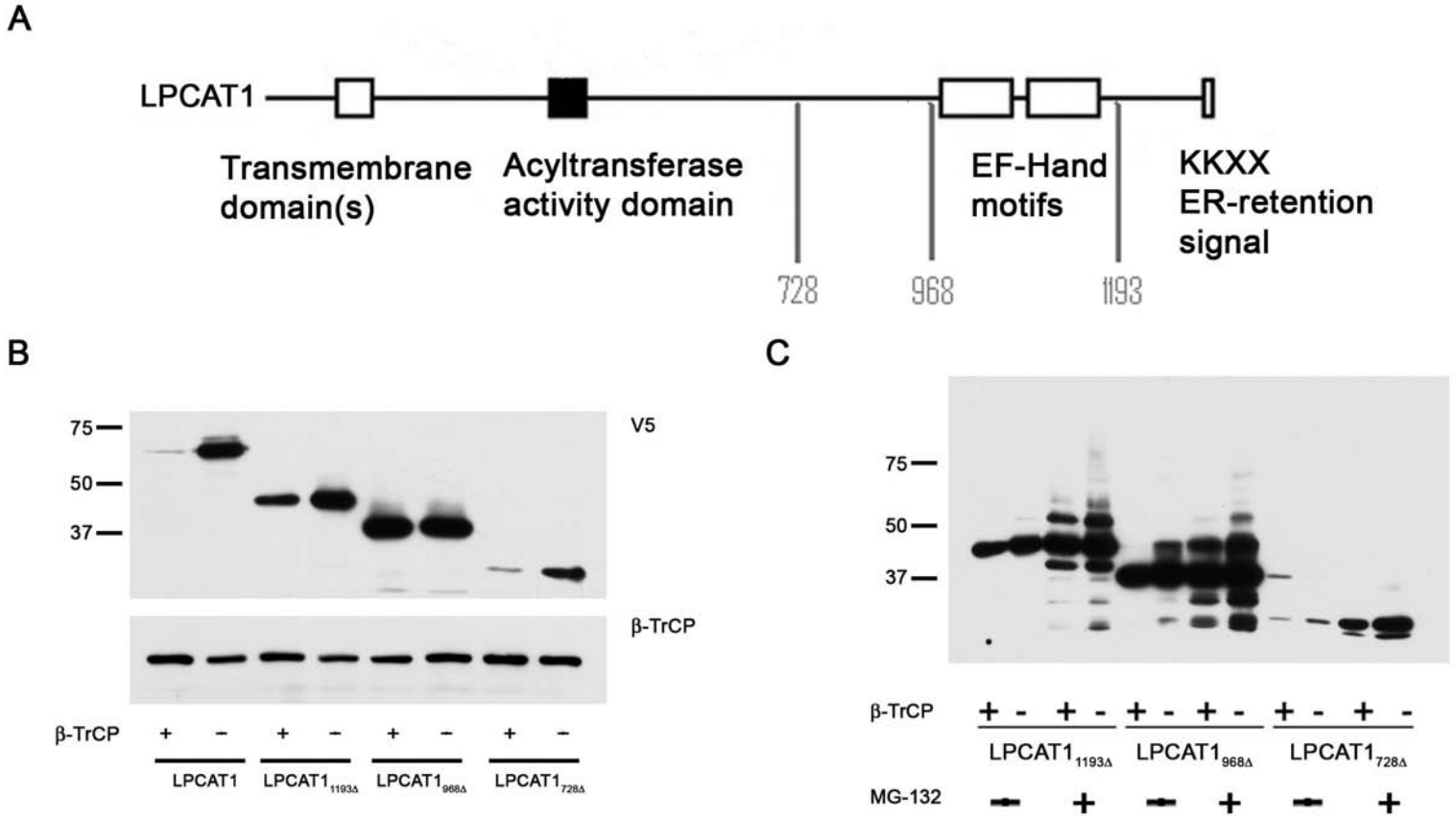
A
LPCAT1
Transmembrane domain(s)
Acyltransferase activity domain
EF-Hand motifs
KKXX ER-retention signal
728
968
1193
B
75
50
37
V5
β-TrCP
β-TrCP + − + − + − + −
LPCAT1
LPCAT1 1193Δ
LPCAT1 968Δ
LPCAT1 728Δ
C
75
50
37
β-TrCP + - + - + - + - + - + -
LPCAT1 1193Δ
LPCAT1 968Δ
LPCAT1 728Δ
MG-132 - + - + - +

CHAPTER V

SUMMARY AND FUTURE STUDIES

Lung epithelial cells are unique in that they secrete a lipid mixture that differs from the composition of lipid normally found in animal membranes. LPCAT1 functions in a key re-acylation/remodeling step to generate surfactant DPPtdCho phospholipid, a unique substance essential for mammalian life. LPCAT1 is a biosynthetic enzyme also essential for phospholipid synthesis, although very limited data is currently available on its regulation. The *de novo* PtdCho pathway complements LPCAT1 remodeling by synthesizing both saturated and unsaturated PtdCho. Acyltransferase activity and its possible role in DPPtdCho synthesis was first described as the Lands cycle [143]. However, this pathway, until recently, has been neglected. Similarly, little is known about the molecular behavior of the terminal enzyme in the *de novo* pathway, CPT1. My studies provide fundamentally new insight into the molecular regulation of these two enzymes at the level of protein turnover important to lipid synthesis. I demonstrate how phospholipid synthesis between the remodeling and *de novo* pathways is also linked by physiological interaction between LPCAT1 and CPT1 to maintain surfactant phospholipid balance in lung epithelia.

Ubiquitination is a common regulatory mechanism for maintaining steady-state levels of LPCAT1 and CPT1 proteins in mammalian cells. Interestingly, the degradative pathway utilized for control of levels of these two enzymes differs. Processing of CPT1 involves multi-ubiquitination and sorting through the endosome/lysosome pathway (Chapters II and III) while LPCAT1 is poly-ubiquitinated and degraded though the proteasome (Chapter IV). These pathways are not mutually exclusive and potential exists that both LPCAT1 and CPT1 are cleared at either site of disposal depending on cellular needs.

Endosomal sorting of ubiquitinated cargo has been best described by the recycling of cell surface receptor tyrosine kinases. This mechanism involves the binding of cell surface recognition ligands that leads to phosphorylation of receptors. This phosphorylation event targets the receptors for ubiquitination. Receptor ubiquitinated cargo trafficking appears to be mediated by adaptor molecules harboring an alpha-helical ubiquitin-interacting motif like the UIM domain but more than sixteen purtative ubiquitin-binding domains have been described [159, 160]. Ubiquitin-binding domains often specifically target the ubiquitin Leu8, Ile44, and Leu73 hydrophobic patch. The importance of ubiquitin as a multi-functional modification is highlighted in the fact that there are multiple binding motifs that recognize ubiquitin. Indeed, even proteins with similar functions such as the endosomal sorting complex required for transport (ESCRT-0, ESCRT-I, ESCRT-II, and ESCRT-III) complexes use different binding motifs to recognize ubiquitin. For instance, ESCRT-0 (Hrs/STAM) binds ubiquitinated proteins through its UIM for incorporation into the early endosomal pathway [161, 162]. In a subsequent step, ESCRT-I, a complex of three proteins, binds ubiquitin though the NH_2-terminal ubiquitin-conjugating enzyme E2 variant (UEV) domain located within Vps23/TSG101 [60]. The association of ESCRT-I with cargo is required for sorting of ubiquitinated proteins into the multi-vesicular body (MVB) system thought to be the initial recycling endosome. Interestingly, the UEV is related to E2 ubiquitin-conjugating enzymes but lacks catalytic activity [163]. ESCRT-II utilizes GRAM-like Ub binding in EAP45 (GLUE) domains for binding of ubiquitinated cargo [163]. Cell trafficking machinery utilize different ubiquitin binding domains, and recently, it was discovered that UBDs even appear to incorporate redundancies within the specific ESCRT complexes that make use of UBDs on different complex subunits highlighting the importance of the ubiquitinated cargo sorting [164].

Ubiquitin, as a signal, is often necessary for protein degradation, but alone may not be sufficient for cargo sorting and trafficking. Indeed, in addition to cytosolic

ubiquitin-binding adaptor molecules, DUBs may also play an important role. DUBs regulate the equilibrium ubiquitination state of enzymes that serve as substrates for the post-translational modification. In specific endosomal compartments where DUB concentration may be increased, enzymes containing differently conjugated ubiquitin chains may be recognized or targeted by specific DUBs for modification. In this way, different ubiquitinated proteins/receptors may enter the endocytic pathway and dissociate, processes that are also controlled by DUBs and add another layer of complexity to ubiquitinated cargo trafficking. Ultimately, this allows ubiquitinated enzymes to be trafficked to different subcellular locations and either undergo degradation or return to another cellular organelle.

Endosomal compartments contain the machinery necessary for enzyme trafficking to the lysosome, trans-Golgi network, or plasma membrane. As ubiquitin is further studied, an emerging concept is that it acts as a fluid signal capable of marking a protein for degradation, structurally modifying secondary structure to confer altered enzymatic activity, and trafficking and recycling enzymes from different organelles and the plasma membrane to the central MVB. Like phosphorylation, ubiquitination is a reversible post-translational modification that serves multiple functions. Although ubiquitin modification is often thought of as a marker for degradation, it is overlooked that ubiquitin is a fluid modification that can be removed by many DUBs within the cell. For example, ESCRT-0 complexes harbor SH3 phosphorylation domains as well as VHS domains that allow for binding of DUBs and incorporation of ubiquitinated cargo into endosome vesicles. Furthermore, two different DUBs, associated molecule with SH3 domain of STAM (AMSH) and ubiquitin isopeptidase Y (UBPY), have been observed associating with ESCRT-0/STAM for entry into the endosomal compartment. While UBPY cleaves both K-48- and K-63-linked ubiquitin chains, AMSH preferentially cleaves K-63-linked chains. In this manner, a system of DUBs and endosome-resident ligases may differentially target or effect transport of cargo by modifying the identity of

the ubiquitin chain linkages associated with a particular enzyme within the endosome. This modification creates an equilibrium of the pools of differentially modified enzymes which have various fates, whether it be recycling or degradation.

Because of the complex system involved with sorting and trafficking of ubiquitinated cargo, there are many possible avenues to pursue to further analyze the regulation of ubiquitinated CPT1. My studies have thus far shown CPT1 as a ubiquitinated enzyme which is trafficked through the endosome/lysosome pathway (Chapters II and III). Future studies could assess the repertoire of molecular binding partners of ubiquitinated CPT1 involved in the trafficking of CPT1 to the lysosome. Molecules such as TSG101 or GGA may be the initial proteins responsible for recognition of ubiquitinated CPT1 after it is ubiquitinated by a specific E3 ubiquitin ligase, possibly β-TrCP. This might involve analysis of the binding partners responsible for maintaining CPT1 retention within the endocytic pathway through initial immunoprecipitation experiments and more sophisticated approaches (yeast 2-hybrids, mass spectrometry, etc.). As there appears to be redundancy within the molecules involved in sorting of ubiquitinated cargos, CPT1 trafficking through the late endosomes to the lysosome may or may not rely on interactions of specific proteins within the ESCRT complexes.

LPCAT1 is also ubiquitinated, but unlike CPT1, its fate appears to be primarily degradation by the 26S proteasome. Studies are still ongoing for the identification of LPCAT1 ubiquitinated lysine residue(s) and the binding site for the putative E3 ubiquitin ligase β-TrCP within LPCAT1. As mentioned above, LPCAT1 is membrane-bound, but it is not an integral membrane protein like CPT1. Hydrophobicity plot programs reveal the possibility of three transmembrane domains within LPCAT1. It is also possible that LPCAT1 has only one true transmembrane domain. A single anchoring hydrophobic domain would act as a membrane tether while the other hydrophobic residue domains would aid in formation of a lipid binding pocket needed for either LysoPtdCho or

palmitoyl-CoA. After modification and binding site identification, it would be interesting to determine the function of LPCAT1 transmembrane domains, EF-hand motifs, and a di-lysine KKXX carboxyl-terminal tail believed to be associated with ER retention. The role of these domains in regulating LPCAT1 turnover has yet to be determined.

The function of an EF-hand-like domain within LPCAT1's carboxyl-terminus is of interest. In this regard, LPCAT1 is regulated by Ca^{2+} concentrations. Divalent ion concentrations in the mM range decrease LPCAT1 activity and both Mg^{2+} and Ca^{2+} have been shown to regulate the enzyme. Ca^{2+} regulation is consistent with other enzymes involved with lipid biogenesis [100]. Cellular cytosolic Ca^{2+} increase could be the result of bacterial infection (influx) or release from the mitochondria, resulting in increased calcium-activated neutral proteinases (e.g. calpains). Increased cytosolic Ca^{2+} can trigger apoptosis by activation of Ca^{2+}-dependent endonucleases [165, 166], calpain activation [167], activation of calcium/calmodulin-dependent protein kinase II phosphorylation of Akt leading to caspase activation [168], among other pathways that contribute to apoptosis. The regulation of LPCAT1 activity by Ca^{2+} could be the result of i) conformational changes with EF-hand motifs that inactivate the enzyme, ii) conformational changes with EF-hand motifs that preferentially target LPCAT1 for degradation, or iii) redistribution caused by EF-hand motifs binding Ca^{2+} [169] of LPCAT1 from the ER to the Golgi, plasma membrane, nucleus or other cellular organelles, altering its function.

The ability of LPCAT1 to bind Ca^{2+} is likely due to EF-Hand binding motifs. The EF-hand motif is best known for its role in Ca^{2+} binding to calmodulin. The properties of these motifs have been extensively studied and it has been discovered that they are composed of a helix-loop-helix structure. The motifs usually function in pairs with the domain linker region forming two small beta-sheets between the two motifs. A conformational change has, at least in part, been attributed to the way in which the motif binds and chelates Ca^{2+}. First, it is thought that the more flexible amino-terminal loop

coordinates Ca^{2+} followed by a repositioning of the carboxyl-terminal ligands necessary for completing the Ca^{2+} coordination sphere [170]. In calmodulin, the actions of Ca^{2+} are cooperative, as the binding of one Ca^{2+} increases the binding of an additional Ca^{2+} ion on the second motif. This cooperativity supports the close proximity and interactions leading to further conformational changes between the two motif tertiary structures.

Binding motif-induced conformational changes, even if slight, can cause significant changes in enzyme activity, stability, or other cellular processing. To determine if Ca^{2+} binding occurs at the proposed EF-hand motifs within LPCAT1, an internal deletion from amino acid 384-477, or mutation to important EF-hand domain residues, could be generated and the mutant proteins expressed in cells. Ca^{2+} sensitivity could then be evaluated by the effect of Ca^{2+} on LPCAT activity. Interestingly, within the 384-477 amino acid region of LPCAT1, up to four EF-hand motifs are candidate regions for study. If the LPCAT1 mutant(s) devoid of EF-hand-like domains are shown to retain enzyme activity and are resistant to the inhibitory effects of divalent ions, then the results would be confirmatory of the negative role of Ca^{2+} on LPCAT activity. There is little doubt that the binding of Ca^{2+} to LPCAT1 would cause conformational changes, but how the conformational change contributes to the overall loss of enzymatic activity has not been explored. Future *in vitro* experiments could entail purifying wild-type LPCAT1 and internal deletion mutants and testing both wild-type LPCAT1 and the internal EF-hand deletion mutants on Ca^{2+} responses. If the EF-hand binding motif contributes to the loss of LPCAT activity, the isolated internal deletion mutant acyltransferase activity would likely be unaffected by Ca^{2+} concentrations and remain highly active. These studies could be extended to models of pneumonia using bacteria, such as PA103 that are known to cause an influx of Ca^{2+} into cells to demonstrate biological relevance of studies of LPCAT1 regulation [155].

A calcium-induced conformational change (Fig. 29A, B) may also work in tandem with a localization change or may allow LPCAT1 to be exposed to proteolysis,

ubiquitination or other modifications. LPCAT1 is normally found in the ER membrane. It is hypothesized that the di-lysine KKXX carboxyl-terminal tail of LPCAT1 causes retrograde trafficking of LPCAT1 from the Golgi back to the ER. Immunofluorescence data suggest LPCAT1 localizes to the ER and Golgi [11]. Preliminary experiments using immunofluorescence and treatment of cells with calcium ionophore and H. *flu*, have allowed me to determine that intercellular Ca^{2+} regulates LPCAT1 trafficking (Figure 31). Similar experiments, involving lower concentrations Ca^{2+} appeared not to alter LPCAT1 localization, however [155]. Therefore, further investigation is necessary to determine the ability of physiologic levels of intracellular calcium to alter LPCAT1 localization. The mechanism by which LPCAT1 localization is shifted from the ER to the nucleus is still under investigation. Translocation of membrane proteins to the nucleus is not well described in the literature, but in yeast, translocation of gln3 from the Golgi to the nucleus has been observed [171]. It is possible that LPCAT1 binds calcium, causing a conformational change, which exposes a nuclear import signal or masks a nuclear export signal after a conformational change is initiated by Ca^{2+} binding. This process may or may not involve protease cleavage induced by elevated cytosolic Ca^{2+}, leading to translocation of the LPCAT1 fragment, with a masked nuclear export signal, to the nucleus. Such an event has been observed with Golgi protein p115, although, it does not contain a nuclear export signal [172]. It is unclear what role a LPCAT1 fragment would play in apoptosis or lipid synthesis, however. Preliminary primary structural analysis using the NetNES 1.1 server suggests that LPCAT1 may contain a nuclear export signal [173]. It is also possible that different cellular Ca^{2+} levels may dictate different LPCAT1 localization. Another possible change in localization could result from the masking of the di-lysine ER retention signal, thereby resulting in altered LPCAT1 localization by prevention of retrograde transport from the Golgi to the ER (Fig. 29C). A change in localization event could also affect substrate availability or expose LPCAT1 to different proteases or ligases associated with the Golgi or nuclear compartments. Ca^{2+}-bound

LPCAT1 may also be less stable due to an increased susceptibility to proteolysis, ubiquitination, or other modifications which may or may not be dependent on localization (Fig. 29D, E). The Ca^{2+} influx mechanism may be involved if increased Ca^{2+} levels are shown to reduce cellular LPCAT1 protein levels. Caspase inhibitors/substrates, calpain inhibitors, and proteasome inhibitors are among the agents that could be utilized to determine the mechanism by which LPCAT1 is regulated at high Ca^{2+} concentrations.

Finally, I propose a basic mechanism for the regulation of CPT1 and LPCAT1, from observations emerging from my work, now depicted in Figure 30. As shown in Figure 2, the *de novo* and LysoPtdCho remodeling pathways are responsible for PtdCho/DPPtdCho synthesis in lung epithelia. I propose that an increase in lipid synthesis, resulting from increased LPCAT1 activity, increases the phospholipid/cholesterol ratio thereby reducing local concentrations of sterols (e.g. cholesterol), thereby causing upregulation in the sterol regulatory element binding protein (SREBP) transcription factor. Next, SREBP causes increased transcription of 3-hydroxy-3-methylglutaryl-CoA reductase (HMG-CoA reductase) and CCT (and possibly CPT1) genes leading to increased mRNA and protein levels that would explain the data observed in Figure 9D [101, 174, 175]. Although previous studies suggest that CPT1 activity within cells is not increased by SREBP, the effect of the transcription factor on CPT1 transcript levels has not been explored [174, 175]. Increased HMG-CoA reductase activity then elevates farnesyl and geranyl production, which may stimulate β-TrCP lipid modification, causing its translocation to cellular membranes as observed for other proteins [176]. Once tethered to the Golgi membrane, β-TrCP is juxtaposed or in proximity to CPT1, allowing the E3 subunit to ubiquitinate the *de novo* enzyme, leading to CPT1 trafficking and degradation through the lysosome pathway. LPCAT1 also appears to be ubiquitinated by β-TrCP (Chapter IV), possibly in a phosphorylation-dependent manner, as LPCAT1 is a substrate for *in vitro* PKC phosphorylation (Fig. 24),

before its degradation. Finally, preliminary data suggest that LPCAT1 localization may be regulated by an increase in cytosolic Ca^{2+} (Fig. 31).

As a whole, the studies in this thesis expand our understanding of the regulatory mechanisms that influence lung phospholipid homeostasis, specifically focusing on the enzymatic behavior of two critical enzymes (CPT1 and LPCAT1) in surfactant biosynthesis. The fundamental mechanisms that control levels of each of these proteins in mammalian epithelia might serve as a springboard to generate novel interventions of degradative pathways that eventually preserve lung surfactant levels during pro-inflammatory stress.

Figure 29. Possible mechanisms of LPCAT1 regulation by increased Ca^{2+}

(A) Diagram of LPCAT1. (B) After an increase in cellular Ca^{2+} levels within the cytosol, the EF-hand motifs of LPCAT1 bind Ca^{2+} and the protein undergoes a conformational change. (C) Conformational change may cause the burying of the di-lysine ER-retention signal, burying of a nuclear export signal, or the exposing of a nuclear import signal, changing LPCAT1 localization. A change in conformation may also leave LPCAT1 more susceptible to (D) ubiquitination or (E) cleavage by calpain or caspase to lead to LPCAT1 loss of stability.

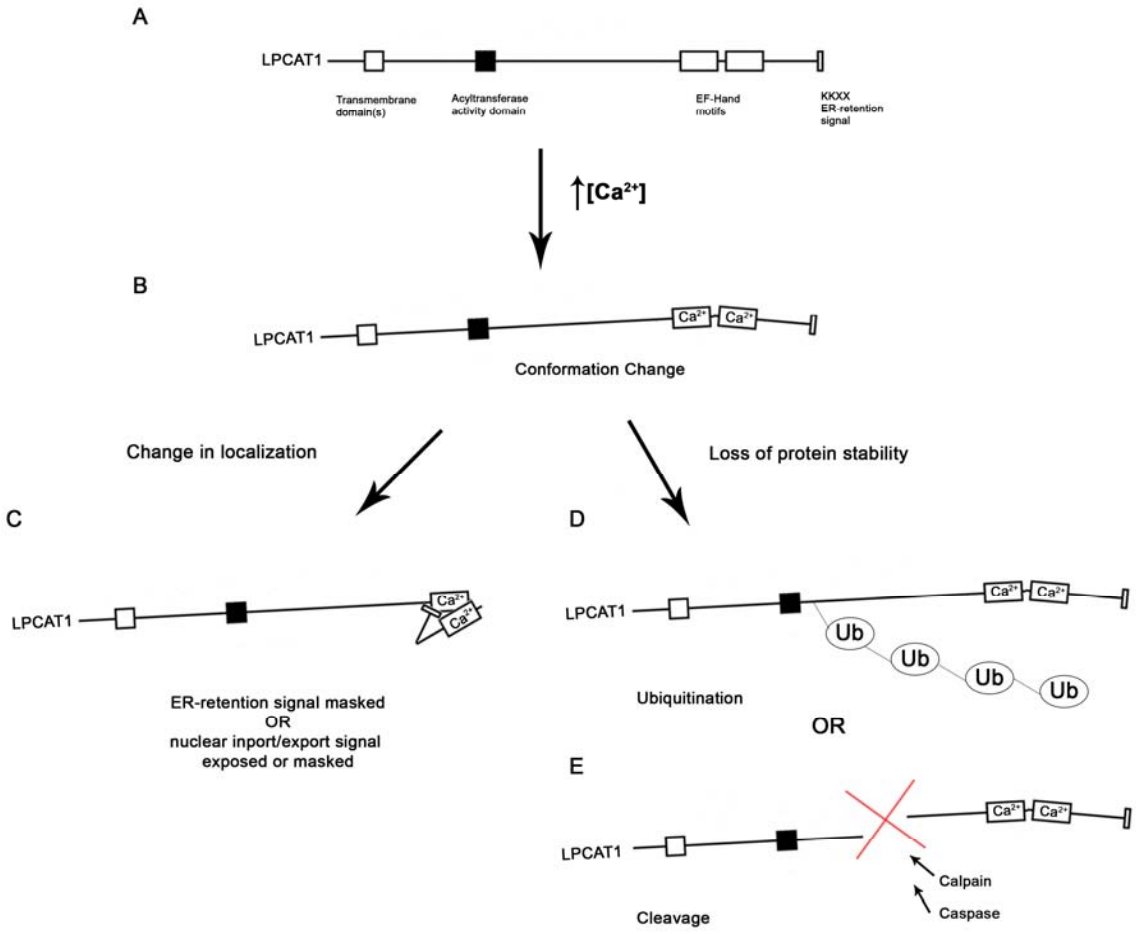
A
LPCAT1
Transmembrane domain(s)
Acyltransferase activity domain
EF-Hand motifs
KKXX ER-retention signal
↑[Ca2+]
B
LPCAT1
Ca2+
Ca2+
Conformation Change
Change in localization
Loss of protein stability
C
LPCAT1
Ca2+
Ca2+
ER-retention signal masked
OR
nuclear inport/export signal
exposed or masked
D
LPCAT1
Ca2+
Ca2+
Ub
Ub
Ub
Ub
Ubiquitination
OR
E
LPCAT1
Ca2+
Ca2+
Calpain
Caspase
Cleavage

Figure 30. Proposed overall mechanism of CPT1 and LPCAT1 regulation

A diagram of a proposed, overall mechanism of CPT1 and LPCAT1 regulation, from data presented in this thesis. The cartoon and proposed regulatory events link the *de novo* and remodeling pathways. Both the *de novo* and remodeling pathways contribute to phospholipid synthesis. I propose that an increase in lipid synthesis reduces local concentrations of sterols (e.g. cholesterol) causing increases in the SREBP transcription factor. SREBP causes increased transcription of CCT, HMG-CoA reductase, and possibly CPT1 genes leading to increased mRNA and protein levels. Increased HMG-CoA reductase activity elevates farnesyl and geranyl production, which may stimulate β-TrCP lipid modification causing its translocation to cellular membranes. Once tethered to the Golgi membrane, β-TrCP is near CPT1 and it ubiquitinates the *de novo* enzyme before its trafficking and degradation through the lysosomal pathway. LPCAT1 also appears to be ubiquitinated by β-TrCP, possibly in a phosphorylation-dependent manner. Finally, preliminary data suggests that LPCAT1 localization may be regulated by an increase in cytosolic Ca^{2+}.

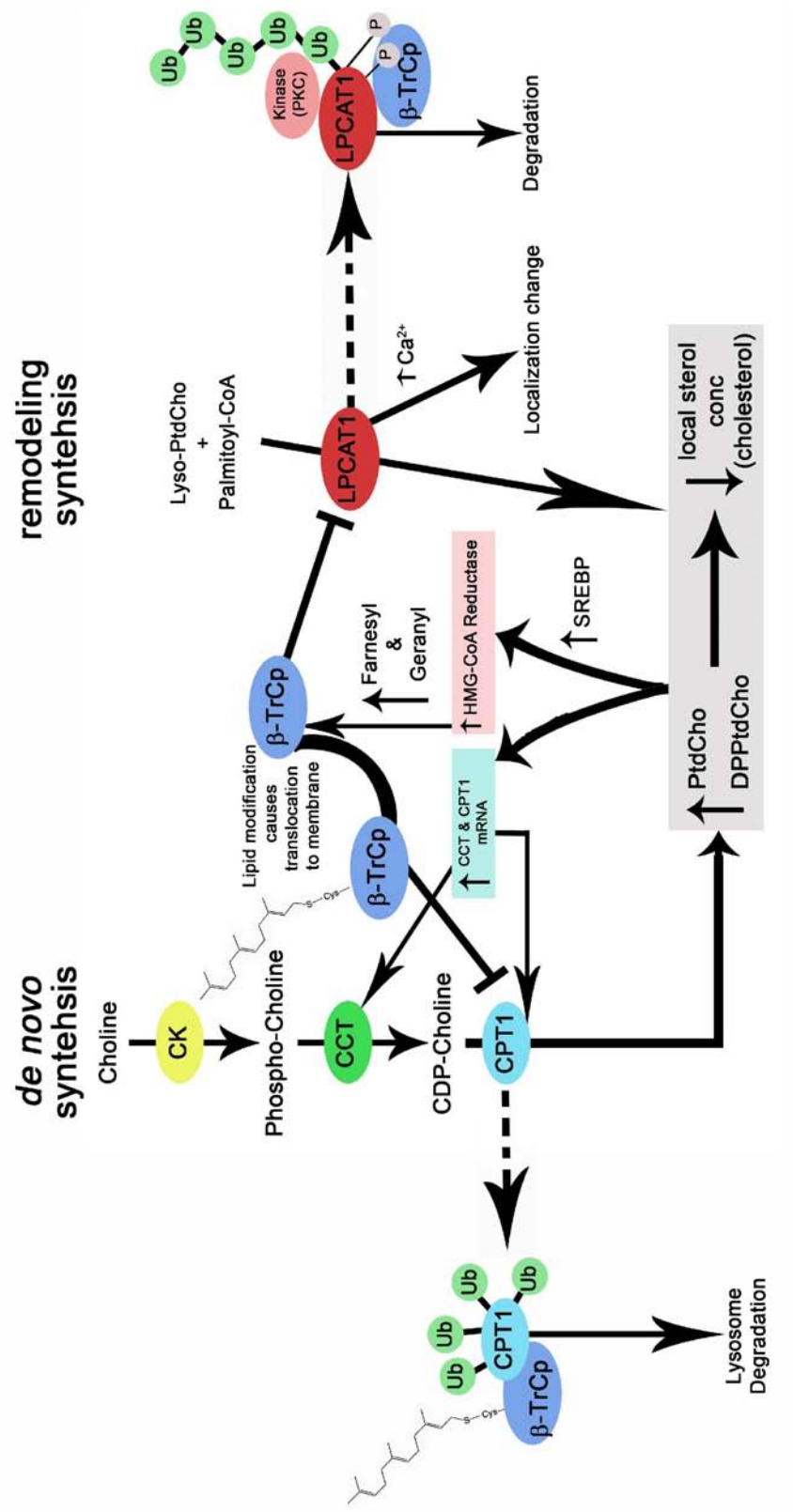
de novo
syntehsis
Choline
CK
Phospho-Choline
CCT
CDP-Choline
CPT1
remodeling
syntehsis
Lyso-PtdCho
+
Palmitoyl-CoA
LPCAT1
Ca2+
Localization change
Degradation
Kinase
(PKC)
β-TrCp
Ub
P
Lipid modification
causes
translocation
to membrane
Farnesyl
&
Geranyl
HMG-CoA Reductase
SREBP
CCT & CPT1
mRNA
PtdCho
DPPtdCho
local sterol
conc
(cholesterol)
Lysosome
Degradation

APPENDIX

Figure 31. Intracellular calcium levels may regulate LPCAT1

LPCAT1 contains several proposed EF-hand motifs associated with Ca^{2+} binding. The role of calcium on LPCAT1 expression was examined. One biological pathogen that causes pneumonia that also regulates cell calcium is *Haemophilus influenza (*H. *flu).* I incubated MLE cells in medium containing 5 mM, or 10 mM calcium with Ca^{2+} ionophore or H. *flu* (1:200). Cells visualized under the control conditions of 3mM Ca^{2+} and Ca^{2+} ionophore show minimal nuclear localization [155]. (A) An increase in medium Ca^{2+} concentrations to 5 mM or 10 mM and treatment with Ca^{2+} ionophore for 1-1.5 h appears to shift localization of LPCAT1 to the nucleus. Here, I used Alexa568 emission signals to visualize within cell nuclei and comparison in the bright field images. (B) Treatment of MLE cells in 5 mM Ca^{2+} in culture medium with H. *flu* was sufficient to alter localization of LPCAT1 from the ER to the nucleus. In future studies, I will incubate MLE cells in 1.8 mM (normal surfactant Ca^{2+} concentration levels) and 3 mM Ca^{2+}-containing media with H. *flu* to determine if bacterial infection alone is sufficient to alter LPCAT1 localization.

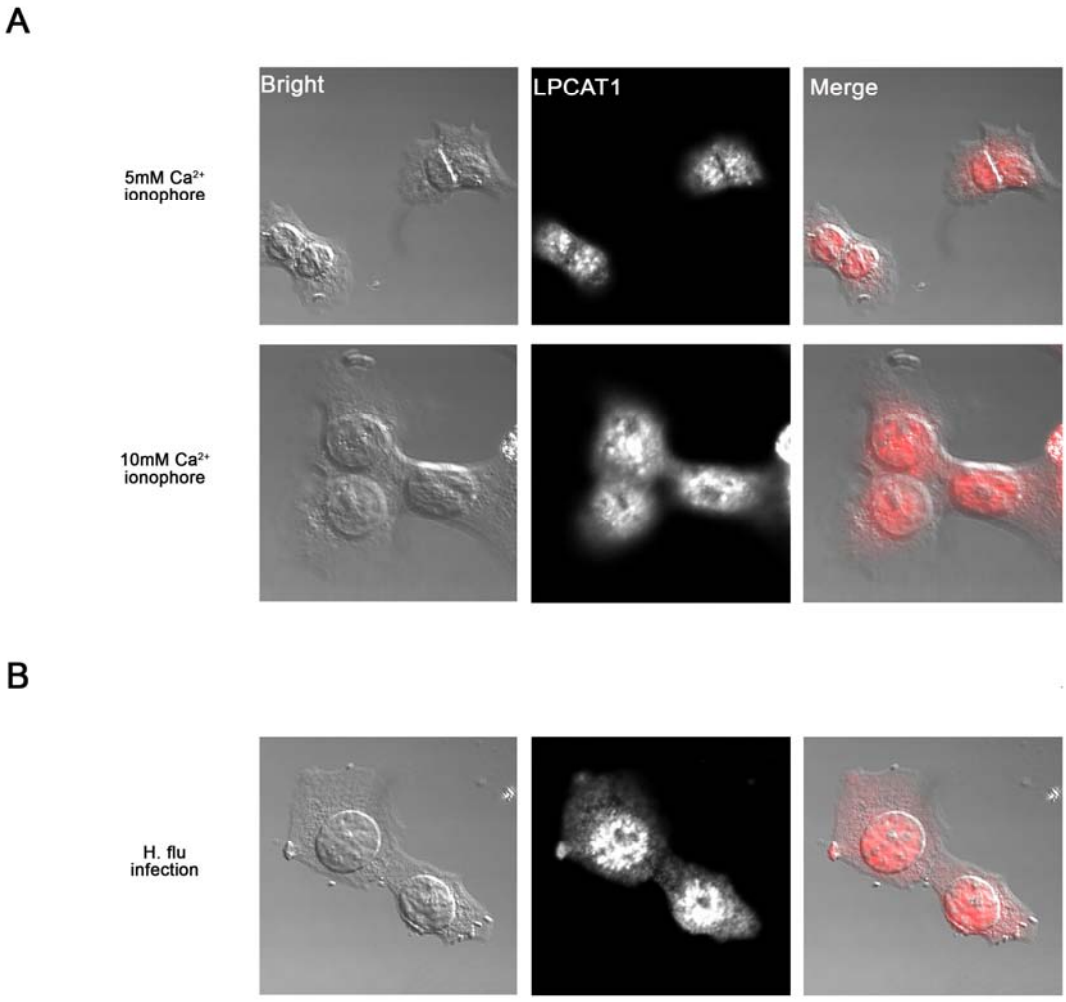
A
Bright
LPCAT1
Merge
5mM Ca2+ ionophore
10mM Ca2+ ionophore
B
H. flu infection

REFERENCES

1. Dobbs, L.G., et al., *Secretion of surfactant by primary cultures of alveolar type II cells isolated from rats.* Biochim Biophys Acta, 1982. **713**(1): p. 118-27.

2. King, R.J., *Pulmonary surfactant.* J Appl Physiol, 1982. **53**(1): p. 1-8.

3. Griese, M., et al., *Nebulization of a bovine surfactant in cystic fibrosis: a pilot study.* European Respiratory Journal, 1989. **10**(9): p. 1989-94.

4. Anzueto, A., et al., *Effects of aerosolized surfactant in patients with stable chronic bronchitis: a prospective randomized controlled trial.[comment]*. Jama., 1997. **278**(17): p. 1426-31.

5. Gross, I., et al., *Influence of epidermal growth factor on fetal rat lung development in vitro.* Pediatr Res, 1986. **20**(5): p. 473-7.

6. McMaster, C.R. and R.M. Bell, *Phosphatidylcholine biosynthesis via the CDP-choline pathway in Saccharomyces cerevisiae. Multiple mechanisms of regulation.* J Biol Chem, 1994. **269**(20): p. 14776-83.

7. Clement, J.M. and C. Kent, *CTP:phosphocholine cytidylyltransferase: insights into regulatory mechanisms and novel functions.* Biochem Biophys Res Commun, 1999. **257**(3): p. 643-50.

8. Mallampalli, R.K., et al., *Tumor necrosis factor-alpha inhibits expression of CTP:phosphocholine cytidylyltransferase.* J Biol Chem, 2000. **275**(13): p. 9699-708.

9. Lauber, K., et al., *Apoptotic cells induce migration of phagocytes via caspase-3-mediated release of a lipid attraction signal.* Cell, 2003. **113**(6): p. 717-30.

10. Chen, X., et al., *Identification and characterization of a lysophosphatidylcholine acyltransferase in alveolar type II cells.* Proc Natl Acad Sci U S A, 2006. **103**(31): p. 11724-9.

11. Nakanishi, H., et al., *Cloning and characterization of mouse lung-type acyl-CoA:lysophosphatidylcholine acyltransferase 1 (LPCAT1). Expression in alveolar type II cells and possible involvement in surfactant production.* J Biol Chem, 2006. **281**(29): p. 20140-7.

12. Smith, S.W., S.B. Weiss, and E.P. Kennedy, *The enzymatic dephosphorylation of phosphatidic acids.* J Biol Chem, 1957. **228**(2): p. 915-22.

13. Hjelmstad, R.H. and R.M. Bell, *sn-1,2-diacylglycerol choline- and ethanolaminephosphotransferases in Saccharomyces cerevisiae. Nucleotide sequence of the EPT1 gene and comparison of the CPT1 and EPT1 gene products.* J Biol Chem, 1991. **266**(8): p. 5094-103.

14. Hjelmstad, R.H. and R.M. Bell, *sn-1,2-diacylglycerol choline- and ethanolaminephosphotransferases in Saccharomyces cerevisiae. Mixed micellar analysis of the CPT1 and EPT1 gene products.* J Biol Chem, 1991. **266**(7): p. 4357-65.

15. Henneberry, A.L. and C.R. McMaster, *Cloning and expression of a human choline/ethanolaminephosphotransferase: synthesis of phosphatidylcholine and phosphatidylethanolamine.* Biochem J, 1999. **339 (Pt 2)**: p. 291-8.

16. Horibata, Y. and Y. Hirabayashi, *Identification and characterization of human ethanolaminephosphotransferase1.* J Lipid Res, 2007. **48**(3): p. 503-8.

17. Mason, R.J. and J. Nellenbogen, *Synthesis of saturated phosphatidylcholine and phosphatidylglycerol by freshly isolated rat alveolar type II cells.* Biochim Biophys Acta, 1984. **794**(3): p. 392-402.

18. den Breejen, J.N., J.J. Batenburg, and L.M. van Golde, *The species of acyl-CoA in subcellular fractions of type II cells isolated from adult rat lung and their incorporation into phosphatidic acid.* Biochim Biophys Acta, 1989. **1002**(3): p. 277-82.

19. Heath, R.J. and C.O. Rock, *A conserved histidine is essential for glycerolipid acyltransferase catalysis.* J Bacteriol, 1998. **180**(6): p. 1425-30.

20. Craig, J., *The Distribution of Surface Active Material in the Lungs of Infants with and without Respiratory Distress.* Biol Neonat, 1964. **7**: p. 185-202.

21. Thom, M.L. and R.D. Zachman, *The enzymes of lecithin biosynthesis in human neonatal lungs. IV. Phosphorylcholine cytidyltransferase.* Pediatr Res, 1975. **9**(4): p. 201-5.

22. McMahan, M.J., et al., *Surfactant associated protein (SAP-35) in amniotic fluid from diabetic and nondiabetic pregnancies.* Obstet Gynecol, 1987. **70**(1): p. 94-8.

23. Cheong, N., et al., *Functional and trafficking defects in ATP binding cassette A3 mutants associated with respiratory distress syndrome.* J Biol Chem, 2006. **281**(14): p. 9791-800.

24. Garmany, T.H., et al., *Surfactant composition and function in patients with ABCA3 mutations.* Pediatr Res, 2006. **59**(6): p. 801-5.

25. McCormack, F.X. and J.A. Whitsett, *The pulmonary collectins, SP-A and SP-D, orchestrate innate immunity in the lung.* J Clin Invest, 2002. **109**(6): p. 707-12.

26. Rooney, S.A., S.L. Young, and C.R. Mendelson, *Molecular and cellular processing of lung surfactant.* Faseb J, 1994. **8**(12): p. 957-67.

27. Schmitz, G. and G. Muller, *Structure and function of lamellar bodies, lipid-protein complexes involved in storage and secretion of cellular lipids.* J Lipid Res, 1991. **32**(10): p. 1539-70.

28. Osanai, K., R.J. Mason, and D.R. Voelker, *Pulmonary surfactant phosphatidylcholine transport bypasses the brefeldin A sensitive compartment of alveolar type II cells.* Biochim Biophys Acta, 2001. **1531**(3): p. 222-9.

29. Chevalier, G. and A.J. Collet, *In vivo incorporation of choline- 3 H, leucine- 3 H and galactose- 3 H in alveolar type II pneumocytes in relation to surfactant synthesis. A quantitative radoautographic study in mouse by electron microscopy.* Anat Rec, 1972. **174**(3): p. 289-310.

30. van Helvoort, A., et al., *Mice without phosphatidylcholine transfer protein have no defects in the secretion of phosphatidylcholine into bile or into lung airspaces.* Proc Natl Acad Sci U S A, 1999. **96**(20): p. 11501-6.

31. Weaver, T.E., C.L. Na, and M. Stahlman, *Biogenesis of lamellar bodies, lysosome-related organelles involved in storage and secretion of pulmonary surfactant.* Semin Cell Dev Biol, 2002. **13**(4): p. 263-70.

32. Agassandian, M., et al., *Oxysterols trigger ABCA1-mediated basolateral surfactant efflux.* Am J Respir Cell Mol Biol, 2004. **31**(2): p. 227-33.

33. Zhou, J., et al., *Upregulation of surfactant synthesis triggers ABCA1-mediated basolateral phospholipid efflux.* J Lipid Res, 2004. **45**(9): p. 1758-67.

34. Agassandian, M., et al., *Pseudomonas aeruginosa and sPLA2 IB stimulate ABCA1-mediated phospholipid efflux via ERK-activation of PPARalpha-RXR.* Biochem J, 2007. **403**(3): p. 409-20.

35. Yamano, G., et al., *ABCA3 is a lamellar body membrane protein in human lung alveolar type II cells.* FEBS Lett, 2001. **508**(2): p. 221-5.

36. Edwards, V., et al., *Ultrastructure of lamellar bodies in congenital surfactant deficiency.* Ultrastruct Pathol, 2005. **29**(6): p. 503-9.

37. Wikenheiser, K.A., et al., *Simian virus 40 large T antigen directed by transcriptional elements of the human surfactant protein C gene produces pulmonary adenocarcinomas in transgenic mice.* Cancer Res, 1992. **52**(19): p. 5342-52.

38. Wikenheiser, K.A., et al., *Production of immortalized distal respiratory epithelial cell lines from surfactant protein C/simian virus 40 large tumor antigen transgenic mice.* Proc Natl Acad Sci U S A, 1993. **90**(23): p. 11029-33.

39. Jackowski, S., et al., *Disruption of CCTbeta2 expression leads to gonadal dysfunction.* Mol Cell Biol, 2004. **24**(11): p. 4720-33.

40. Trauner, M., M. Arrese, and M. Wagner, *Fatty liver and lipotoxicity.* Biochim Biophys Acta. **1801**(3): p. 299-310.

41. Cui, Z., M. Houweling, and D.E. Vance, *Expression of phosphatidylethanolamine N-methyltransferase-2 in McArdle-RH7777 hepatoma cells inhibits the CDP-choline pathway for phosphatidylcholine biosynthesis via decreased gene expression of CTP:phosphocholine cytidylyltransferase.* Biochem J, 1995. **312 (Pt 3)**: p. 939-45.

42. d'Azzo, A., A. Bongiovanni, and T. Nastasi, *E3 ubiquitin ligases as regulators of membrane protein trafficking and degradation.* Traffic, 2005. **6**(6): p. 429-41.

43. Berridge, M.J., P. Lipp, and M.D. Bootman, *The versatility and universality of calcium signalling.* Nat Rev Mol Cell Biol, 2000. **1**(1): p. 11-21.

44. Sun, L. and Z.J. Chen, *The novel functions of ubiquitination in signaling.* Current Opinion in Cell Biology, 2004. **16**(2): p. 119-26.

45. Pickart, C.M., *Ubiquitin in chains.* Trends Biochem Sci, 2000. **25**(11): p. 544-8.

46. Wang, X., et al., *Ubiquitination of serine, threonine, or lysine residues on the cytoplasmic tail can induce ERAD of MHC-I by viral E3 ligase mK3.* J Cell Biol, 2007. **177**(4): p. 613-24.

47. Ikeda, F. and I. Dikic, *Atypical ubiquitin chains: new molecular signals. 'Protein Modifications: Beyond the Usual Suspects' review series.* EMBO Rep, 2008. **9**(6): p. 536-42.

48. Tyers, M. and A.R. Willems, *One ring to rule a superfamily of E3 ubiquitin ligases.* Science, 1999. **284**(5414): p. 601, 603-4.

49. Deshaies, R.J. and C.A. Joazeiro, *RING domain E3 ubiquitin ligases.* Annu Rev Biochem, 2009. **78**: p. 399-434.

50. Wang, C., et al., *Identification of FBL2 as a geranylgeranylated cellular protein required for hepatitis C virus RNA replication.* Molecular Cell, 2005. **18**(4): p. 425-34.

51. Yu, H., et al., *Identification of a novel ubiquitin-conjugating enzyme involved in mitotic cyclin degradation.* Curr Biol, 1996. **6**(4): p. 455-66.

52. Grima, B., et al., *The F-box protein slimb controls the levels of clock proteins period and timeless.* Nature, 2002. **420**(6912): p. 178-82.

53. Carroll, J.L., Jr., et al., *Pulmonary-specific expression of tumor necrosis factor-alpha alters surfactant lipid metabolism.* Am J Physiol Lung Cell Mol Physiol, 2002. **282**(4): p. L735-42.

54. Salome, R.G., et al., *Effects of intratracheal instillation of TNF-alpha on surfactant metabolism.* J Appl Physiol, 2000. **88**(1): p. 10-6.

55. Ryan, A.J., et al., *Alveolar sphingolipids generated in response to TNF-alpha modifies surfactant biophysical activity.* J Appl Physiol, 2003. **94**(1): p. 253-8.

56. Haas, T.L., et al., *Recruitment of the linear ubiquitin chain assembly complex stabilizes the TNF-R1 signaling complex and is required for TNF-mediated gene induction.* Mol Cell, 2009. **36**(5): p. 831-44.

57. Fujita, K. and S.M. Srinivasula, *Ubiquitination and TNFR1 signaling.* Results Probl Cell Differ, 2009. **49**: p. 87-114.

58. Woodman, P., *ESCRT proteins, endosome organization and mitogenic receptor down-regulation.* Biochem Soc Trans, 2009. **37**(Pt 1): p. 146-50.

59. Fernandez-Sanchez, E., et al., *Constitutive and regulated endocytosis of the glycine transporter GLYT1b is controlled by ubiquitination.* J Biol Chem, 2009. **284**(29): p. 19482-92.

60. Teo, H., D.B. Veprintsev, and R.L. Williams, *Structural insights into endosomal sorting complex required for transport (ESCRT-I) recognition of ubiquitinated proteins.* J Biol Chem, 2004. **279**(27): p. 28689-96.

61. Mori, S., C.H. Heldin, and L. Claesson-Welsh, *Ligand-induced polyubiquitination of the platelet-derived growth factor beta-receptor*. J Biol Chem, 1992. **267**(9): p. 6429-34.

62. Mori, S., et al., *Degradation process of ligand-stimulated platelet-derived growth factor beta-receptor involves ubiquitin-proteasome proteolytic pathway.* J Biol Chem, 1995. **270**(49): p. 29447-52.

63. Baron, V. and M. Schwartz, *Cell adhesion regulates ubiquitin-mediated degradation of the platelet-derived growth factor receptor beta.* J Biol Chem, 2000. **275**(50): p. 39318-23.

64. Haglund, K., et al., *Multiple monoubiquitination of RTKs is sufficient for their endocytosis and degradation.* Nat Cell Biol, 2003. **5**(5): p. 461-6.

65. Malik, B., et al., *Regulation of epithelial sodium channels by the ubiquitin-proteasome proteolytic pathway.* Am J Physiol Renal Physiol, 2006. **290**(6): p. F1285-94.

66. Mallampalli, R.K., et al., *Lipid deprivation increases surfactant phosphatidylcholine synthesis via a sterol-sensitive regulatory element within the CTP:phosphocholine cytidylyltransferase promoter.* Biochem J, 2002. **362**(Pt 1): p. 81-8.

67. Horowitz, A.D., et al., *Preferential uptake of small-aggregate fraction of pulmonary surfactant in vitro.* Am J Physiol, 1997. **273**(2 Pt 1): p. L468-77.

68. Bruno, M.D., et al., *Transcriptional regulation of the murine surfactant protein-A gene by B-Myb.* J Biol Chem, 1999. **274**(39): p. 27523-8.

69. Chander, A., et al., *Protein kinase C in ATP regulation of lung surfactant secretion in type II cells.* Am J Physiol, 1995. **268**(1 Pt 1): p. L108-16.

70. Rooney, S., *Phospholipid composition, biosynthesis, and secretion*, in *Comparative Biology of the Normal Lung*, R. Parent, Editor. 1992, CRC: Boca Raton. p. 511-544.

71. Ciechanover, A., *The ubiquitin-proteasome proteolytic pathway.* Cell, 1994. **79**(1): p. 13-21.

72. Goldberg, A.L., *Functions of the proteasome: the lysis at the end of the tunnel.* Science, 1995. **268**(5210): p. 522-3.

73. Coux, O., K. Tanaka, and A.L. Goldberg, *Structure and functions of the 20S and 26S proteasomes.* Annu Rev Biochem, 1996. **65**: p. 801-47.

74. Rock, K.L., et al., *Inhibitors of the proteasome block the degradation of most cell proteins and the generation of peptides presented on MHC class I molecules.* Cell, 1994. **78**(5): p. 761-71.

75. Fenteany, G., et al., *Inhibition of proteasome activities and subunit-specific amino-terminal threonine modification by lactacystin.* Science, 1995. **268**(5211): p. 726-31.

76. Lee, D.H. and A.L. Goldberg, *Proteasome inhibitors: valuable new tools for cell biologists.* Trends Cell Biol, 1998. **8**(10): p. 397-403.

77. Bonifacino, J.S. and L.M. Traub, *Signals for sorting of transmembrane proteins to endosomes and lysosomes.* Annu Rev Biochem, 2003. **72**: p. 395-447.

78. Roederer, M., R. Bowser, and R.F. Murphy, *Kinetics and temperature dependence of exposure of endocytosed material to proteolytic enzymes and low pH: evidence for a maturation model for the formation of lysosomes.* J Cell Physiol, 1987. **131**(2): p. 200-9.

79. Pratt, M.R., et al., *Direct measurement of cathepsin B activity in the cytosol of apoptotic cells by an activity-based probe.* Chem Biol, 2009. **16**(9): p. 1001-12.

80. McMaster, C.R. and R.M. Bell, *CDP-choline:1,2-diacylglycerol cholinephosphotransferase.* Biochim Biophys Acta, 1997. **1348**(1-2): p. 100-10.

81. Chen, B.B. and R.K. Mallampalli, *Masking of a nuclear signal motif by monoubiquitination leads to mislocalization and degradation of the regulatory enzyme cytidylyltransferase.* Mol Cell Biol, 2009. **29**(11): p. 3062-75.

82. Butler, P.L. and R.K. Mallampalli, *Cross-talk between remodeling and de novo pathways maintains phospholipid balance through ubiquitination,* in *J Biol Chem*. 2009.

83. Winston, J.T., et al., *The SCFbeta-TRCP-ubiquitin ligase complex associates specifically with phosphorylated destruction motifs in IkappaBalpha and beta-catenin and stimulates IkappaBalpha ubiquitination in vitro.* Genes Dev, 1999. **13**(3): p. 270-83.

84. Orian, A., et al., *SCF(beta)(-TrCP) ubiquitin ligase-mediated processing of NF-kappaB p105 requires phosphorylation of its C-terminus by IkappaB kinase.* Embo J, 2000. **19**(11): p. 2580-91.

85. Feldman, M. and F.G. van der Goot, *Novel ubiquitin-dependent quality control in the endoplasmic reticulum.* Trends Cell Biol, 2009. **19**(8): p. 357-63.

86. Skowyra, D., et al., *F-box proteins are receptors that recruit phosphorylated substrates to the SCF ubiquitin-ligase complex.* Cell, 1997. **91**(2): p. 209-19.

87. Jackowski, S. and P. Fagone, *CTP: Phosphocholine cytidylyltransferase: paving the way from gene to membrane.* Journal of Biological Chemistry, 2005. **280**(2): p. 853-6. Epub 2004 Nov 9.

88. Henneberry, A.L., M.M. Wright, and C.R. McMaster, *The major sites of cellular phospholipid synthesis and molecular determinants of Fatty Acid and lipid head group specificity.* Molecular Biology of the Cell, 2002. **13**(9): p. 3148-61.

89. Sinha Roy, S., et al., *Inhibition of cholinephosphotransferase activity in lung injury induced by 2-chloroethyl ethyl sulfide, a mustard analog.* J Biochem Mol Toxicol, 2005. **19**(5): p. 289-97.

90. Fisher, A.B. and C. Dodia, *Role of acidic Ca2+-independent phospholipase A2 in synthesis of lung dipalmitoyl phosphatidylcholine.* American Journal of Physiology, 1997. **272**(2 Pt 1): p. L238-43.

91. Walkey, C.J., G.B. Kalmar, and R.B. Cornell, *Overexpression of rat liver CTP:phosphocholine cytidylyltransferase accelerates phosphatidylcholine synthesis and degradation.* Journal of Biological Chemistry, 1994. **269**(8): p. 5742-9.

92. Shindou, H., et al., *A single enzyme catalyzes both platelet-activating factor production and membrane biogenesis of inflammatory cells. Cloning and characterization of acetyl-CoA:LYSO-PAF acetyltransferase.* J Biol Chem, 2007. **282**(9): p. 6532-9.

93. Ye, G.M., et al., *Cloning and characterization a novel human 1-acyl-sn-glycerol-3-phosphate acyltransferase gene AGPAT7.* DNA Seq, 2005. **16**(5): p. 386-90.

94. Soupene, E., H. Fyrst, and F.A. Kuypers, *Mammalian acyl-CoA:lysophosphatidylcholine acyltransferase enzymes.* Proceedings of the National Academy of Sciences of the United States of America, 2008. **105**(1): p. 88-93.

95. Cao, J., et al., *Molecular identification of a novel mammalian brain isoform of acyl-CoA:lysophospholipid acyltransferase with prominent ethanolamine lysophospholipid acylating activity, LPEAT2.* J Biol Chem, 2008. **283**(27): p. 19049-57.

96. Chen, M. and L.A. Brown, *Histamine stimulation of surfactant secretion from rat type II pneumocytes.* Am J Physiol, 1990. **258**(4 Pt 1): p. L195-200.

97. Nicholas, T.E., J.H. Power, and H.A. Barr, *The pulmonary consequences of a deep breath.* Respir Physiol, 1982. **49**(3): p. 315-24.

98. Dietl, P., et al., *Pulmonary consequences of a deep breath revisited.* Biol Neonate, 2004. **85**(4): p. 299-304.

99. Zhou, J., et al., *Adenoviral gene transfer of a mutant surfactant enzyme ameliorates pseudomonas-induced lung injury.* Gene Ther, 2006. **13**(12): p. 974-85.

100. Chen, B.B. and R.K. Mallampalli, *Calmodulin binds and stabilizes the regulatory enzyme, CTP: Phosphocholine cytidylyltransferase.* Journal of Biological Chemistry, 2007. **282**: p. 33494-33506.

101. Kast, H.R., et al., *CTP:phosphocholine cytidylyltransferase, a new sterol- and SREBP-responsive gene.* J Lipid Res, 2001. **42**(8): p. 1266-72.

102. Kimbrel, E.A. and A.L. Kung, *The F-box protein beta-TrCp1/Fbw1a interacts with p300 to enhance beta-catenin transcriptional activity.* J Biol Chem, 2009. **284**(19): p. 13033-44.

103. Mallampalli, R.K., et al., *Betamethasone activation of CTP:cholinephosphate cytidylyltransferase in vivo is lipid dependent.* Am J Respir Cell Mol Biol, 1994. **10**(1): p. 48-57.

104. Bligh, E.G. and W.J. Dyer, *A rapid method of total lipid extraction and purification.* Can J Biochem Physiol, 1959. **37**(8): p. 911-7.

105. Harayama, T., et al., *Identification of a novel noninflammatory biosynthetic pathway of platelet-activating factor.* Journal of Biological Chemistry, 2008. **283**(17): p. 11097-106.

106. Storrie, B., et al., *Recycling of golgi-resident glycosyltransferases through the ER reveals a novel pathway and provides an explanation for nocodazole-induced Golgi scattering.* J Cell Biol, 1998. **143**(6): p. 1505-21.

107. Jordan, M.A., D. Thrower, and L. Wilson, *Effects of vinblastine, podophyllotoxin and nocodazole on mitotic spindles. Implications for the role of microtubule dynamics in mitosis.* J Cell Sci, 1992. **102 (Pt 3)**: p. 401-16.

108. Chen, B.B. and R.K. Mallampalli, *Masking of a nuclear signal motif by monoubiquitination leads to mislocalization and degradation of the regulatory enzyme, CCT•*. Mol. Cell. Biol., 2009. **29**: p. 3062-3075.

109. McCoy, D.M., Fisher K., Ryan, A.J., Mallampalli, R.K., *Transcriptional regulation of lung cytidylyltransferase in developing transgenic mice.* Am J Respir Cell Mol Biol, 2006. **35**: p. 394-402.

110. Mallampalli, R.K., et al., *Betamethasone modulation of sphingomyelin hydrolysis up-regulates CTP:cholinephosphate cytidylyltransferase activity in adult rat lung.* Biochem J, 1996. **318 (Pt 1)**: p. 333-41.

111. Miller, J.C. and P.A. Weinhold, *Cholinephosphotransferase in rat lung. The in vitro synthesis of dipalmitoylphosphatidylcholine from dipalmitoylglycerol.* J Biol Chem, 1981. **256**(24): p. 12662-5.

112. Agassandian, M., et al., *Oxysterols Inhibit phosphatidylcholine synthesis via ERK docking and phosphorylation of CTP:Phosphocholine cytidylyltransferase.* Journal of Biological Chemistry, 2005. **280**(22): p. 21577-87. Epub 2005 Mar 23.

113. Bladergroen, B.A., et al., *Inhibition of phosphatidylcholine and phosphatidylethanolamine biosynthesis in rat-2 fibroblasts by cell-permeable ceramides.* Eur J Biochem, 1999. **264**(1): p. 152-60.

114. O, K.M. and P.C. Choy, *Effects of fasting on phosphatidylcholine biosynthesis in hamster liver: regulation of cholinephosphotransferase activity by endogenous argininosuccinate.* Biochem J, 1993. **289 (Pt 3)**: p. 727-33.

115. Voziyan, P.A., C.M. Goldner, and G. Melnykovych, *Farnesol inhibits phosphatidylcholine biosynthesis in cultured cells by decreasing cholinephosphotransferase activity.* Biochem J, 1993. **295 (Pt 3)**: p. 757-62.

116. Wilgram, G.F. and E.P. Kennedy, *Intracellular Distribution of Some Enzymes Catalyzing Reactions in the Biosynthesis of Complex Lipids.* J Biol Chem, 1963. **238**: p. 2615-9.

117. Vance, J.E. and D.E. Vance, *Does rat liver Golgi have the capacity to synthesize phospholipids for lipoprotein secretion?* J Biol Chem, 1988. **263**(12): p. 5898-909.

118. Katzmann, D.J., M. Babst, and S.D. Emr, *Ubiquitin-dependent sorting into the multivesicular body pathway requires the function of a conserved endosomal protein sorting complex, ESCRT-I.* Cell, 2001. **106**(2): p. 145-55.

119. Helliwell, S.B., S. Losko, and C.A. Kaiser, *Components of a ubiquitin ligase complex specify polyubiquitination and intracellular trafficking of the general amino acid permease.* J Cell Biol, 2001. **153**(4): p. 649-62.

120. Chau, V., et al., *A multiubiquitin chain is confined to specific lysine in a targeted short-lived protein.* Science, 1989. **243**(4898): p. 1576-83.

121. Thrower, J.S., et al., *Recognition of the polyubiquitin proteolytic signal.* Embo J, 2000. **19**(1): p. 94-102.

122. Deribe, Y.L., et al., *Regulation of epidermal growth factor receptor trafficking by lysine deacetylase HDAC6.* Sci Signal, 2009. **2**(102): p. ra84.

123. Bao, J., et al., *Threonine phosphorylation diverts internalized epidermal growth factor receptors from a degradative pathway to the recycling endosome.* J Biol Chem, 2000. **275**(34): p. 26178-86.

124. Hicke, L., *Gettin' down with ubiquitin: turning off cell-surface receptors, transporters and channels.* Trends Cell Biol, 1999. **9**(3): p. 107-12.

125. van Kerkhof, P., et al., *Proteasome inhibitors block a late step in lysosomal transport of selected membrane but not soluble proteins.* Mol Biol Cell, 2001. **12**(8): p. 2556-66.

126. Dupre, S. and R. Haguenauer-Tsapis, *Deubiquitination step in the endocytic pathway of yeast plasma membrane proteins: crucial role of Doa4p ubiquitin isopeptidase.* Mol Cell Biol, 2001. **21**(14): p. 4482-94.

127. Hicke, L., H.L. Schubert, and C.P. Hill, *Ubiquitin-binding domains.* Nat Rev Mol Cell Biol, 2005. **6**(8): p. 610-21.

128. Urbanowski, J.L. and R.C. Piper, *Ubiquitin sorts proteins into the intralumenal degradative compartment of the late-endosome/vacuole.* Traffic, 2001. **2**(9): p. 622-30.

129. Harayama, T., H. Shindou, and T. Shimizu, *Biosynthesis of phosphatidylcholine by human lysophosphatidylcholine acyltransferase 1.* J Lipid Res, 2009. **50**(9): p. 1824-31.

130. Tsien, R.Y., *The green fluorescent protein.* Annual Review of Biochemistry, 1998. **67**: p. 509-44.

131. Piper, R.C. and J.P. Luzio, *Ubiquitin-dependent sorting of integral membrane proteins for degradation in lysosomes.* Current Opinion in Cell Biology, 2007. **19**(4): p. 459-65.

132. Lucero, P. and R. Lagunas, *Catabolite inactivation of the yeast maltose transporter requires ubiquitin-ligase npi1/rsp5 and ubiquitin-hydrolase npi2/doa4.* FEMS Microbiol Lett, 1997. **147**(2): p. 273-7.

133. Galan, J.M. and R. Haguenauer-Tsapis, *Ubiquitin lys63 is involved in ubiquitination of a yeast plasma membrane protein.* Embo J, 1997. **16**(19): p. 5847-54.

134. Gitan, R.S. and D.J. Eide, *Zinc-regulated ubiquitin conjugation signals endocytosis of the yeast ZRT1 zinc transporter.* Biochem J, 2000. **346 Pt 2**: p. 329-36.

135. Madshus, I.H., *Ubiquitin binding in endocytosis--how tight should it be and where does it happen?* Traffic, 2006. **7**(3): p. 258-61.

136. Pelham, H.R., *Membrane traffic: GGAs sort ubiquitin.* Current Biology, 2004. **14**(9): p. R357-9.

137. Wang, J., et al., *PI4P promotes the recruitment of the GGA adaptor proteins to the trans-Golgi network and regulates their recognition of the ubiquitin sorting signal.* Molecular Biology of the Cell, 2007. **18**(7): p. 2646-55.

138. Ikeda, H. and T.K. Kerppola, *Lysosomal localization of ubiquitinated Jun requires multiple determinants in a lysine-27-linked polyubiquitin conjugate.* Molecular Biology of the Cell, 2008. **19**(11): p. 4588-601.

139. Kim, P.K., et al., *Ubiquitin signals autophagic degradation of cytosolic proteins and peroxisomes.* Proceedings of the National Academy of Sciences of the United States of America, 2008. **105**(52): p. 20567-74.

140. Kopito, R.R., *Aggresomes, inclusion bodies and protein aggregation.* Trends Cell Biol, 2000. **10**(12): p. 524-30.

141. Chin, L.S., J.A. Olzmann, and L. Li, *Parkin-mediated ubiquitin signalling in aggresome formation and autophagy.* Biochem Soc Trans. **38**(Pt 1): p. 144-9.

142. Murai-Takebe, R., et al., *Ubiquitination-mediated regulation of biosynthesis of the adhesion receptor SHPS-1 in response to endoplasmic reticulum stress.* J Biol Chem, 2004. **279**(12): p. 11616-25.

143. Lands, W.E., *Metabolism of glycerolipids. 2. The enzymatic acylation of lysolecithin.* J Biol Chem, 1960. **235**: p. 2233-7.

144. Hubner, A., et al., *Multisite phosphorylation regulates Bim stability and apoptotic activity.* Mol Cell, 2008. **30**(4): p. 415-25.

145. Pasdar, M., Z. Li, and V. Chlumecky, *Plakoglobin: kinetics of synthesis, phosphorylation, stability, and interactions with desmoglein and E-cadherin.* Cell Motil Cytoskeleton, 1995. **32**(4): p. 258-72.

146. Miranda, F.F., et al., *Structural and stability effects of phosphorylation: Localized structural changes in phenylalanine hydroxylase.* Protein Sci, 2004. **13**(5): p. 1219-26.

147. Raiborg, C., T.E. Rusten, and H. Stenmark, *Protein sorting into multivesicular endosomes.* Curr Opin Cell Biol, 2003. **15**(4): p. 446-55.

148. Nakatsukasa, K. and J.L. Brodsky, *The recognition and retrotranslocation of misfolded proteins from the endoplasmic reticulum.* Traffic, 2008. **9**(6): p. 861-70.

149. Chen, B.B. and R.K. Mallampalli, *Masking of a nuclear signal motif by monoubiquitination leads to mislocalization and degradation of the regulatory enzyme, CCT•*. Molecular and Cellular Biology, 2009. **29**: p. 3062-3075.

150. Bridges, J.P., Shannon, J. M., *LPCAT1 regulates phospholipid synthesis and is required for the transition to air breathing.* Journal of Clinical Investigation, 2010.

151. Hoseki, J., R. Ushioda, and K. Nagata, *Mechanism and components of endoplasmic reticulum-associated degradation.* J Biochem. **147**(1): p. 19-25.

152. Omura, S., et al., *Lactacystin, a novel microbial metabolite, induces neuritogenesis of neuroblastoma cells.* J Antibiot (Tokyo), 1991. **44**(1): p. 113-6.

153. Frescas, D. and M. Pagano, *Deregulated proteolysis by the F-box proteins SKP2 and beta-TrCP: tipping the scales of cancer.* Nat Rev Cancer, 2008. **8**(6): p. 438-49.

154. Kanemori, Y., K. Uto, and N. Sagata, *Beta-TrCP recognizes a previously undescribed nonphosphorylated destruction motif in Cdc25A and Cdc25B phosphatases.* Proc Natl Acad Sci U S A, 2005. **102**(18): p. 6279-84.

155. Agassandian, M., et al., *14-3-3{zeta} escorts CCT{alpha} for calcium-activated nuclear import in lung epithelia.* Faseb J, 2009.

156. Orrenius, S., M.J. McCabe, Jr., and P. Nicotera, *Ca(2+)-dependent mechanisms of cytotoxicity and programmed cell death.* Toxicol Lett, 1992. **64-65 Spec No**: p. 357-64.

157. Eckenhoff, R.G. and A.P. Somlyo, *Rat lung type II cell and lamellar body: elemental composition in situ.* Am J Physiol, 1988. **254**(5 Pt 1): p. C614-20.

158. Chandra, S., et al., *Calcium sequestration in the Golgi apparatus of cultured mammalian cells revealed by laser scanning confocal microscopy and ion microscopy.* J Cell Sci, 1991. **100 (Pt 4)**: p. 747-52.

159. Hurley, J.H., S. Lee, and G. Prag, *Ubiquitin-binding domains.* Biochem J, 2006. **399**(3): p. 361-72.

160. Oldham, C.E., et al., *The ubiquitin-interacting motifs target the endocytic adaptor protein epsin for ubiquitination.* Curr Biol, 2002. **12**(13): p. 1112-6.

161. Williams, R.L. and S. Urbe, *The emerging shape of the ESCRT machinery.* Nat Rev Mol Cell Biol, 2007. **8**(5): p. 355-68.

162. Bilodeau, P.S., et al., *Vps27-Hse1 and ESCRT-I complexes cooperate to increase efficiency of sorting ubiquitinated proteins at the endosome.* J Cell Biol, 2003. **163**(2): p. 237-43.

163. Alam, S.L., et al., *Structural basis for ubiquitin recognition by the human ESCRT-II EAP45 GLUE domain.* Nat Struct Mol Biol, 2006. **13**(11): p. 1029-30.

164. Shields, S.B., et al., *ESCRT ubiquitin-binding domains function cooperatively during MVB cargo sorting.* J Cell Biol, 2009. **185**(2): p. 213-24.

165. Kyprianou, N., H.F. English, and J.T. Isaacs, *Activation of a Ca2+-Mg2+-dependent endonuclease as an early event in castration-induced prostatic cell death.* Prostate, 1988. **13**(2): p. 103-17.

166. Wyllie, A.H., G.J. Beattie, and A.D. Hargreaves, *Chromatin changes in apoptosis.* Histochem J, 1981. **13**(4): p. 681-92.

167. Squier, M.K., et al., *Calpain activation in apoptosis.* J Cell Physiol, 1994. **159**(2): p. 229-37.

168. Fujikawa, K., et al., *Calcium/calmodulin-dependent protein kinase II (CaMKII) regulates tumour necrosis factor-related apoptosis inducing ligand (TRAIL)-mediated apoptosis of fibroblast-like synovial cells (FLS) by phosphorylation of Akt.* Clin Exp Rheumatol, 2009. **27**(6): p. 952-7.

169. Tazmini, G., et al., *Membrane localization of RasGRP1 is controlled by an EF-hand, and by the GEF domain.* Biochim Biophys Acta, 2009. **1793**(3): p. 447-61.

170. Gifford, J.L., M.P. Walsh, and H.J. Vogel, *Structures and metal-ion-binding properties of the Ca2+-binding helix-loop-helix EF-hand motifs.* Biochem J, 2007. **405**(2): p. 199-221.

171. Puria, R., S.A. Zurita-Martinez, and M.E. Cardenas, *Nuclear translocation of Gln3 in response to nutrient signals requires Golgi-to-endosome trafficking in Saccharomyces cerevisiae.* Proc Natl Acad Sci U S A, 2008. **105**(20): p. 7194-9.

172. Mukherjee, S. and D. Shields, *Nuclear import is required for the pro-apoptotic function of the Golgi protein p115.* J Biol Chem, 2009. **284**(3): p. 1709-17.

173. la Cour, T., et al., *Analysis and prediction of leucine-rich nuclear export signals.* Protein Eng Des Sel, 2004. **17**(6): p. 527-36.

174. Lagace, T.A., M.K. Storey, and N.D. Ridgway, *Regulation of phosphatidylcholine metabolism in Chinese hamster ovary cells by the sterol regulatory element-binding protein (SREBP)/SREBP cleavage-activating protein pathway.* J Biol Chem, 2000. **275**(19): p. 14367-74.

175. Ridgway, N.D. and T.A. Lagace, *Regulation of the CDP-choline pathway by sterol regulatory element binding proteins involves transcriptional and post-transcriptional mechanisms.* Biochem J, 2003. **372**(Pt 3): p. 811-9.

176. Wright, L.P. and M.R. Philips, *Thematic review series: lipid posttranslational modifications. CAAX modification and membrane targeting of Ras.* J Lipid Res, 2006. **47**(5): p. 883-91.